# DETERMINING MOLECULAR MECHANSIMS OF DNA NON-HOMOLOGOUS END JOINING PROTEINS

Katherine S. Pawelczak

Accepted by the Faculty of Indiana University, in partial
fulfillment of the requirements for the degree of Doctor of Philosophy.

                                                                      _____

Ronald Wek, Ph.D., Chair

_____

John Turchi, Ph.D.

Doctoral Committee

_____

Suk-Hee Lee, Ph.D.

June 4, 2010

_____

Yuchiro Takagi, Ph.D.

ii

ACKNOWLEDGEMENTS

I would like to thank my family for supporting me through five years of hard work. My mother was a constant source for advice, particularly as she was defending her own dissertation. My father, who always has expressed a sincere interest in my research, and was a supportive cheerleader. My brother Eli, who served as a great sounding board for all of my complaints over the years. My soon-to-be in-laws, who have been wonderful during the last five years. My fiancé, Josh Miller, who has supported me both financially and emotionally as I progressed through the graduate program. He never left my side, and I couldn't have done it without him. I also have to thank my advisor, Dr. John Turchi, for teaching me everything I know. He has trained me for eight years, and I literally owe my entire scientific career to him. After working as his technician for 3 years, I became his graduate student and it served to be the best decision I have ever made. John is a wonderful mentor, phenomenal biochemist and great friend. His family, wife Karen and two children Meg and Alaina, have been supportive as well as I "grew up" as a scientist in John's lab. I would also like to thank my committee for providing great assistance for my entire graduate career, Dr. Ron Wek, Dr. Zhong-Yin Zhang, Dr. Suk-Hee Lee and Dr. Yuichiro Takagi. I would also like to acknowledge the Turchi lab members, who have been an integral part of my doctorate education. My good friends Brooke Andrews, Dr. Sarah Shuck, Emily Short, Dr. Kambiz Tahmaseb, Dr. Jason Lehman, Dr. Steve Patrick, Dr. Kelly Trego, Victor Anciano and Derek Woods. These people have helped me become the biochemist I am today.

ABSTRACT

Katherine S. Pawelczak

Determining molecular mechanisms of DNA Non-Homologous End Joining proteins

DNA double strand breaks (DSB), particularly those induced by ionizing radiation (IR) are complex lesions and if not repaired, these breaks can lead to genomic instability, chromosomal abnormalities and cell death.  IR-induced DSB often have DNA termini modifications including thymine glycols, ring fragmentation, 3' phosphoglycolates, 5' hydroxyl groups and abasic sites.  Non-homologous end joining (NHEJ) is a major pathway responsible for the repair of these complex breaks. Proteins involved in NHEJ include the Ku 70/80 heterodimer, DNA-PKcs, processing proteins including Artemis and DNA polymerases μ and λ, XRCC4, DNA ligase IV and XLF.  The precise molecular mechanism of DNA-PK activation and Artemis processing at the site of a DNA DSB has yet to be elucidated.  We have investigated the effect of DNA sequence and structure on DNA-PK activation and results suggest a model where the 3' strand of a DNA terminus is responsible for annealing and the 5' strand is involved in activation of DNA-PK.  These results demonstrate the influence of DNA structure and orientation on DNA-PK activation and provide a molecular mechanism of activation resulting from compatible termini, an essential step in microhomology-mediated NHEJ.  Artemis, a nuclease implicated in processing of DNA termini at a DSB during NHEJ, has been demonstrated to have both DNA-PK independent 5'-3' exonuclease activities and DNA-PK dependent endonuclease activity.  Evidence suggests that either the enzyme contains two different active sites

for each of these distinct processing activities, or the exonuclease activity is not intrinsic to the Artemis polypeptide.  To distinguish between these possibilities, we sought to determine if it was possible to biochemically separate Artemis endonuclease activity from exonuclease activity.  An exonuclease-free fraction of Artemis was obtained that retained DNA-PK dependent endonuclease activity, was phosphorylated by DNA-PK and reacted with an Artemis specific antibody.  These data demonstrate that the exonuclease activity thought to be intrinsic to Artemis can be biochemically separated from the Artemis endonuclease.  These results reveal novel mechanisms of two critical NHEJ proteins, and further enhance our understanding of DNA-PK and Artemis activity and their role in NHEJ.


Ronald C. Wek, Ph.D., Chair

TABLE OF CONTENTS

Curriculum Vitae

LIST OF TABLES

Table 1: Oligonucleotide sequences

Table 2: Purification table of [His]6-Artemis protein preparation

LIST OF FIGURES

# ABBREVIATIONS

DSB = double-strand break

IR = ionizing radiation

NHEJ = non-homologous end joining

HDR = homology directed repair

DNA-PK = DNA dependent protein kinase

DNA-PKcs = DNA dependent protein kinase catalytic subunit

Pol = polymerase

LIV/X4 = ligase IV / XRCC4

PNKP = human polynucleotide kinase-phosphatase

PIKK = (PI-3) kinase-like kinases

Ku 80 CTR = Ku 80 C-terminal region

dsDNA = double-strand DNA

ssDNA = single-strand DNA

SS/DS junction = single-strand/double-strand junction

nt = nucleotides

SAXS = small angle X-ray scattering

vWA = von Willebrand Factor A

XLF = XRCC4-like factor

## 1. Background and Significance

### 1.1. DNA damage

Genetic mutations accumulating over millions of years have lead to positive

adaptations and changes that have created the extreme diversity that is seen in the

multitudes of organisms today.  However, in an individual's life span, genetic change

can be detrimental as it can lead to phenotypical alterations that negatively impact

physiology.  Such genetic change can occur following damage to an organism's

DNA, creating a genetic mutation that is propogated as individual cells divide and

pass this mutation on to daughter cells.  DNA damage that results in a heritable

change in DNA can occur from both endogenous and exogenous sources.  DNA

damage from endogenous sources like replication errors and oxidative source

includes base loss, base modification, formation of abasic sites, and single-strand and

double-strand breaks.  Damage from exogenous sources like UV light, ionizing

radiation and a variety of chemotherapeutic agents include photo-induced DNA

lesions, chemical base modification, single and double-strand breaks, inter-strand

crosslinks, protein-DNA crosslinks and other DNA lesions.  This thesis focuses on

DNA double strand breaks (DSB) and examines the regulatory system in place in the

cell to counteract this type of damage.

#### 1.1.1. DNA double strand breaks

DNA double strand breaks (DSB) have been a topic widely studied over the

years in part because of the ability for unrepaired DSB to induce genomic instability,

chromosomal translocation, carcinogenesis and cell death [1].  Cellular DSB can arise

from both endogenous and exogenous sources (Figure 1).  Endogenous DSB can
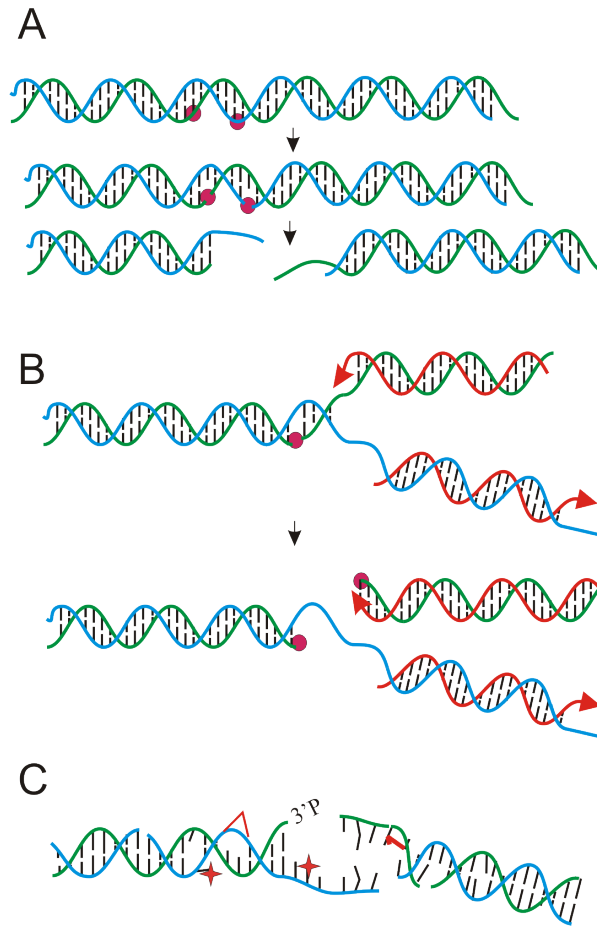
**Figure 1. DNA double strand breaks (DSB). (A)** Single-strand breaks (SSB) arising from reactive oxygen species (ROS) that are located in close proximity to each other in the genome can lead to a DNA DSB. SSB locations are indicated by red circles. **(B)** DNA polymerase-driven attempts to replicate past a nick in the leading strand template of DNA can result in a DNA DSB. Nicks are indicated by red circles and newly replicated DNA is indicated by red strands. **(C)** Exogenous DNA damaging agents like ionizing radiation (IR) produce DNA DSB with a variety of end modifications and various forms of DNA damage around the DNA terminus.

occur from reactive oxygen species that create dual lesions in close proximity to each other. DSB can also arise from replication fork stalling that lead to fork collapse or attempts to replicate past a nick in a leading strand template [2]. In addition, certain genomic recombination events, including V(D)J recombination, induce DSB through endonuclease processing [3]. Finally, endogenous DSB can result from physical stress that occurs during separation of chromosomes in mitosis [4]. DSB are also produced from a variety of exogenous DNA damaging agents, such as ionizing radiation (IR) and certain chemotherapeutic agents like bleomycin and camptothecin [5].

### 1.1.2. Ionizing radiation induced DNA DSB

DNA double strand breaks produced by ionizing radiation typically do not have blunt, unmodified termini. Instead, DNA termini at the site of a break induced by IR can have a variety of DNA lesions that present as end modifications, base damages and base alterations. It has been suggested that many of these DNA moieties can occur in a clustered region, potentially near the site of the initial break, and the presence of these multiple lesions could increase the mutagenesis rate that can arise from IR [6]. DNA modifications include thymine glycols, ring fragmentation, 3' phosphoglycolates, 5' hydroxyl groups and abasic sites. Regions of single-strand DNA that arise from strand breakage can occur at a DSB as well, leaving a single-strand overhang region at the site of the break. These diverse forms of damage and structure at the site of DNA DSB are likely to impact rate and overall repair of the DSB. As the structural complexity found at the site of DSB increases, the ability of repair decreases [7]. It is becoming increasingly apparent that the assortment of

secondary DNA lesions found at the site of an IR-induced break presents challenges

for their repair. Due to the complexities in the DNA lesions produced by IR, one

could imagine that different enzymes or pathways would be required to process

different types of DNA lesions found at termini towards the joining or resolution of

DNA DSB.

## 1.2. Repairing DNA DSB

The cell has developed two major pathways that are responsible for the repair

of DNA DSB, homology directed repair (HDR) that is based homologous

recombination and non-homologous end joining (NHEJ). The mechanism controlling

the pathway choice for repair of DNA DSB in mammalian cells has not yet been

clearly defined. However, it is thought that NHEJ, rather than HDR, is the

predominant pathway for repair of DSB, particularly those induced by IR and other

exogenous agents. A contributing factor to this hypothesis is that HDR requires a

sister chromatid in close proximity that is used as a template in repair of the DSB and

thus is restricted to S/G2 [8]. This mechanism has provided the nickname "error-

free" repair for HDR, as little to no loss of genetic material occurs, particularly if the

template used is completely homologous. Importantly, specific DNA damage may be

retained in HDR and require further repair or processing following initial HDR. Non-

dividing or cells not in S phase do not have a homologous donor, and as the majority

of DNA damage from exogenous sources affects cells without a donor, NHEJ is

thought to be responsible for the repair of most DSB caused by IR and other

exogenous agents. Due to its ability to repair a DSB without a homologous template,

NHEJ has been referred to as the "error-prone" pathway, as it is able to bring together

two DNA ends that potentially have little to no homology at the site of the break. While in theory a simple mechanism, continuing research is showing that joining of two non-homologous DNA ends by NHEJ is in fact a sophisticated and complex mechanism of DNA repair.

### 1.2.1. Non-homologous end joining

NHEJ, found to be active throughout all phases of the cell cycle, is responsible for the joining of a DNA DSB. The pathway is most efficient *in vitro* at processing blunt termini that require no modification at the terminus prior to ligation. However, NHEJ is also proficient at joining two DNA ends that have non-homologous overhang regions, and frequently this involves the removal or addition of nucleotides at the site of the break [9]. Despite the term "non-homologous" end joining, it has been shown that there can be a greater tendency to join two broken ends that contain sequences with 1-4 nucleotides that are complementary [10], dubbed more recently as areas of microhomology. It is suggested that to align these ends of DNA at regions of microhomology, processing that results in the loss or addition of nucleotides must occur [11-13].

There are four specific steps in NHEJ; DNA termini recognition, bridging of the DNA ends also known as formation of the synaptic complex, DNA end processing, and finally DNA ligation (Figure 2). After a DSB occurs, the heterodimeric protein Ku, made up of 70 and 80 kDa subunits, binds to the end of the break. Once Ku is bound, it recruits the 465 kDa DNA-PK catalytic subunit (DNA-PKcs). Together, these proteins make up a heterotrimeric complex called the DNA-dependent protein kinase, or DNA-PK. The formation of this complex may aid in
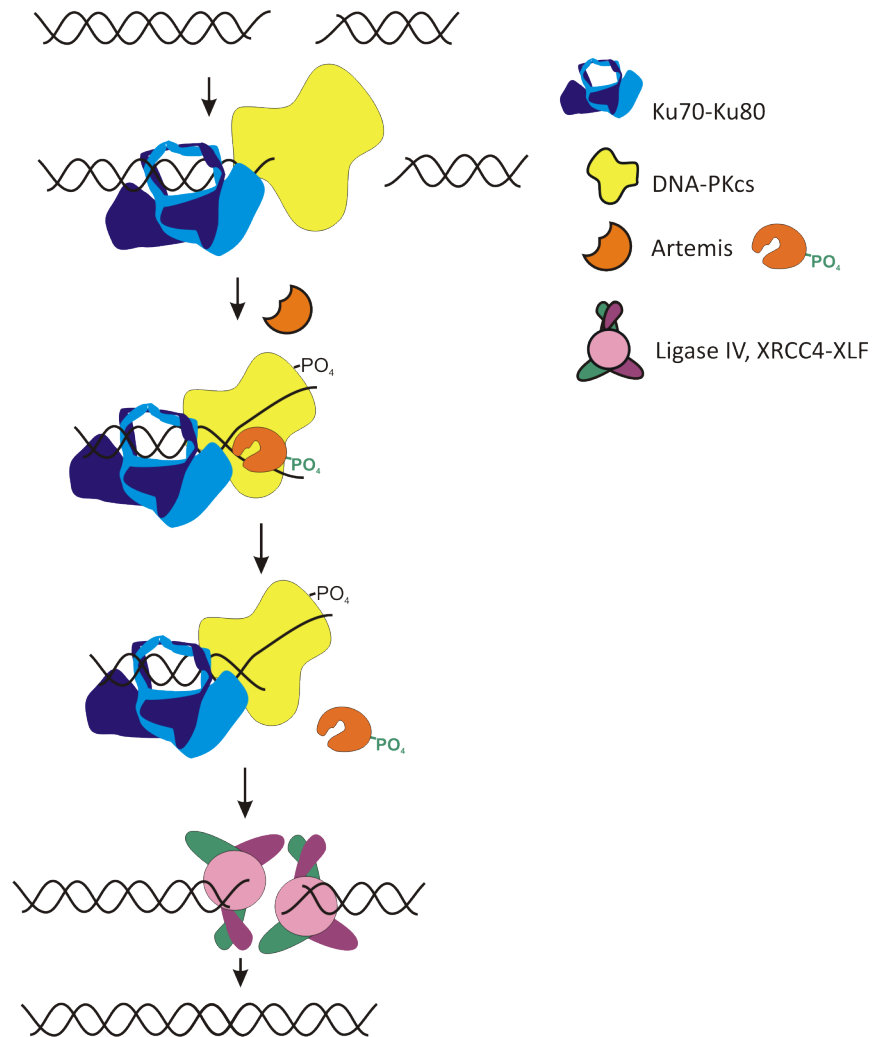
**Figure 2. The Non-Homologous End Joining (NHEJ) pathway.** Following a DNA DSB induced by IR, the heterodimeric Ku (Ku 70 and Ku 80) complex is recruited to the DNA terminus, binds to the DNA and recruits the DNA-dependent protein kinase catalytic subunit (DNA-PKcs). DNA-PKcs forms a heterotrimeric complex with Ku and its serine/theonine protein kinase activity is activated once bound to the DNA terminus. Autophosphorylation and phosphorylation of other target proteins occurs. Artemis, in the presence of DNA-PK and ATP, becomes active and is able to endonucleolytically cleave DNA termini that require processing. Ligase IV/XRCC4/XLF complex is recruited to DNA termini and catalyze ligation of the DNA DSB.

stabilizing the two DNA ends at the site of the break, forming a synaptic complex that secures the two ends together [14]. The catalytic activity of DNA-PK is activated once bound to DNA, and this unique serine/threonine protein kinase phosphorylates downstream target proteins needed for completion of the pathway [15].

As mentioned earlier, IR does not frequently produce clean blunt-end breaks, and in fact regularly produces a number of complex breaks that contain DNA discontinuities at the terminus that require processing before proper ligation can occur. Artemis is the main nuclease known to process DNA termini in NHEJ, by degrading DNA single-strand overhangs with its 5' exonuclease and 5' or 3' endonuclease activity [16, 17]. Cells containing defective Artemis are hypersensitive to radiation treatment [18]. Polymerases responsible for adding bases at the termini include pol $\beta$, $\mu$, and $\lambda$. Pol $\mu$ is of particular interest, as its concentration is increased in cells after IR exposure it is found in a complex with Ku and the Ligase IV/XRCC4 complex [19].

After processing of the DNA termini, DNA ligase IV is responsible for ligating the DSB. Ligase IV is able to ligate double-stranded DNA that has either compatible overhangs or blunt-ends [20], making it the perfect ligase for a repair pathway that does not require homology. DNA ligase IV is found in a complex with XRCC4, and the flexibility of this complex is apparent by the fact that the complex can ligate one strand even if the second strand can't be ligated (perhaps because of a 5' OH) [21]. XLF, a recently identified protein found to be involved in NHEJ just recently [22] , was found to interact with Ligase IV/XRCC4 and found to be required for NHEJ and can complement DNA repair defects. Even more recent evidence has

shown that XLF is in a complex with Ligase IV/XRCC4, and it is believed to be needed for stimulating the ligase activity of the complex [21].

### 1.3. Ku 70/Ku 80

#### 1.3.1. Background

Ku, initially discovered as an autoantigen, is one of the first proteins to bind to DNA at a double strand break in NHEJ [23]. Ku is extremely abundant in the cell, at about 400,000 molecules per cell [24]. This DNA binding protein, found predominantly in the nucleus, is typically found as a stable heterodimeric complex of 70 and 86 kDa subunits [25]. Mice deficient in either Ku 70 or Ku 80 were found to have low levels of the remaining subunit, indicating that the heterodimer is the stable form found in the cell [26, 27]. Ku can also form a heterotrimeric complex with the 469 kDa DNA-PKcs when bound to DNA, forming the ~610 kDa DNA-PK complex. Very recent work from the Ramsden lab suggests that Ku also has enzymatic activity, 5' AP lyase activity, used in NHEJ (not BER) to remove AP sites near DSB. Overall, Ku has been implicated in other cellular pathways, including telomere length regulation, but its main role has been shown to be crucial to NHEJ-mediated DNA repair in eukaryotes [28].

#### 1.3.2. Ku and DNA binding

Ku binds to specific DNA structures in a sequence independent fashion. Kinetic studies have shown that Ku has a high affinity for DNA termini with values ranging from $1.5\text{-}4.0 \times 10^{-10}\ M^{-1}$, [29] and Ku can bind to double-stranded DNA termini that have 5' or 3' single-strand overhangs or blunt ends [23, 30]. Other studies have reported Ku interacting with a variety of other DNA structures, including

nicked DNA, circular plasmid DNA, and single-strand DNA [31]. However, due to

more recent structural and biochemical on Ku, it is unlikely that this heterodimer can

bind and DNA that does not have a free terminus. DNA length also plays a crucial

role in Ku-DNA binding. Photocrosslinking studies have revealed that Ku 70 is

positioned closer to the DNA terminus and Ku 80 is positioned distally to the

terminus [32, 33]. The size and shape of these molecules requires a DNA length of

14-18 base-pairs for successful binding of one Ku molecule [30]. Kinetic analysis

has revealed that Ku can bind to 1-site DNA (DNA substrate able to accommodate

one Ku molecule) in a noncooperative fashion. Substrates long enough to bind two

Ku molecules, however, result in positive cooperativity, with the second Ku molecule

loading onto the DNA and forming more contacts with the first Ku molecule already

loaded on the DNA substrate (potentially stabilizing both Ku molecules) [34]. This

and other studies led to the hypothesis that multiple Ku molecules can bind to DNA

in a length-dependent fashion and line up on the substrate, much like beads on a

string, although the biological significance of this activity is unclear.

The "beads on a string" model of multiple Ku molecules binding to a substrate

is consistent with data showing that Ku, once bound to the end of a double strand

break, can translocate inward along the length of DNA in an ATP-independent

manner. This movement is thought to coincide with the recruitment of DNA-PKcs to

the site of the break, and is required for DNA-PK to gain access to the end of the

DNA substrate [34]. Interestingly, discontinuities in the DNA strucuture, such as

bulky cisplatin lesions, do not significantly diminish Ku binding capacity, but can

inhibit translocation of Ku along the length of DNA [35]. This impairment of Ku

movement along the DNA was also found to inhibit LIV/XRCC4 stimulated ligation, presumably because without translocation of Ku along the DNA, the ligase complex is unable to efficiently bind to the DNA [36]. A recent study has addressed the issue of Ku translocating on DNA *in vivo*, where the DNA is coated in histones and other DNA binding proteins. These large proteins could prevent the ring-like structure of Ku from sliding onto the end of DNA and moving along the length of it, as suggested by numerous *in vitro* experiments over the years. Roberts and Ramsden demonstrated that Ku is capable of peeling away as much as 50 base-pairs of DNA from around the histone octamer structure at the terminus of a double strand break, thus allowing for DNA-PK to slide along the DNA without the need for chromatin remodeling [37].

*1.3.3. Ku structure*

The structural features of Ku as revealed by various methods support much of the biochemical evidence gathered about Ku over the years. The two Ku subunits have a great deal of sequence similarity and both contain regions that contribute to the main DNA binding domain of the heterodimer [38]. The Ku crystal structure reveals a ring-like shape that does not appear to undergo any major change in conformation after binding DNA [39]. This ring-like structure allows for Ku to slide onto the DNA terminus, but the shape and geometry of the molecule renders it difficult if not impossible to bind to and interact with DNA in the absence of a free end. It is hypothesized that two turns of DNA can fit through the channel in this ring-like structure. The non-specific interaction between the sugar-phosphate backbone of DNA and the amino acids of the Ku ring structure is supporting evidence for Ku

binding to DNA double-strand breaks in a sequence-independent manner [39]. The

C-terminal region of Ku 80, which is too flexible for X-ray crystallography and

missing from the heterodimer solved structure, has been examined in solution based

structural studies. This work has revealed a 30 amino acid flexible linker region

with a cluster of six alpha helixes, with the final 12 amino acid residues largely

disordered. This region is important for interaction with DNA-PKcs, and will be

discussed in detail later in this chapter [40, 41].

## 1.4. DNA-PK

### 1.4.1. Background

DNA dependent protein kinase catalytic subunit (DNA-PKcs) is the largest

protein kinase in the cell reported to date at 469 kDa. Sequence analysis places

DNA-PKcs as a member of the phosphatidylinositol-3 (PI-3) kinase-like-kinase

(PIKK) suerpfamily (along with ATM, ATR, mTOR, SMG-1 and TRRAP). Grouped

together because of their similar catalytic domains, the PIKKs catalytic domains have

significant homology with the catalytic domains of the phosphoinositide (PI-3)-

kinases. However, the PIKKs use their catalytic domains to phosphorylate protein

targets on serine or threonine residues rather than lipids. DNA-PKcs, like other

family members, has a C-terminus kinase domain that is relatively small compared to

the rest of the polypeptide (5-10 %), and is flanked by a FAT and FAT-C domains,

whose roles are not yet clearly understood. The N-terminal region is not well

conserved, but is predicted to have multiple alpha-helical HEAT repeats [42].

DNA-PKcs was identified as playing a role in NHEJ because DNA-PKcs

binds to the site of a DSB following binding of the heterodimer protein Ku.

Furthermore, glioma cell lines that contain a defect in the gene encoding DNA-PKcs have been shown to be defective in NHEJ and are radiation sensitive [43]. This is supported by data showing that the binding affinity of the 465 kDa DNA-PK catalytic subunit (DNA-PKcs) to the site of a DNA DSB is increased 100-fold in the presence of Ku [44], and the serine/threonine protein kinase activity is increased at least 6-fold by the presence of Ku [30]. Once bound to DNA, DNA-PKcs is able to phosphorylate substrate proteins, preferentially targeting serines and threonines that are followed by a glutamine (S-T/Q) [1]. As DNA-PK kinase activity is required for efficient DNA end joining [45], and inhibition of the kinase by specific inhibitors decreases end joining [46], a large body of work has supported the idea of physiological importance of phosphorylation on different protein substrates by DNA-PK. It has also been suggested that DNA-PK kinase activity plays a role in the DNA damage checkpoint or apoptotic signaling pathways [47].

*1.4.2. DNA-PK structure and activation: the role of DNA*

As described earlier, the working model for DNA-PK activation requires Ku binding to the site of a DSB, followed by recruitment of the DNA-PKcs to the terminus. Once bound, these proteins form a protein complex, termed DNA-PK, which exists in a dynamic state on each DNA terminus of the DSB. DNA-PK is a unique kinase as it is activated only upon binding to the ends of double-stranded DNA [47, 48]. However, one of the biggest challenges in the field is understanding the molecular mechanisms that drive activation of DNA-PK by DNA. This dependence on DNA for activity has led to the conclusion that DNA-PK makes direct contact with DNA, as supported by numerous studies reviewed in [32], including a

study showing the importance of a leucine rich region that appears to be at least partially responsible for the direct interaction between the kinase and the DNA [49]. Significant structural and biochemical advances with DNA-PK are aiding our understanding of DNA-PK activation.

The DNA terminus resulting from an IR-induced DSB can vary in structure, size, and chemistry, each of which may play an important role in DNA-PK activation. Like Ku, it has been shown that DNA-PK is activated by fully duplex DNA [50]. However, hairpin structures or supercoiled plasmids result in little or no kinase activity. Furthermore, DNA-PK is preferentially activated by DNA with 3' pyrimidine-rich termini, but activity is severely inhibited by cisplatin-DNA adducts [51]. These results are attributed to the catalytic subunit of DNA-PK, as there is no strong evidence for sequence-bias or strand bias with Ku and DNA, nor are cisplatin lesions thought to inhibit Ku binding. Interestingly, chemical modifications to DNA termini such as biotin and fluoroscein do not inhibit kinase activity [14, 51].

A large amount of *in vitro* biochemical analysis regarding the activation of the catalytic subunit has previously been determined in the absence of Ku. Such studies were made possible because DNA-PKcs has an affinity for DNA *in vitro*, specifically in low salt buffer, even in the absence of Ku [52]. This assay technique results in interesting data stating that DNA-PKcs is preferentially activated by single-strand DNA ends (in a Ku-independent reaction) [53]. More recently groups have undertaken studies with the heterotrimeric complex that is made up of Ku 70, Ku 80 and DNA-PKcs. This could be considered to be the more physiologically relevant form of studying DNA-PK, as there is no evidence that DNA-PKcs binds to or is

activated by DNA in the cell in the absence of Ku 70/80. Studies from our lab working with the heterotrimeric complex have revealed that DNA-PK is preferentially activated by 3' pyrimidine-rich sequences, and this supports the theory that single-strand ends of DNA may play an important role in DNA. Furthermore, studies have suggested that melting of the DNA terminus to expose single-strand ends may be necessary for DNA-PK to bind in a stable complex with DNA and lead to optimal activation of the kinase [54]. Clearly, DNA terminal structure, sequence and chemistry have an impact on activation of DNA-PK.

Advances in structural studies have complemented and extended our understanding of DNA-PK with respect to the role of DNA in activation of the kinase. Electron crystallographic studies have shown an open channel in the DNA-PKcs structure that can plausibly interact with double-stranded DNA [55]. Due to the enormity of the catalytic subunit (465 kDa), structural reconstructions, primarily from cryo EM analysis, have resulted in fairly low resolution images. These studies have revealed, among other things, structural data to support the theory that the catalytic subunit undergoes conformational changes upon binding to DNA and these changes play an important role in efficient NHEJ [56, 57]. More recently, higher resolution reconstruction (7 Å) of DNA-PKcs was achieved. In this study, Williams et al. show that DNA-PK displays handedness, with a head and base region with two side connections that create a tunnel-like hollow channel within the protein that is the proposed binding site for DNA. Docking experiments revealed that the kinase domain could fit in either the head or base regions, although homology docking work with PI3Kgamma as a model indicate that the base region is the more plausible

position. Within the central opening is an alpha-helical like protrusion, a likely candidate for direct interaction with DNA. The authors propose that about 1 turn of the dsDNA would need to enter this channel to interact with this alpha-helical region. Interestingly, what appears to be a smaller cavity, only large enough to fit single-strand DNA, is located above the larger central channel [58]. A crystal structure of DNA-PKcs together with truncated forms of Ku 70 and Ku 80 have resulted in a structure of DNA-PK with the highest resolution yet accomplished, at 6.6 Å, where the overall shape is discernable. This reveals that an alpha helical region of HEAT repeats result in a bending of the protein structure into a hollow circular structure, like that described by the cryo EM data discussed above. Interestingly, these authors place the catalytic domain in the top portion, or head region, of this circular structure, and show that there is a small HEAT repeat region inside the structure that probably binds DNA [59].

Previous biochemical studies have suggested that once double strand DNA is threaded through the kinase, it can fray to expose a certain length of single strand DNA. Each of these strands can then be inserted into what are seen from the structural data as two cavitities [53, 55] or, alternatively, one cavity on the perimeter of the molecule that may be an active site and has the dimensions to accommodate single-strand DNA [58] (Figure 3). It is important to point out that the higher resolution structural data that has been generated suggests that there is a DNA binding alpha-helical region within the core of the circular cavity of DNA-PK and this supports the model of threading of DNA through the kinase [59]. However, this does not rule out the possibility that after threading, DNA could be separating and

wrapping around the kinase to activate via interactions in another cavity in a *cis* or *trans* fashion. In fact, data showing that the kinase has alpha-helical HEAT repeats scattered throughout the polypeptide and distributed around the structure indicates that the DNA could also interact in various positions on the periphery of the kinase, which could result in activation of DNA-PK by DNA. These structural and biochemical studies indicate that DNA is in fact important for activating the kinase, probably through a direct interaction that involves threading of the DNA through the circular structure of DNA-PK.

### 1.4.3. DNA-PK activation: the role of protein interactions

While the role of DNA is crucial as the name applies, protein-protein interactions are also necessary for DNA-PK activation and are predominantly provided by the Ku heterodimer. Two regions of Ku were not observed in the crystal structure, the C-terminal regions (CTR) of Ku 80 and Ku 70. Ku 80 CTR is a region that has historically been shown to play an important role in DNA-PK activation. Kinetic analysis has shown that DNA-PKcs undergoes an extreme increase in activity when bound to a Ku-DNA complex as compared to just DNA alone, suggesting that a Ku-DNA-PKcs interaction is necessary for optimal activation of the enzyme. Interestingly, incubating DNA-PKcs with Ku molecules missing the CTR of Ku 80 results in significantly reduced DNA-PK kinase activity, and it has been revealed that only the last 12 amino acids of the region are required for an interaction with DNA-PKcs [38, 60]. While this region is difficult to crystallize because of the extreme flexibility it exhibits, solution based structural studies have shown that the CTR of Ku

16

80 contains a long flexible linker region with a cluster of six alpha helices that ends with the final 12 amino acid residues classified as highly disordered [40, 41].

Despite results revealing that the CTR of Ku 80 both physically interacts with DNA-PKcs and is needed for optimal kinase activity, it is still unclear if this region promotes activation through recruitment of DNA-PKcs to the DSB or through direct contact with the DNA-PKcs polypeptide to activate the kinsae. Intial *in vivo* studies showed that DNA-PKcs does not accumulate at DNA DSB in cells that are Ku 80 null, indicating that perhaps the CTR of Ku 80 is needed for recruitment of DNA-PKcs to the DSB [61]. Interestingly, studies also revealed that Ku 80 CTR truncations result in a level of radiosensitivity in cells that is similar to that seen with DNA-PKcs null cells, and this Ku 80 truncation mutant phenotype is postulated to be from lack of recruitment of DNA-PKcs to the site of a break. However, controversial and more recent *in vitro* and *in vivo* studies show that DNA-PKcs is recruited to the site of a DSB in the absence of the CTR of Ku 80 (but with the remaining heterotrimeric protein intact) [62]. These results indicate that deletion of the Ku 80 CTR does not disrupt recruitment of DNA-PKcs to a DNA terminus. Although Weterings et al. reported seeing only a 50 % decrease in kinase activation with mutant Ku that was missing the CTR of Ku 80, our lab has shown that DNA-PK kinase activity is severely inhibited by loss of the Ku 80 CTR, with kinase levels near background level when incubated with truncated Ku (Bennet et al., unpublished). This would indicate that while recruitment of DNA-PKcs to the site of DSB is not dependent on Ku 80 CTR, kinase activation, and therefore repair of DSB, is dependent on the Ku 80 CTR. Interestingly, new structural data suggests that the Ku

80 CTR extends considerably from the remainder of the Ku heterodimer, and is

attached to the core by the disordered, flexible region.  The flexibility coupled with

the distance of the c-terminal region afforded by the 30 residue linker from the core

suggests that region could easily recruit and then retain interaction with DNA-PKcs at

the site of a DSB.  It is also possible that this disordered region interacts with other

parts of the Ku molecule to induce a conformational change that could in turn activate

the kinase.  These possibilities raise the question of whether the CTR of Ku 80 is

responsible for DNA-PKcs recruitment, retainment, activation or potentially plays a

role in all three of these possibilities [63].  Clearly, further studies need to be done to

determine the exact role of Ku 80 CTR in DSB repair.

## 1.5.  Protein-protein interactions: synaptic complex of a DNA DSB

Successful repair of a DSB requires that the two ends of the DNA are brought

together to allow for ligation by Ligase 4/XRCC4/XLF.  Emerging data over the

years has indicated that NHEJ proteins must bind to DNA in order to bring the two

ends together into a synaptic complex to allow for the ligation reaction.  Ku and

DNA-PKcs are recognized as the first proteins to bind to the site of the damage and

may be responsible for the recruitment of other proteins in the pathway.  This leads to

the hypothesis that this protein complex could be responsible for bringing the two

ends of DNA together and maintaining them in a synaptic complex.  Furthermore, it

is possible that regions of microhomology at each DNA termini play a role in

efficient end-joining, but these ends must be held in close proximity to allow for

ligation.  A synaptic complex formation could provide the necessary stablization that

would keep complementary ends at each fragment within proximity to each other (Figure 3).

Many studies suggest that Ku, DNA-PKcs or the heterotrimeric complex (Ku and DNA-PKcs) play a crucial role in synapses of DNA ends. Atomic force microscopy revealed a complex of Ku and the two DNA ends of a linearized plasmid, suggesting that Ku holds the two termini together in a synaptic complex [64]. Data showing that Ku can transfer between two strands of DNA, whether they contain homologous or non-homologous sequence regions, also suggests that Ku is responsible for the juxtaposition of DNA ends [65, 66]. More recent electron microscopy as well as two-photon fluorescence cross-correlation spectroscopy has revealed that two DNA ends are in fact brought together by two DNA-PKcs molecules into a synaptic complex and biochemical analysis revealed that kinase activation occurs following synaptic formation of the complex [14, 67].

SAXS structural data suggests that both the DNA-PKcs and Ku play a role in stabilizing two DNA termini in a synaptic complex, as the Ku 80 CTR is made up of a dynamic arm that is significantly extended from the core of the molecule such that it could interact with a DNA-PKcs molecule across the synapses, and furthermore shows that DNA-PKcs can form head-to-head dimers [63]. The SAXS work shows that the dimensions coupled with the extreme flexibility of the C-terminus region of Ku 80 are ample enough to allow interactions with both the DNA-PKcs bound at the same DSB terminus, as well as across the DSB to a DNA-PKcs molecule bound to the opposing terminus, contacting the molecule in a *trans* fashion [63].
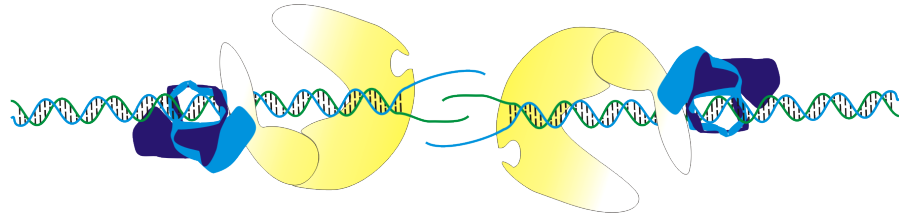
**Figure 3. DNA-PK synaptic complex.** DNA threads through the ring-like structure of the Ku heterodimer (depicted in blue) and through a channel in DNA-PKcs (depicted in yellow). Following threading of the DNA, strand separation occurs, and DNA-DNA, protein-DNA and protein-protein interactions may all play a role in bringing the two DNA-PK molecules bound to each DNA terminus into a synaptic complex.

This would suggest that the CTR of Ku 80 indeed is responsible for retaining DNA-PKcs at the site of break, perhaps through a tethering mechanism that retains the kinase in a synaptic complex at the DSB site. Recent biochemical data from our laboratory and structural SAXS data also suggest that the CTR of Ku 80 can form a dimer. Our lab generated the 16 kDa Ku 80 C-terminus fragment indicated to be important for DNA-PK activation, and cross-linking data shows a homodimer being formed with this mutant protein. SAXS data suggests that the Ku 80 CTR can interact with the remainder of the Ku polypeptide in a total of five possible different possible positions [63]. This Ku80 CTR homodimerization may facilitate tethering of the two DNA termini at a DSB to enhance synaptic complex formation and end-joining activity (Figure 4). These results all suggest that protein-protein interactions, at least in part, play a role in formation of a synaptic complex for joining of the two DNA termini at the site of a DSB. The role of protein-DNA interactions in formation of a synaptic complex will be discussed in Chapter 3.

## 1.6.  DNA-PK phosphorylation targets

As it appears that the main role of active DNA-PK is in NHEJ, considerable work has been done to map DNA-PK dependent phosphorylation sites of the core NHEJ protein machinery and uncover the *in vivo* relevance of these phosphorylation events. Many of the original NHEJ investigators believed that DNA-PK phosphorylation of downstream components in the pathway was important for both recruitment to the DSB and subsequent activation of the key NHEJ proteins.
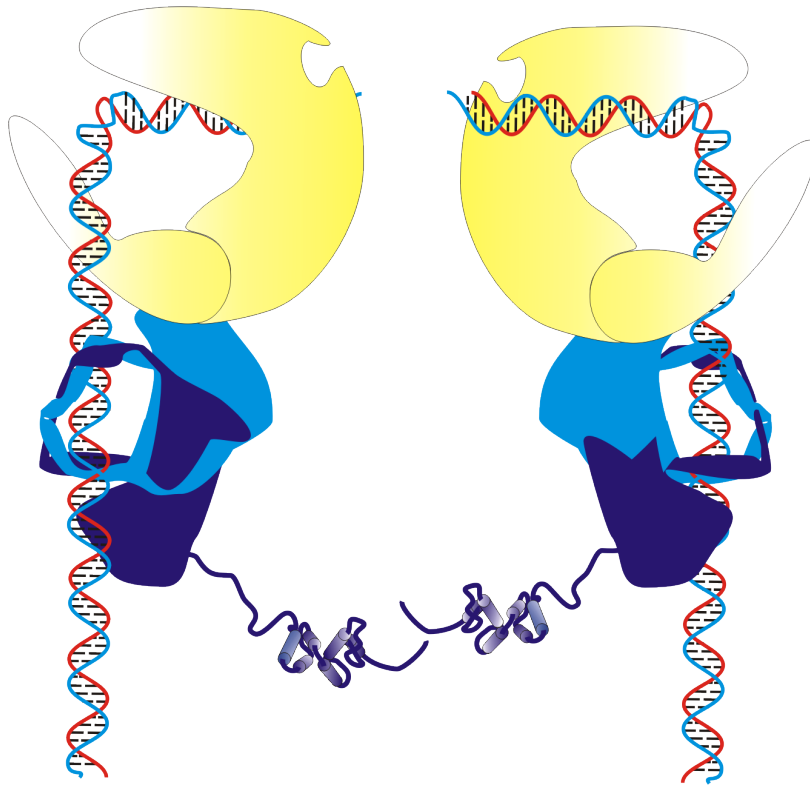
**Figure 4. Ku 80 C-term interactions.** The Ku 80 CTR (depicted in dark blue and extending out from the Ku molecule) is a highly flexible region with a cluster of six α-helical repeats at the terminus. Ku 80 CTR can interact with regions of the Ku heterodimer including itself, and this CTR-CTR interaction may promote synaptic complex formation. Interactions between Ku 80 CTR and DNA-PKcs can also occur and may also play a role in synapsis of the DNA termini.

*In vitro* and *in vivo* studies of the key players revealed very few physiologically

relevant phosphorylation sites. Work done with XLF, a ligation stimulating factor in

NHEJ, revealed two serine DNA-PK phosphorylation sites, but mutation of these

residues to alanine did not appear to have any effect on DNA binding, recruitment to

a DNA DSB, or IR sensitivity [68]. While it appears that assembly of DNA-PK on

DNA ends plays a role in recruitment of the XRCC4-ligase 4 complex to the site of a

DSB, no phosphorylation sites within the XRCC4-ligase 4 have been identified as

necessary for recruitment [69]. It is possible that another DNA-PK dependent

phosphorylation event, like autophosphorylation (further discussed below) is

important for recruitment of the ligase complex. Two residues were identified *in*

*vitro* within ligase 4 as potential DNA-PK phosphorylation sites, but again, these sites

did not have an effect on the ligase's end-joining activity [70]. As Ku is one of the

first proteins to bind to and make direct contact with DNA at the site of a DSB, as

well as form a heterotrimeric complex via a direct interaction with DNA-PKcs, it is

rational that Ku is phosphorylated by DNA-PK [38, 60]. One phosphorylation site

was identified in the N-terminus of Ku 70 and three were identified in the C-terminus

of Ku80, a region that is important for the kinase activity of DNA-PK [71].

However, further analysis revealed that while these residues are phosphorylated *in*

*vitro,* DNA-PK is not required for *in vivo* phosphorylation of Ku nor is

phosphorylation of these Ku residues required for NHEJ [72].

*1.6.1. DNA-PK autophosphorylation*

Of the multiple protein substrates identified *in vitro* as DNA-PK

phosphorylation targets, only two proteins within the NHEJ pathway have functional

*in vivo* roles upon phosphorylation by DNA-PK. Artemis, a DNA nuclease implicated in end processing in the NHEJ pathway, gains endonucleolytic activity on DNA substrates following DNA-PK phosphorylation [73, 74]. This enzyme is discussed in greater detail. The other DNA-PK dependent phosphorylation substrate that has been shown to shown to have *in vivo* relevance is DNA-PK itself. Early studies with DNA-PK revealed that autophosphorylation of the kinase resulted in decreased kinase activity [75], and this reduction in activity was attributed to dissociation of the DNA-PK catalytic subunit from the Ku and DNA bound complex, or the "active" complex. These studies demonstrate the dynamic complex that forms at a DNA DSB, and reveals a physiological role for DNA-PK autophosphorylation [75, 76]. Further experiments mapped the autophosphorylation sites within DNA-PKcs and initially identified a cluster of six sites within residues 2609-2647 [77]. Interestingly, mutational analysis of these residues revealed that autophosphorylation of any one of the sites alone is not necessary for NHEJ as determined by radiosensitivity assays. However, when all six of the serine or threonine residues were mutated to alanine (dubbed the ABCDE mutant), cells displayed similar high levels of radiosensitivity as cells that were DNA-PKcs null [76]. When this cluster was mutated, repair of IR-induced DSB was reduced [78]. These studies further demonstrate the importance of DNA-PK autophosphorylation *in vivo*. Several more autophosphorylation sites have been identified, and to date the ABCDE mutant and the PQR mutant [78, 79] are the clusters that appear to be the most biologically relevant. Interestingly, each of these mutant clusters display severe radiosensitivity, yet the mutant DNA-PK still maintains full kinase activity and can associate with and

dissociate from DNA DSB. The major defect exhibited by the two mutants described is a disruption in DNA end processing during NHEJ. Further studies have shown that autophosphorylation at the ABCDCE sites renders DNA termini accessible for end processing, but not by DNA-PK dissociation. Instead, it is proposed that following autophosphorylation of ABCDE, DNA-PK remains bound but undergoes a conformational change so that DNA ends are now made accessible to end processing factors and the ligase complex, and DNA-PK remains in position on the DNA termini to support a synaptic complex (discussed later in this chapter). This signifies that a major role of DNA-PK in NHEJ involves regulation of end processing and formation of a synaptic complex to drive repair of the DSB [80, 81]. This model is further supported by recent evidence showing that autophosphorylation of DNA-PKcs occurs in *trans*, both *in vitro* and *in vivo* [82]. This indicates that a synaptic complex is formed, thus allowing for *trans* autophosphorylation between two DNA-PK molecules located at each termini of the DNA DSB. Furthermore, this synaptic complex could protect ends from processing until autophosphorylation occurs and alters the complex formation, liberating ends for processing [83]. Recent *in vivo* photobleaching studies [61] and *in vitro* structural data support the model that autophosphorylation does render DNA termini accessible for processing, and this occurs because of a conformational change in DNA-PKcs following autophosphorylation. Small angle X-ray scattering (SAXS) data revealed major conformational changes throughout the DNA-PKcs structure, including an opening up of the head and palm regions that have previously been postulated to encircle the DNA. This structural change not only releases DNA termini for processing, but most

25

likely results in dissociation of DNA-PKcs from the DNA [63]. While additional work is needed to fully understand the mechanism of DNA-PKcs dissociation and clearly define the residues involved, it is clear that DNA-PK autophosphorylation plays two important roles, one involved in DNA termini accessibility and the other in dissociation.

## 1.7. End processing events

Once the DNA termini have been recognized, bound, and stabilized by the DNA-PK heterotrimeric complex, processing of the DNA ends needs to occur to remove DNA discontinuities that would interfere with ligation needs to occur. As mentioned earlier, DNA DSB induced by IR can be very complex, and a variety of DNA terminal structures can occur from one DSB to another. Depending on the complexity of the DNA discontinuity, an assortment of different processing enzymes is required to remove DNA damage at the site of the break to allow for ligation. It has also been shown that nucleotide processing (typically 1-4 NT) can occur at a DNA terminus to reveal regions of complementary at the DNA ends, and NHEJ can then proceed through annealing of these regions [84]. Enzymes implicated in DNA processing, include but are not limited to, FEN-1 [85], polynucleotide kinase (PNK) [86], Werner protein [87, 88], MRN [89], DNA polymerase $\mu$ and $\lambda$ [16], and the nuclease Artemis [74].

### 1.7.1. Family X polymerases

A DSB induced by IR frequently has non-complementary ends that need to be joined by NHEJ, and this step can require polymerases to fill in single-strand overhang regions or gaps. Of the four X family of polymerases, pol $\mu$, DNA pol $\lambda$

26

and TdT have been implicated in NHEJ [19, 90, 91]. All have a BRCT domain in the N-terminus that is responsible for protein-protein interactions that aid in recognizing and repairing a DNA DSB, but TdT has been implicated in only playing a role in V(D)J initiated NHEJ, while pol μ and pol λ are thought to play a role in overall NHEJ [92]. Pol λ and pol μ are thought to be recruited to the site of DSB by Ku via an interaction with pol λ BRCT domain [93]. Pol λ was shown to preferentially fill in sequences at a 5' overhang terminal structure generally in a template dependent fashion, thus requiring complementary ends, or regions of microhomology, at either end of the break [94, 95]. Like pol λ, pol μ has been indicated to play a role in DNA end processing during NHEJ. However, its mechanistic role varies from pol λ, as it can support NHEJ of DNA ends with non-complementary sequences by initiating nucleotide synthesis from a 3' overhang on one DNA using a noncomplementary overhang 3' end on the opposite strand as a template [96]. Pol μ has also been shown to add nucleotides in a template-independent manner, with nucleotides being added at the terminus by terminal transferase activity [97, 98]. This polymerization step creates a region at the site of a break that now has microhomology that can be annealed and ligated together by the remaining NHEJ machinery (Ligase IV, XRCC4 and XLF).

### 1.7.2. Artemis

The 78 kDa nuclease, Artemis is known to be responsible for cleaving hair-pins generated during V(D)J recombination. More recently, Artemis has been shown to be play a role in NHEJ repair of IR induced DNA DSB. The role of Artemis in NHEJ is based on *in vivo* data showing that Artemis null cells are more sensitive to

27

IR than wild type counterparts [18]. Artemis has been found to possess 5'-3'
exonucleolytic activity on single-strand DNA, DNA-PK and ATP dependent
endonuclease activity on DNA hairpin structures, and DNA-PK and ATP dependent
endonuclease processing of 3' and 5' single-strand overhangs, with preferential
cleavage at the dsDNA/ssDNA junction [74]. Artemis has also been shown to
remove 3' phosphoglycolate groups from DNA termini, like those generated by IR
[99].

Artemis is a member of the β-CASP family, a new group of the metallo-β-
lactamase fold superfamily made up of enzymes acting on nucleic acids [100, 101].
All β-CASP family members studied to date are enzymes that process nucleic acids
and have two major structural domains, the metallo-β-lactamase domain and the β-
CASP domain (which is embedded in the metallo-β-lactamse domain). Artemis also
has an extended C-terminal region following the β-CASP domain, which appears to
be fairly disordered (unpublished PONDR data). The metallo-β-lactamase domain is
made up of a four-layered β-sandwich that is flanked by α-helices, with zinc
coordination sites located in the sandwich region [102]. Artemis, as a DNA nuclease,
hydrolyses the phosphodiester backbone of DNA, and recent work has revealed a
histidine residue within the β-CASP domain that is critical for the catalytic activity of
Artemis (*in vitro* and *in vivo*) [103]. Higher resolution structural data is needed for a
greater understanding of how this enzyme is activated and regulated, but extensive
biochemical analysis has answered some questions regarding Artemis nuclease
activity.

Artemis has been shown to be phosphorylated by DNA-PK *in vitro* [73] and

*in vivo* [104]. It has been suggested that the stimulation of endonuclease activity of

Artemis requires binding and phosphorylation by DNA-PK which causes a

conformational change in the C-terminal region of Artemis, resulting in relief of

Artemis autoinihibition of the endonuclease active site [73]. DNA-PKcs-mediated

phosphorylation of Artemis has also been suggested to be necessary for Artemis to

retain association with DNA-PK/DNA complex at the site of the break [105]. Other

laboratories suggested that autophosophorylation of DNA-PK results in a

conformational change in the DNA-bound kinase which in turn alters the

conformation of DNA such that it can be easily recognized and cleaved by Artemis

[106, 107]. While each model differs slightly in mechanism, both models suggest

that Artemis endonuclease activity is DNA-PK and ATP dependent. However, many

questions remain regarding DNA-PK dependent Artemis endonuclease activity.

The specifics of DNA cleavage by Artemis have yet to be fully elucidated. It

appears that *in vitro*, DNA-PK dependent Artemis endonuclease activity

preferentially cleaves single-strand overhang DNA around the SS/DS junction on

synthetic oligonucleotide substrate. Biochemical studies performed with DNA

substrates containing a 21 basepair double-strand region with a 15 base 5' single-

strand overhang result in endonuclease cleavage at the SS/DS DNA junction,

generating a 15 base single-strand cleavage product (and a blunt double-strand

product). Paradoxically, Lees-Miller and colleagues report that a similar substrate (25

basepair double-strand substrate with a 15 base 5' single-strand overhang) resulted in

24 and 26 nucleotide excision fragments, indicating that DNA-PK dependendent

Artemis activity can cleave DNA at the n+1 and n-1 positions at the SS/DS junction [106]. 3' overhang substrates (21 basepairs of double-strand DNA with a 15 base single-strand overhang) are preferentially cleaved in the SS region, reducing the 15 base overhang to a 4 to 5 single-strand overhang [74]. According to Yannone and Povirk, single-strand overhang length impacts the cleavage position on 3' overhangs, with longer single-strand overhangs (15 base and 13 base) trimmed to leave a 5 base overhang while a 9 base overhang was trimmed to a 4 base overhang [99]. This group also observed endonuclease activity on plasmid substrates, albeit somewhat decreased compared to longer substrates, with 4, 5 and 6 base overhangs, resulting in 2-4 base cleavage products. Detailed biochemical studies with purified Artemis and DNA-PK further suggest that in the presence of active DNA-PK, Artemis can make small endonuclease cleavage products, or "trim", DNA termini on both the 3' and 5' strand. The authors point out that this versatile activity of Artemis would allow the enzyme to process a variety of DNA structures and chemistries that might exist at a DSB, priming the break site for polymerase-mediated extension and ultimate ligation of the DSB [107]. Artemis has also recently been shown to possesses DNA-PK dependent endonuclease activity on single-strand DNA, with a sequence preference favoring cleavage of thymidines [108]. Despite the details known regarding DNA-PK dependent Artemis cleavage, further studies must be conducted to understand the molecular mechanism of DNA processing by Artemis.

IR induced DNA DSB are complicated and can vary in many different ways at each break site, with the potential for one terminus of the DSB to have a different DNA structure than the opposite terminus. As research progresses in the NHEJ field,

it becomes more evident that there are many proteins involved in the processing of this large variety of damage found at the DNA DSB. With the variety of proteins, including polymerases, nucleases and kinases, it is becoming apparent that the processing steps are not adequately accomplished by just one protein. Rather, it is likely that not every DNA DSB is processed the same way, and that only a subset of the processing proteins are required to repair any individual break. It is not known how the correct protein needed to process a specific DNA discontinuity at the terminus is recruited. However, it is clear that this is a dynamic and complicated process that is likely to involve a variety of proteins, some of which may not yet have been identified.

## 2. Materials and Methods

### 2.1. DNA effector preparation for DNA-PK kinase assays

Single-strand oligonucleotides were purchased from Integrated DNA Technology (IDT, Coralville, IA). Oligonucleotides were synthesized with a 5'-biotin molecule by IDT, as indicated. The single-strand oligonucleotides were gel-purified by preparative denaturing 15 % polyacrylamide gel electrophoresis. Following separation by electrophoresis, oligonucleotides were visualized by UV light shadowing, excised from gel and eluted overnight 3 mL in elution buffer at 4ºC (0.3M NaOAc, 1 mM EDTA and 0.1 % SDS). Following elution, solution was filtered through a sterile syringe filter to remove gel pieces. DNA-containing solution was precipitated by addition of 9 mL of 100 % pure ethanol and 10 µg glycogen and incubated for one hour at -80ºC. Following incubation, samples were centrifuged at 10,000 x $g$ for 30 minutes. Pelleted DNA was resuspended in sterile water and DNA was quantified by absorbance reading at 260 nm. DNA substrates were annealed to complementary oligonucleotides at a 1:1 ratio.

Oligonucleotides for Chapter 3 were annealed as follows. The 24-bp full duplex DNA effector was created by annealing 3'24 to 5'24, and the 30-bp full duplex DNA created by annealing oligonucleotides 3'30 and 5'30. The two Y-shaped effectors were prepared by annealing 3'24+6 to 5'30 and 3'30 to 5'24+6. The 3' overhang effector was prepared by annealing oligonucleotide 3'30 to 5'24. To prepare effectors with 3' overhangs for microhomology studies oligonucleotide 3'24+6T, 3'24+6A or 3'24+6mix were annealed to 5'24 to make the 3' overhang effectors containing homopolymeric T's, A's or with compatible sequences

respectively.  Additionally, the 3'24 oligonucleotide was annealed to 5'30 to make

the 5' overhang effector, and 3'24 was annealed 5'24+6T or 5'24+6A to make the 5'

overhang effectors for microhomology studies.  Sequences of the above DNA

substrates can be found in Table 1.  Duplex DNA was gel-purified by native

polyacrylamide gel electrophoresis to ensure homogeneity, eluted from gel,

precipitated and quantified.  DNA-PK was purified from HeLa cells, and a series of

titrations of both DNA and DNA-PK were performed to determine the appropriate

concentrations to use in kinase assays to accurately assess binding and activation.

## 2.2.  DNA substrate preparation for nuclease assays and mobility gel-shift

Single-strand oligonucleotides from IDT were gel-purified as described

above.  To generate 5' radiolabeled substrates, single-strand oligonucleotides were

incubated with T4 polynucleotide kinase (New England Biolabs), T4 PNK buffer (70

mM Tris-HCl, 10 mM $MgCl_2$, 5 mM Dithiothreitol) and 15 pmol of $[\gamma\text{-}^{32}P]$ ATP

(Perkin Elmer) for 30 minutes at 37ºC.  1 nmol of ATP was added to the reaction for

the last five minutes of incubation to ensure phosphate incorporation into every DNA

molecule.  The reaction was stopped with the addition of 100 mM EDTA and final

volume of reactions was brought up to 50 µL with water.  Residual $[\gamma\text{-}^{32}P]$ ATP not

incorporated into DNA was removed by separation of reaction mix over 300 µL

Sephadex G-50 spin columns.  Radiolabeled DNA oligonucleotides were annealed to

complement and gel purified as described above.  To generate 3' radiolabeled DNA

substrates, single-strand complementary oligonucleotides were annealed and

incubated with $[\alpha\text{-}^{32}P]$ dCTP and Klenow (exo$^-$) fragment for 30 minutes at 37ºC.

Reactions were stopped with the addition of 100 mM EDTA and gel purified as described above.

## 2.3. Protein purification of DNA-PK

Cell free extracts were prepared from 12 L of HeLa cells grown in DMEM supplemented with 10 % Fetal Bovine Serum to $1 \times 10^6$ cells/mL. To prepare extracts, cells were pelleted at 4,000xG for 10 minutes, washed in cold 1x PBS and repelleted. Pellet was resuspended in 20 mL of hypotonic buffer (10 mM Tris-HCl pH 8.0, 1 mM EDTA, 5 mM DTT) and incubated on ice for 20 minutes. Protease inhibitors were added (0.5 mM PMSF and 1 µg/mL each leupeptin and pepstatin) and cells were subjected to 20 strokes of Dounce homogenization. 20 mL of high salt buffer (50 mM Tris-HCl pH 8.0, 10 mM $MgCl_2$, 2 mM DTT, 25 % sucrose and 50 % glycerol) was added 1 mL at a time while stirring extract at 4ºC. 3 mL of saturated AMS was added 1 mL at a time while stirring, and then sample was stirred for an additional 30 minutes at 4ºC. The sample was sedimented at 30,000 x $g$ for one hour at 4ºC and the supernatant was dialyzed overnight against 3 x 1 Liter buffer changes in 10 mM Tris-HCl pH 7.5, 1 mM EDTA, 10 % glycerol and 1 mM DTT (Buffer A) with the addition of 100 mM KCl. Following dialysis, sample was sedimented at 3,000 x $g$ to remove any residual debris and applied at 3 mL/min to a 30 mL sepharose column with double-strand DNA conjugated to it to fractionate protein. The column was washed with 50 mL of Buffer A and bound protein was eluted with Buffer A containing 500 mM KCl. The 5 mL elution fractions were screened for protein using Bradford reagent and a DNA-PK kinase assay was done on the fractions with protein to ensure that they contained DNA-PK. Fractions containing an absorbance greater

34

than 50 % of the maximal absorbance and kinase activity were pooled and dialyzed overnight against Buffer A with 100 mM KCl.  Following dialysis, the remaining sample was further fractionated by chromatography at a flow-rate of 3 mL/min on a 10 mL Heparin column.  The column was washed in Buffer A with 100 mM KCl and bound protein was eluted with a 50 mL linear gradient from 100 mM KCl to 0.6 mM KCl.  The 3 mL fractions were assayed for total protein by Bradford, DNA-PK kinase activity, and Ku binding activity by electrophoretic mobility shift assay (EMSA). Pooled fractions were dialyzed overnight against Buffer A with 100 mM KCl and applied to a 2 mL Q-sepharose ion exchange column at a flow-rate of 1 mL/min.  The column was washed with 10 mL of Buffer A-100 mM KCl and bound protein was eluted with a 20 mL linear gradient from 100 mM KCl to 1.0 M KCl.  The 1 mL fractions were assayed for total protein by Bradford and SDS-PAGE analysis, DNA-PK kinase activity, and Ku binding activity by electrophoretic mobility shift assay (EMSA).  Pooled fractions were dialyzed overnight against Buffer A with 200 mM KCl and 20 % glycerol and aliquots were frozen at -80ºC.

## 2.4.  SDS-PAGE and western blot analysis

Protein samples were separated by SDS-PAGE and either stained with Coomassie Blue or transferred to Immobilon-FL membranes (Millipore, Bedford, MA), probed and then visualized using chemiluminescent detection, and the LAS-3000 imaging system (FujiFilm) was used to document and quantify blots.  $[His]_6$-Artemis was detected in immunoblots using either a monoclonal antibody against the N-terminal $[His]_6$ fusion tag, anti-xpress, (Invitrogen) or a polyclonal antibody

directed against the full length of Artemis (Bethyl Laboratories, Montgomery, TX).

DNA-PKcs was detected using a polyclonal antibody against DNA-PKcs (Abcam).

## 2.5.  Electrophoretic mobility shift assays (EMSA)

EMSAs were performed in 20 µL reactions containing 50 mM NaCl, 10 mM

Tris-HCl pH 7.9, 10 mM $MgCl_2$, 1mM DTT, 100 fmol of 5' radiolabeled double-

strand 30mer DNA substrate (JTILH2.1/JTILH2.2, see Table 1) and 2 µL of each

fraction from a DNA-PK prep.  Protein samples were incubated with DNA for 5

minutes at room temperature.  Separation was performed on a 6 % non-denaturing

polyacrylamide gel, vacuum dried and visualized using PhosphorImager analysis.

## 2.6.  DNA-PK kinase assays

Kinase assays containing a single effector per reaction were performed at 37º

C in a final volume of 20 µl containing 20 mM HEPES, pH 7.5, 8 mM $MgCl_2$, 1 mM

DTT, 5 % glycerol, 125 µM ATP, $[\gamma\text{-}^{32}P]$ ATP (0.5µCi), 6.3 nM DNA-PK, 5 nM

DNA, and 500 µM p53 synthetic peptide.  Taking into account the buffer in which the

DNA-PK preparations were dialyzed, the final KCl concentration of the reactions

ranged from 20 mM to 70 mM.   In addition, to determine the effect of ionic strength,

a series of DNA-PK activation experiments were performed at varying KCl

concentrations and the results demonstrated no significant effect over the range of

concentrations tested (Supplementary Data).  Biotinylated duplex DNA was

incubated with 1 ng Streptavidin (SA) / fmol DNA and incubated on ice for 5 min.

DNA-PK and reaction buffer containing peptide were added to DNA and incubated

on ice for 5 min.  Reactions were initiated with addition of ATP, incubated at 37ºC

for 15 or 30 min, as indicated, and terminated by addition of 20 µl of 30 % acetic

acid. Reactions products were spotted on P81 phosphocellulose filter paper. The paper was washed five times, 5 min. each, in 15 % acetic acid, once in 100 % methanol and allowed to dry. Samples were quantified by PhosphorImager® analysis using ImageQuant software (Molecular Dynamics). Each DNA effector used in the assays to analyze dimeric activation was bound with SA then DNA-PK was added to the DNA and allowed to incubate for 5 min, on ice. Each effector was then added alone to a tube or mixed with the complementary pre-bound effector and allowed to incubate on ice for 5 min. Reaction buffer and peptide were then added to the DNA-DNA-PK mix, the reaction was initiated with ATP and the assay was completed as described above.

## 2.7. DNA-PK autophosphorylation assay

Kinase assays were performed as described above with the following modifications. Reactions contained 20 nM DNA-PK and 1.0 μCi [γ-$^{32}$P] ATP. Where indicated, reactions were performed in a time-dependent manner. Reactions were terminated with addition of SDS buffer and loaded onto an 8 % SDS-PAGE gel. Following electrophoresis, the gel was dried and visualized by PhosphorImager® analysis.

## 2.8. DNA-PK pull down assay

DNA synaptic complex formation was determined by incubating 500 fmol of each biotinylated DNA effector with 10 µL slurry of Streptavidin magnetic beads (Promega) in 500 µL of 10 mM Tris-pH 7.5, 1 mM EDTA, 5 % glycerol, and 0.1 % BSA for 30 minutes to allow for binding to occur. SA-DNA magnetic beads were washed three times to remove excess DNA. DNA-PK was bound to the SA- DNA as

well as to a non-biotinylated DNA effector with a [γ-$^{32}$P] ATP 5' label in a 20 μl

reaction containing 20 mM HEPES, pH 7.5, 8 mM MgCl$_2$, 1 mM DTT, and 5 %

glycerol.  Following a 5 minute incubation period, the DNA-PK-5' labeled DNA

effector complex was added to the SA-DNA-DNA-PK bead mixture and allowed to

incubate at room temperature for an additional 5 minutes.  The beads were collected

in a magnetic separator and the supernatant was removed, beads were gently washed

two times in reaction buffer, and the bound DNA quantified via scintillation counting.

## 2.9.  Cloning and production of [His]$_6$-Artemis

### 2.9.1.  Polymerase Chain Reaction (PCR)

The Artemis gene was amplified via PCR from a B-cell cDNA library using

primers specifically designed to encompass the entire gene, 2220 basepairs.  PCR

primers were synthesized by IDT with the following sequences;

CCCAACCAGGTTATTTGAACATTTT (antisense) and

GTCCCGGACTCTGGGATCGG (sense).  PCR reactions were performed in 20 μL

containing 100 pmol of each primer, 500 μM dNTPS, 2 units Deep Vent DNA

polymerase (NEB), 2 mM MgSO$_4$ and 10 ng of cDNA.  Following initial

denaturation for five minutes at 94ºC the reactions were subjected to 25 three-step

cycles consisting of 30 seconds at 94ºC, 30 seconds at 62ºC and 2 minutes at 72ºC.  A

final incubation at 72ºC. was performed to fully extend the PCR products.  The DNA

product was separated on a 0.8 %  low-melting point agarose gel and bands were

excised.

The gel-purfied PCR product was cloned into a BLUNT-TOPO-II vector

(Invitrogen) to create the pCR-Blunt-Artemis construct.  In-gel ligation was done by

melting agarose plug containing PCR product at 65ºC.  5 µL of melted agarose PCR

product was brought to final reaction mix of 20 µL with 100 ng of TOPO vector, 3

units T4 DNA Ligase (NEB), 10 mM $MgCl_2$ and 1 mM ATP.  This reaction was

incubated overnight at 15ºC.  Following incubation, ligated products were

transformed into bacteria by reheating the ligation products at 65 ºC for five minutes

and adding 5 µL of this mix to 200 µL completent XL-1 Blue *E. coli* cells

(Stratagene).  Tubes were placed on ice for 10 minutes, heat shocked at 42ºC for 2

minutes.  Following heat shock, 1 mL of LB media was immediately added to the

reaction tube and reactions underwent shaking at 250 rpm for 1 hour at 37ºC.

Transformed *E. coli* was spread on agar plates containing 200 µg/mL Ampicillin and

incubated overnight at 37ºC.  Colonies were selected from plates, expanded in LB

media and plasmid DNA purified using Qiagen mini-prep spin column.  Restriction

enzyme analysis was performed to ensure proper insertion of Artemis gene into the

TOPO vector.  Following verification, the Artemis gene was excised from the TOPO

vector with Xba I and was filled in with Sequenase and dNTP's to create a blunt end

at the XbaI site and then further digested with KpnI.  The fragment was then gel

purified and cloned into the pRSETC vector (Invitrogen) to incorporate an N-terminal

$His_6$ tag.  The $His_6$-tagged Artemis gene was excised using Xba I and Not I, and

cloned into the pBacPAK8 vector (Clontech) to create BacPAK8-Art-His.

Sequencing analysis verified the insert sequence.

## 2.9.3. *Baculovirus production*

The BacPAK8-Art-His construct was transfected into SF9 insect cells in conjunction with *Bsu*36I-digested BacPAK6 viral DNA to generate recombinant baculovirus. All baculovirus methods take place at room temperature, including growing of SF9 cells, unless otherwise mentioned. Briefly, 2 mL of SF9 insect cells at $5 \times 10^5$ cells/mL in complete Grace's insect media (Clontech) supplemented with 10 % FBS were placed in a 35 mm tissue culture dish and allowed to adhere for one hour at room temperature. Once attached, the cells were washed with PBS and placed in 2 mL of media containing no FBS (basic media) for 30 minutes. During this incubation time, 500 ng of BacPAK8-Art-His was incubated with 5 µL of pBacPAK 6 that had been digested Bsu36I (provided by Clontech kit) in a final volume of 96 µL. 4 µL of the transfection agent Bacfectin (Clontech) was added to the mix and incubated for 15 minutes. Basic media was removed from adherent cells and the total volume of transfection mixture was slowly added to the adherent cells and incubated for 5 hours. Following incubation, 1.5 mL of complete media was added to the dish and the plate was incubated for 72 hours. After 72 hours the media, which contains viruses produced by the transfected cells, was removed and saved in a sterile tube.

The supernatant removed from the cells described above contains your target virus, but often it will contain a mixture of other viruses as well. To isolate recombinant viruses, a plaque purification assay was completed. Serial dilutions of the virus were made to give final dilutions of $10^{-1}$ to $10^{-3}$. 6-well dishes with $1 \times 10^6$ SF9 insect cells plated on them were infected with these dilutions. To accomplish this, media was removed from the cells and 200 µL of virus dilutions were added to

each dish and carefully placed to incubate for one hour in a location that will not

disturb the small amount of liquid on the plate. 4 % sterile low melting agarose was

melted during this incubation and mixed with warm Grace's media to generate a 1 %

agarose solution. Following viral incubation on cells, the inoculum was removed and

1.5 mL of the warm agarose/media solution was added to the cells and allowed to set

until firm. 1.5 mL of media was then added on top of the agarose layer and the cells

were incubated for 5 days. Following incubation, media was removed and 1 mL of

0.03 % neutral red dye (diluted in sterile 1x PBS) was added on top of the agarose

and allowed to soak into agarose for 1 hour. The dye was then removed, plates were

inverted and stored overnight in the dark to allow for plaques to "clear". Areas of

cells that have died due to viral infection will appear as clear spots in red dye.

Following clearing, plaques appeaing as clear areas were picked using glass Pasteur

pipettes and resuspended in 1 mL of media. Viruses were allowed to diffuse out

overnight, and the resulting supernatant was called the plaque purified primary virus.

This plaque purified virus can now be amplified to generate a passage one (P1) stock

by adding it to $5x10^5$ SF9 cells on 6-well dishes, allowing to incubate for five days

and removing supernatant that is now the P1 virus. To screen this virus and ensure

that it is producing the His-Artemis gene, infected cells that P1 was removed from

were scraped off of plates into 500 µL of 1x SDS loading buffer and western blot

analysis was done on these samples as described above using anti-artemis to

determine if the virus produced was accurate. As western blot analysis revealed the

presence of Artemis in the infected cells, the P1 was further amplified into a P2 virus

by infecting 50 mL of SF9 cells at $5x10^5$ cells/mL with 50 µL of P1 virus and

incubating for 5 days.  Cells were pelleted and supernatant was saved as P2.  A

plaque assay was done to determine the viral titer on the P2 virus.  Briefly, plaque

assays to titer virus are done as described above except plaques (clear spots following

addition of red dye to plates) are counted.  The following equation is used to

determine titers.

Titer (pfu/mL) = (# of plaques * 5) / dilution factor

# of plaque is multiplied by 5 because only 200 µL of a viral dilution was used in this

assay and the equation calls for a titer in mL.

One amplification of P2 produced 25 plaques a plate with a virus dilution of $10^{-5}$:

(25*5) / .00001 = 1.25 x $10^7$ pfu/ml

Following determination of the P2, the P2 virus was amplified to create a P3.  The

following equation is used to determine how much virus to infect cells with.  An MOI

of 0.1 is needed to amplify virus.

(MOI) * (# of cells) / viral titer = ml of virus to use

 100 mL of SF9 cells at 5x$10^5$ cells/mL were infected with 400 µL of P2 virus to

generate a P3 virus.  The P3 virus was subsequently titered and a titer of 1x$10^8$

pfu/mL was determined.

## 2.10.  Protein expression and purification of [His]$_6$-Artemis

200 mL of SF9 cells at 1x$10^6$ cells/mL were infected with P3 baculovirus at an

MOI of 10, driving expression of the [His]$_6$-Artemis protein for 48 hours.  Infected

cells were sedimented at 4,000 x g at 4ºC for 15 min and washed once in PBS,

repelleted and resuspended in buffer P50/10 (50 mM KPi, pH 7.85, 10mM KCl, 10 %

glycerol, 5 mM imidazole).  All buffers used in protein purification were

supplemented with protease inhibitors (0.5 mM PMSF and 1 µg/mL each leupeptin and pepstatin). Cells were lysed by Dounce homogenization and sonication, and extract was sedimented at 10,000 x $g$ at 4°C for 30 minutes. The supernatant was retrieved, and KCl was added to adjust the salt concentration to 500 mM KCl. The high-salt extract was batch adsorbed to 10 mL of Phosphocellulose matrix equilibrated in buffer P50/500 (50 mM KPi, pH 7.85, 500 mM KCl, 10 % glycerol, 5 mM imidazole). The matrix and cell extract slurry was applied to a 30 mL syringe with a frit at the bottom of it and the flow-through was collected and immediately applied at a flow rate of 0.3 mL/min to a 2 mL Nickel-agarose column equilibrated in the same buffer. The flow-through material was re-applied and the column subsequently washed with 20 mL buffer P50/500 followed by a 20 mL wash with P50/10. Bound protein was eluted in P50/10 with 200 mM imidazole. The 0.5 mL fractions were collected and screened for protein using Bradford reagent. Fractions containing an absorbance greater than 50 % of the maximal absorbance were pooled and dialyzed overnight against buffer P10/200 (10 mM KPi, pH 7.85, 200 mM KCl, 10 % glycerol, 2 mM DTT). A portion of protein pooled from the Nickel-agarose column was dialyzed overnight against Buffer A (50 mM Tris, pH 7.5, 200 mM KCl, 20 % glycerol, 1 mM DTT), aliquoted and stored directly at -80° C. Following dialysis, the remaining sample was further fractionated by chromatography at a flow-rate of 1 mL/min on a 5mL CHT-Hydroxyapatite (HAP) column (Biorad) equilibrated in buffer P10/200. The column was washed with buffer P10/200 and bound protein was eluted with a 25 mL linear gradient from 10 mM KPi to 500 mM KPi. All of the 1 mL fractions were assayed for total protein and screened for

exonuclease activity.  Pooled fractions were dialyzed overnight against Buffer A and frozen at -80º C.

## 2.11.  DNA-PK phosphorylation of Artemis

To assay phosphorylation status of Artemis by DNA-PK, kinase assays were performed at 37ºC in a final volume of 20 µL containing 50 mM HEPES, pH 7.5, 100 mM KCl, 10 mM $MgCl_2$, 0.2 mM EGTA, 0.1 mM EDTA, 1 mM DTT, 125 µM ATP, $[\gamma\text{-}^{32}P]$-ATP (1.0 µCi), 100 nM 30-bp full duplex DNA, 60 nM DNA-PK and varying concentrations of $[His_6]$-Artemis, as indicated.  DNA-PK was added to buffer and DNA and incubated on ice for 5 minutes, followed by addition of Artemis.  Reactions were initiated with the addition of ATP, incubated at 37ºC for 30 minutes, and terminated by addition of SDS loading dye.  Reactions were heated at 95ºC for 5 minutes and separated by SDS-PAGE.  Gels were dried and phosphorylated products were visualized by PhosphorImager analysis.

## 2.12.  *In vitro* exonuclease assays

The 5' radiolabeled DNA substrate (CCCCTATCCTTTCCGCGTCCTTACTTCCCC) used for single-strand nuclease assays was radiolabeled as described above with $[\gamma\text{-}^{32}P]$ ATP [51].  To generate the 3' radiolabeled DNA substrate for single-strand nuclease assays, complementary oligonucleotide were annealed, extended and labeled with $[\alpha\text{-}^{32}P]$ dCTP and Klenow (exo⁻) fragment.  The extension reactions were performed for 30 minutes at 37ºC, followed by a chase reaction containing 1mM dCTP to ensure full extension.  The DNA was denatured at 95ºC in formamide buffer and separated on a 12 % polyacrylamide/urea denaturing gel.  The radiolabeled band was visualized using

film, excised, eluted from the gel piece as described above, ethanol precipitated and resuspended in water. Single-strand nuclease assays were carried out in a final volume of 15 µL in nuclease buffer (25 mM Tris, pH 8.0, 10 mM KCl, 10 mM MgCl$_2$, 1 mM DTT) with 50 fmol of radiolabeled DNA and varying amounts of Artemis (as indicated) at 37ºC for 30 minutes. Reactions were terminated by the addition of formamide loading dye, heated at 95ºC for 5 min, loaded onto a 12 % polyacrylamide/urea denaturing gel, and products were visualized by PhoshorImager analysis.

## 2.13. *In vitro* endonuclease assays

The 5' radiolabeled hairpin substrate with a 6 base single-strand overhang and the 3' overhang DNA substrates were prepared as described above (2.2), as was the 3' radiolabeled substrate with a 5' single-strand overhang. Endonuclease assays were carried out in a final volume of 10 µL containing nuclease buffer with 50ng/ul of BSA, varying amounts of Artemis, 50 nM of DNA-PK, 250 fmol of radiolabeled DNA and 250 µM ATP (unless otherwise indicated). Reactions were incubated, terminated and visualized as described above for single-strand nuclease assays.

| Name | Sequence | Notes |
|---|---|---|
| | *General DNA substrates* | Complementary to 2.2 |
| JT ILH 2.1 | CCCCTATCCTTTCCGCGTCCTTACTTCCCC | Used as general double-strand 30-mer substrate |
| JT ILH 2.2 | GGGGAAGTAAGGACGCGGAAAGGATAGGGG | |
| | | |
| | *Effectors for DNA-PK* | |
| 3'24 | Biotin-TAGATGGACTATCGCAGCACTGTA | |
| 3'30 | Biotin-TAGATGGACTATCGCAGCACTGTACGGCTT | |
| 3'24+6 | Biotin-TAGATGGACTATCGCAGCACTGTAGCCGAA | |
| 3'24+6A | Biotin-TAGATGGACTATCGCAGCACTGTAAAAAAA | |
| 3'24+6T | Biotin-TAGATGGACTATCGCAGCACTGTATTTTTT | |
| 3'24+6-mix | Biotin-TAGATGGACTATCGCAGCACTGTAAAGCCG | |
| 5'24 | TACAGTGCTGCGATAGTCCATCTA | |
| 5'30 | AAGCCGTACAGTGCTGCGATAGTCCATCTA | |
| 5'24+6 | TTCGGCTACAGTGCTGCGATAGTCCATCTA | |
| 5'24+6A | AAAAAATACAGTGCTGCGATAGTCCATCTA | |
| 5'24+6A | TTTTTTTACAGTGCTGCGATAGTCCATCTA | |
| | | |
| | *DNA substrates for Artemis* | |
| KSP 2.0 | GTCCCGGACTCTGGGATCGG | Artemis sense primer |
| KSP 2.1 | CCCAACCAGGTTATTTGAACATTTT | Artemis antisense primer |
| KSP 10.1 | TTTTTGATTACTACGGTAGTAGCTACGTAGCTACTACCGTAGTAAT | Art hairpin substrate |
| KSP 10.2 | ACTGAGTCCTACAGAAGGATCTTTTTTTTTTTTTT | Anneal to KSP 10.2C |
| KSP 10.2C | GATCCTTCTGTAGGACTCAGT | Makes 3' overhang Art substrate |
| KSP 11.1 | TTTTTTTTTTTTTTTAAGCTTGCATGCCTGCAGGTCGAC | anneal to KSP 11.0C |
| KSP 11.0C | GGTCGACCTGCAGGCATGCAAGCTT | Makes 5' overhang art substrate |
| KSP 11.2 | AAAAAAAAAAAAAAAAAGCTTGCATGCCTGCAGGTCGAC | aneal to KSP 11.0C |
| KSP 11.3 | GTAGATGGACTATCGCAGCACTGTA | anneal to 5'30 and for Art 5' overhang substrate |

**Table 1.** Oligonucleotide sequences. All sequences are 5′-3′ with biotin modifications as indicated.

## 3. Influence of DNA sequence and strand structure on DNA-PK activation

### 3.1. Introduction

While it is known that activation of DNA-PK is an important step in NHEJ [43], the exact molecular mechanism of DNA-PK activation remains to be elucidated. It is known that to be activated, the protein kinase must bind DNA, and structural studies have observed a channel in the DNA-PK catalytic subunit large enough to accommodate double strand DNA [58]. This suggests that DNA threads through a channel in the DNA-PK complex. After the DNA-DNA-PK complex is formed, a DNA-PK dimer is formed, creating a synaptic complex that results in the two DNA termini to be joined being brought into close proximity [109]. This complex most likely initiates the recruitment of other NHEJ proteins and ultimate ligation of the DNA.

Biochemical studies suggest that melting of the DNA terminus to form single-strand ends is needed for a stable DNA-PK-DNA complex to be formed [54]. This information can be used to extend the model that strand separation occurs, and the resulting single-strand termini can be inserted into one or more active sites on the kinase after synapsis of the two DNA-PK bound termini has occurred [14].

To determine the underlying mechanism of activation of DNA-PK, we reported that the activation of DNA-PK is influenced by the strand orientation and specific base composition of a double strand DNA effector, with 3' pyrimidine/5' purine –rich termini (Figure 5) resulting in a greater level of DNA-PK activation than DNA effectors with 3' purine/5'pyrimidine –rich termini [51]. A study published shortly after showed that DNA sequence

47
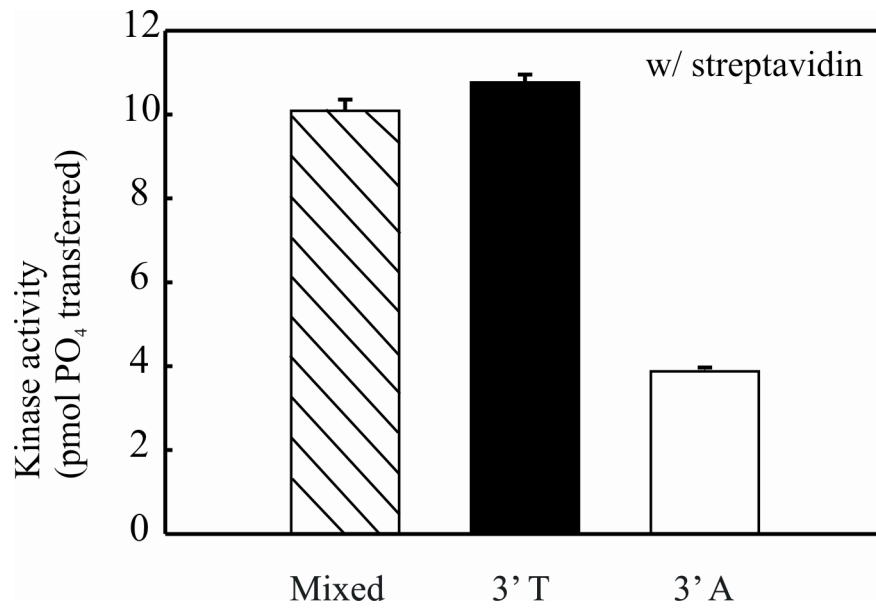
**Figure 5. Effect of DNA strand orientation and sequence bias on DNA-PK activation.** 30mers containing 15 homopolymeric bases of 3'-dT or 3'-dA and a control 30mer of mixed sequence were assayed for DNA-PK activation. Reactions contained 20 nM DNA-PKcs, 3.3 nM Ku and 5 nM SA – DNA, as indicated. Results are presented as the pmol of $^{32}$P transferred to the synthetic p53 peptide in a 30 min reaction. Reactions were performed in triplicate and the mean and standard error of the mean are presented.

strongly influences joining of blunt end DNA substrates via NHEJ [9].  This data

confirmed our findings, and clearly demonstrates the importance of analyzing how

DNA sequence composition affects the activation of DNA-PK.

We have continued our studies of DNA-PK activation by designing DNA

effectors that address how sequence, orientation and structure influence activation of

DNA-PK, and these results are presented in this chapter.  Our experiments also

indicate that using DNA effectors with compatible termini resulted in increased

activity compared to effectors with non-compatible termini.  A strand orientation

preference was observed in these reactions and a model based on these results is

presented.  These results demonstrate the influence of DNA structure and orientation

on DNA-PK activation and provide a molecular mechanism of activation resulting

from compatible termini, an essential step in microhomology-mediated NHEJ.

## 3.2.  Results

Endogenous human DNA-PK was purified from 12 Liters of Hela cells as

described in Materials and Methods.  Briefly, extracts were fractionated on a 50 mL

cisplatin-damaged double-strand DNA-Sepharose column, heparin-Sepharose column

and Q-Sepharose column.  DNA-PK containing fractions were identified by protein

concentration as determined by Bradford assay, DNA-PK kinase activity, Ku-binding

activity and Coomassie staining of SDS gels.  DNA-PK kinase activity was

determined as described in Materials and Methods.  Briefly, fractions were incubated

with a double-strand DNA substrate (ie, the effector) as it has been shown that

double-strand DNA activates this unique kinase, as well as with a synthetic peptide

that contains an embedded serine residue that DNA-PK will phosphorylate.

49

Reactions were initiated with [$\gamma$-$^{32}$P] ATP, incubated and spotted on P81 paper, and results are presented as pmol of phosphate transferred to the synthetic peptide. Ku binding activity was determined as described in Materials and Methods, with fractions incubated with $^{32}$P-labeled double-stranded 30 base-pair DNA and separated on a native polyacrylamide gel. A representative Coomassie stained 8 % SDS gel from a single prep is shown in Figure 6, and shows that the DNA-PK heterotrimer (DNA-PKcs, 465 kDa and Ku 70 kDa and 80 kDa) is purified to greater than 90 % homogeneity. This is considered highly purified, as the heterotrimeric complex is not tagged or over-expressed.

Previous data revealed that DNA-PK is differentially activated by 3' pyrimidine and 5' purine-rich DNA termini, indicating that one DNA strand might be more important for activation than another. Therefore, we designed a set of DNA effectors to determine how each strand of DNA plays a role in activation of the kinase. Single-strand oligonucleotides were synthesized, gel purified and annealed to generate double-strand DNA effectors for use in DNA-PK kinase assays. DNA effectors were designed with one strand containing a biotin molecule on the 5' terminus, so that when incubated with Streptavidin, only one DNA termini was accessible for DNA-PK binding (Figure 7). This *in vitro* design allowed us to manipulate DNA structure, sequence and chemistry at the DNA-PK/DNA interaction site so as to better understand how specific DNA effectors influenced activation of DNA-PK. DNA effectors were designed with 3' or 5' single-strand 6-base overhang structures or Y-shaped 6-base termini on the accessible terminus, or as full duplexes (Figure 7). Full sequences can be found in Table 1.
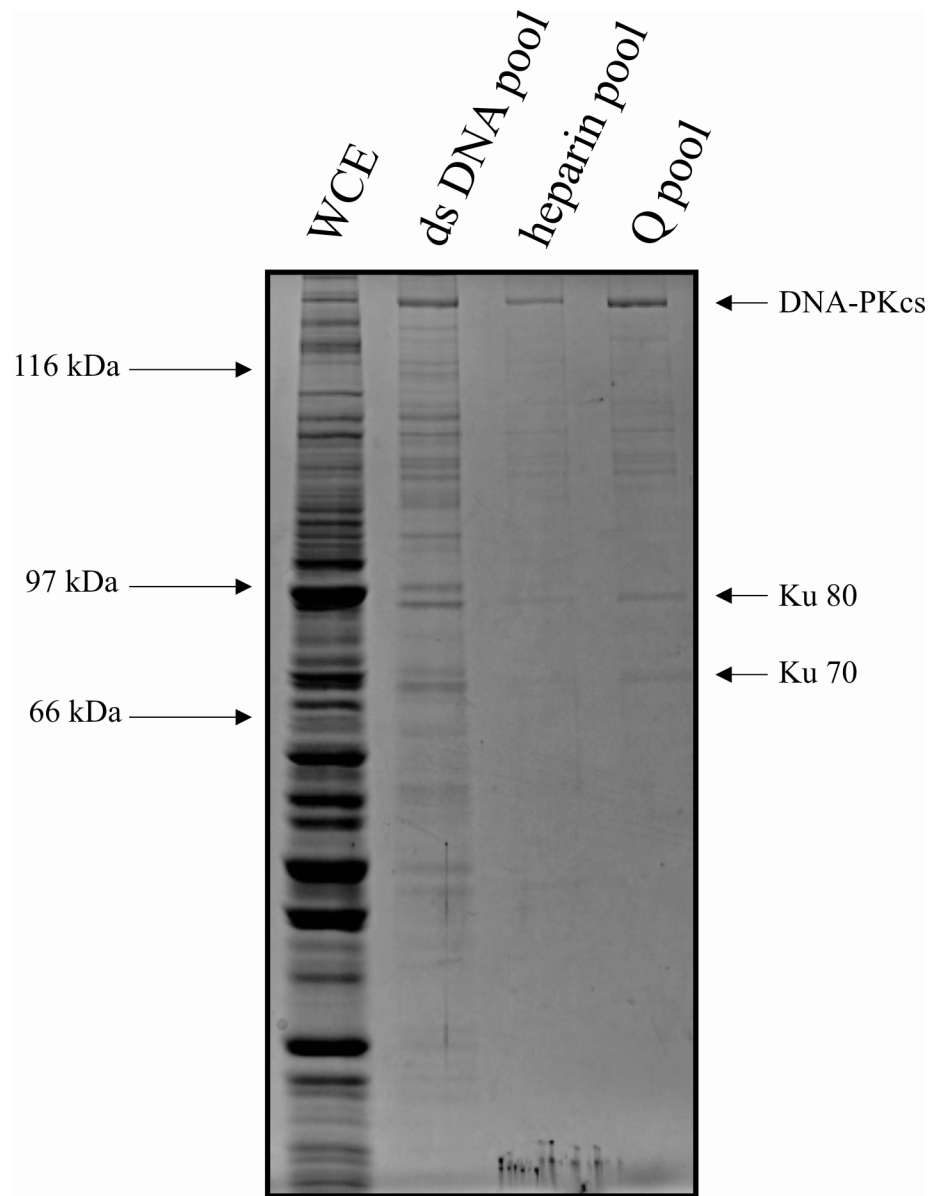
**Figure 6. SDS-PAGE of a DNA-PK protein preparation.** DNA-PK was purified as described in Materials and Methods: Equal volumes of the whole cell extract (WCE) and elution pools from each chromatography column used to fractionate DNA-PK were separated on an 8 % SDS – PAGE gel and stained with Coomassie Blue. The position and molecular weights (kDa) of the standards are indicated on the left-hand side and Ku 70, Ku 80 and DNA-PKcs are indicated on the right side.
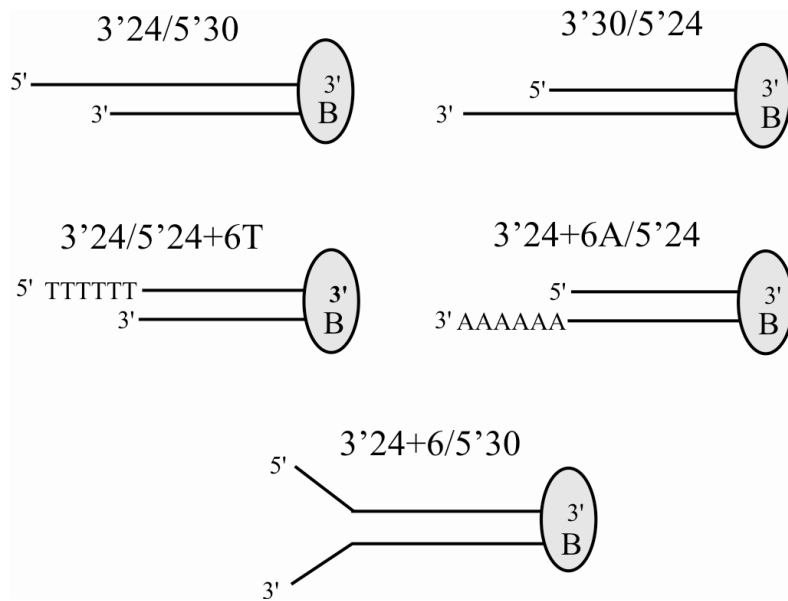
**Figure 7. DNA effectors used to study DNA-PK activation.** Duplex DNA effectors were prepared from gel purified single strand oligonucleotides. The addition of streptavidin, as indicated by the oval, results in blocking of the 5' biotinylated terminus, indicated by the B. The effectors generated have a 3' overhang, 5' overhang or Y-shaped structure at the DNA-PK accessible terminus.

Previous work with DNA-PKcs that has been purified free from Ku and is in a monomeric form showed an increase in kinase activity with DNA effectors that contained single-strand overhangs as compared to full duplex effectors [53]. Importantly, it has been shown *in vivo* that Ku recruits DNA-PKcs to the site of a DNA DSB [61]. This illustrates the necessity of studying how the holoenzyme (Ku and DNA-PKcs) interacts with different DNA terminal structures, and so our experiments contain the heterotrimeric complex as opposed to DNA-PKcs alone. The DNA effectors described above were incubated with DNA-PK and all experiments shown included a 30 base-pair DNA control to ensure that difference seen between DNA effectors was with varying termini was not a result of experimental variation. Results show that although DNA-PK is activated by a 24 base-pair duplex effector, a 30 base-pair duplex effector results in more activity (Figure 8, bars 1 and 4). This was not surprising, as previous work has shown that DNA-PK activity is length dependent, with longer DNA effectors resulting in greater kinase activity [35, 53]. DNA-PK kinase activity resulting from 24 base-pair DNA effectors with an additional 6 base single strand overhang on the 3' or 5' end was no greater than that seen from a full 24 base-pair duplex effector (Figure 8, bars 1, 2, 3). Interestingly, activity from these effectors was actually decreased as compared to the 24 base-pair duplex effector. These results differ from the published results showing that DNA-PKcs is stimulated by single-strand overhangs effectors compared to full duplex DNA [53], and this indicates that in the presence of Ku, DNA-PKcs does not require DNA with a single-strand overhang for maximal activation.

To further examine the inhibition in kinase activity resulting from single-strand DNA overhangs, effectors were designed with 24 base-pairs of duplex DNA with an additional 6 bases of noncomplementary sequence on each strand at the terminus (Y-shaped effectors). Analysis of kinase activation revealed that maximal DNA-PK activation was completely restored (to the level of activity seen from a 30 base-pair duplex DNA effector) with these Y-shaped effectors, as compared to DNA effectors with a single-strand overhang on either terminus (Figure 8A, bar 5 compared to bars 2 and 3). These results suggest that single-stranded ends are not inhibitory to kinase activation. In an effort to rule out any potential differences in DNA-PK activation resulting from sequence or orientation dependent activation, effectors with the identical Y-shaped structure but varied DNA sequence on each strand were designed. These results again demonstrated that DNA-PK activation by the Y-shaped DNA effectors is comparable to the full duplex DNA effectors and furthermore, that any minor differences can be attributed to strand orientation-dependent sequence bias (data not shown). Finally, 24 base-pairs of duplex DNA with homopolymeric 6-base Y-shaped termini or full duplex ends were designed. Results show again that DNA-PK kinase activity is not increased from Y-shaped effectors compared to full duplex DNA effectors of identical length (Figure 8B). These results all demonstrate that in the presence of Ku, DNA-PKcs does not require single-strand termini for maximal activation.
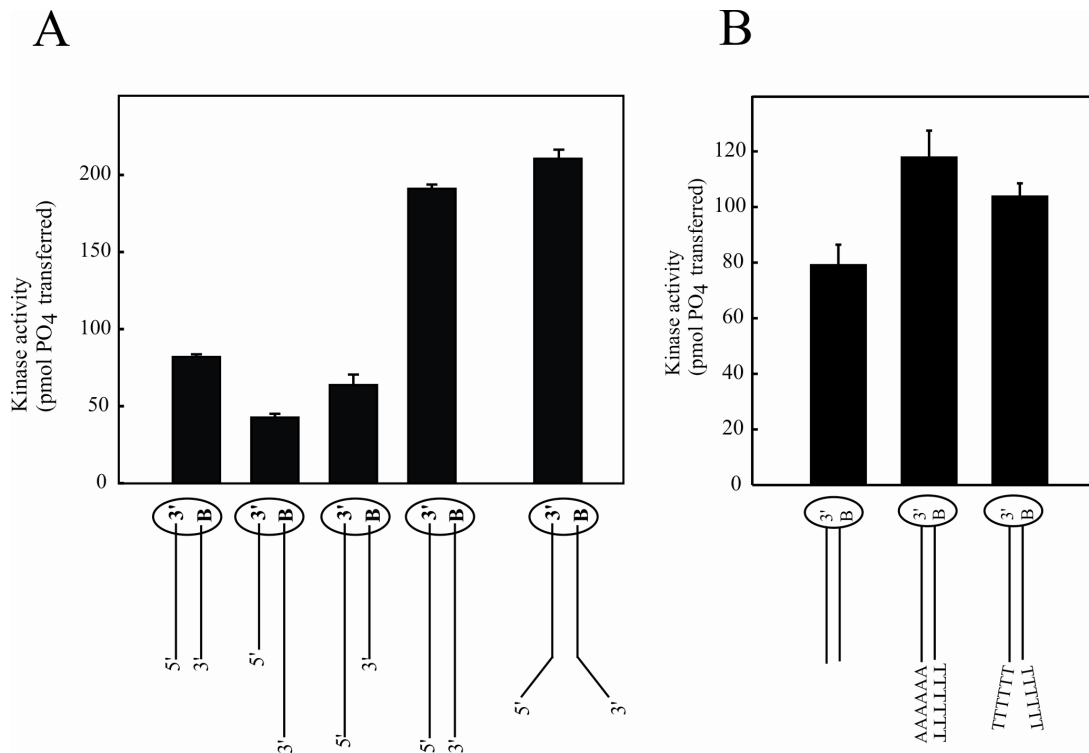
**Figure 8. Effect of DNA overhangs on DNA-PK activation.** DNA-PK kinase assays were conducted with annealed DNA effectors, as described in 'Materials and methods' section. Briefly, 24- and 30-bp full duplex DNA effectors, 3' and 5' 6-bp overhang effectors and Y-shaped effectors were assayed. Reactions contained 6.3 nM DNA-PK and 5 nM SA-DNA, as indicated. Results are presented as the picomoles of $^{32}$P transferred to the synthetic p53 peptide in a 30-min reaction. Reactions were performed in triplicate and the mean and standard deviation are presented.

Figure 8 indicates that DNA-PK is not preferentially activated by DNA that contains single-strand overhang structures as compared to full duplex DNA effectors of the same length. In fact, activity from single-strand overhangs is somewhat reduced compared to full duplex DNA. Furthermore, a difference in activation between the 3' and 5' overhang effectors was observed. Statistical analysis of the results presented in Figure 8A revealed a statistically significant difference (a $P$-value $< .05$) in comparisons with each set of effectors. Despite the convincing statistical analysis, we decided to further investigate the small but significant differences observed between the single-strand overhang effectors. We hypothesized that if there were truly relevant differences in activation with the varying overhang effectors, these differences would be emphasized as a function of DNA concentration. In the standard kinase assays conducted, like that depicted in Figure 5, the DNA concentration (5 nM) is saturating, and so a DNA titration was conducted with each DNA effector to accentuate differences in the resulting kinase activity. DNA-PK kinase activity was assayed with increasing concentrations of 3' and 5' overhang effectors, and a substantial difference in activity over the entire range of effector concentrations was observed (Figure 9). These results confirm that DNA-PK exhibits lower activity from a 3' overhang DNA effector compared to the 5' overhang effector.

Previous studies have suggested that DNA-PK activity is modulated by autophosphorylation. Upon autophosphorylation, the kinase is believed to dissociate from the DNA effector, thus lowering overall kinase activity of DNA-PK [75].
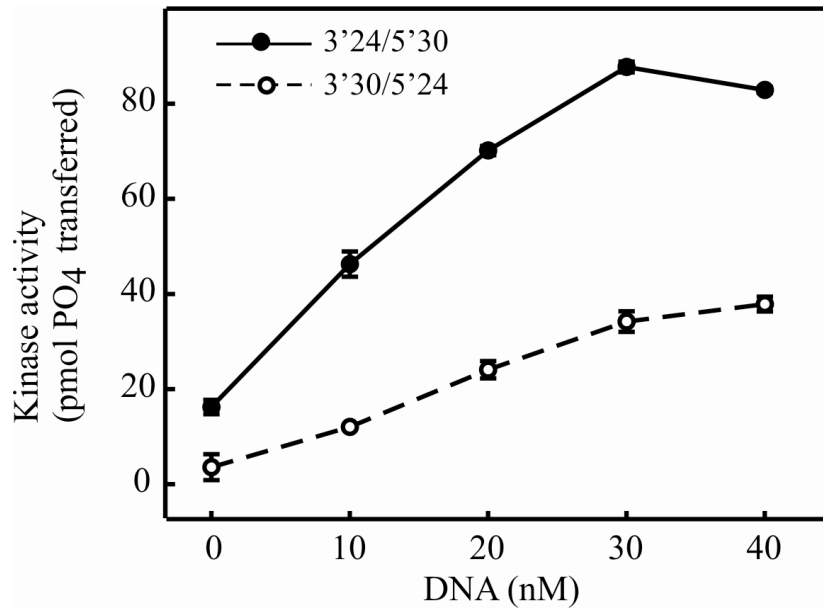
**Figure 9. Titration of DNA effectors containing 3' and 5' overhangs.** DNA effectors with a 3' or 5' 6-base overhangs were pre-bound with excess streptavidin and then assayed for DNA-PK kinase activation as described in Figure 8. Reactions were incubated with increasing concentrations of each effector. Results are presented as the picomoles of ^{32}P transferred to the synthetic p53 peptide in a 30-min reaction. Reactions were performed in triplicate and the mean and standard deviation are presented.

To investigate if the level of DNA-PK autophosphorylation was responsible for the differential peptide phosphorylation observed between 3' and 5' overhang effectors, autophosphorylation kinase assays were performed as described in Materials and Methods. With autophosphorylation assays, DNA-PK itself serves as the protein substrate, and levels of $^{32}$P-labeled DNA-PK are visualized with a PhosphoImager following separation on a SDS denaturing gel. Effectors tested had 3' or 5' single-strand overhangs, Y-shaped termini or blunt termini that were all accessible for DNA-PK binding, with the other termini blocked by streptavidin. Results show that DNA-PK autophosphorylation resulting from the 3' and 5' overhang effectors was significantly reduced when compared with the full duplex 30 base-pair effector (Figure 10). Furthermore, the kinetics of autophosphorylation of DNA-PK was determined with the 30 base-pair duplex effector and the 3' overhang effector (Figure 11A). The results confirm the decreased autophosphorylation obtained with the 3' overhang effector compared to the full duplex DNA (Figure 10). Quantitation of these results shows a time dependent autophosphorylation activity (Figure 11B). The level of autophosphorylation presented in Figures 10 and 11 comparing the overhang effectors and the 30 base-pair duplex effector mimics the level of peptide phosphorylation observed in peptide-based kinase assays (Figure 8A). Interestingly, the level of autophosphorylation resulting from the 24 base-pair effector is the same as that from the 30 base-pair effector (Figure 10, lanes 1 and 4). When measuring peptide phosphorylation by DNA-PK, levels from a 24 base-pair effector are significantly lower than from a 30 base-pair effector (Figure 8, lanes 1 and 4).
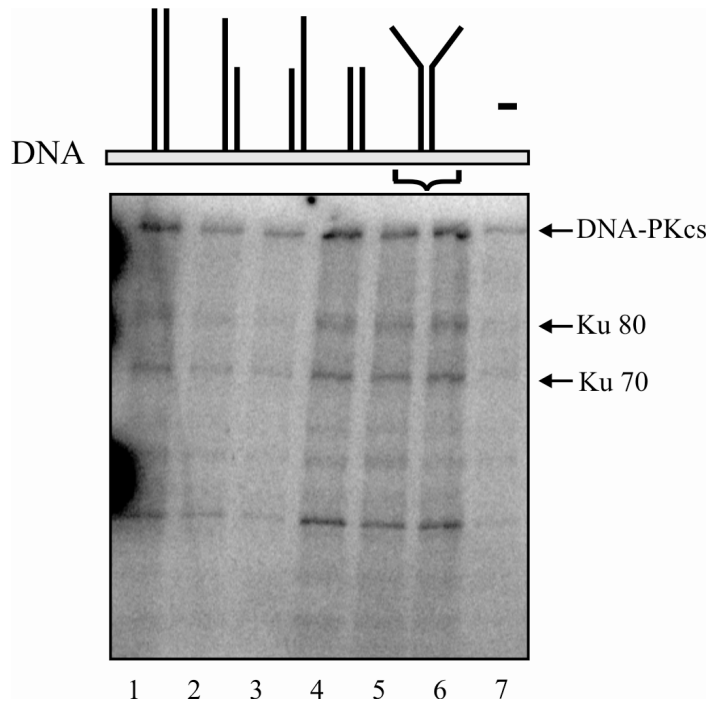
**Figure 10. Autophosphorylation of DNA-PK by full duplex, overhang and Y-shaped effectors.** DNA-PK autophosphorylation was measured with 24- and 30-bp full duplex DNA effectors, 3' and 5' overhang effectors and Y-shaped effectors. Reactions were performed as described in Figure 8, initiated with 1.0 µCi [$\gamma$-$^{32}$P] ATP, and stopped with SDS. Reaction products were separated by 8 % SDS – PAGE. The gel was dried and exposed to a PhosphorImager.
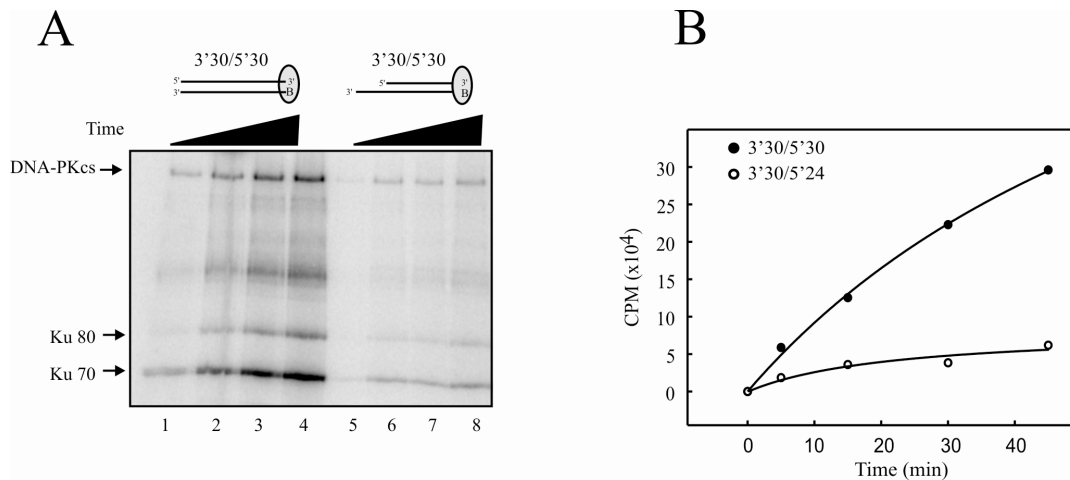
**Figure 11. Time dependent autophosphorylation of DNA-PKcs by full duplex or 3' overhang effectors.** (A) Reactions were performed as described in Figure 10 and stopped with SDS at 5, 15, 30 and 45 minutes. Reactions products were separated by 8 % SDS-PAGE and the gel was dried and exposed to a PhosphorImager. (B) Time-dependent autophosphorylation of DNA-PKcs was quantified using a Phosphorimager and results are presented as cpm of $^{32}$P transferred to DNA-PKcs as time increases.

This is an expected result, as DNA-PK activity has been shown to be length dependent, with longer DNA effectors resulting in greater activity. If DNA-PK autophosphorylation resulting from the full duplex sets of DNA were mimicking the peptide phosphorylation observed in the kinase assays, we would expect to see less autophosphorylation from the 24 base pair effector than from the 30-mer. Importantly, there is no difference in autophosphorylation between the 3' overhang and 5' overhang DNA effectors. These results demonstrate that the reduced activity resulting from the 3' overhang compared to the 5' overhang effector is not due to a disparity in autophosphorylation. However, the increase in autophosphorylation resulting from the 24 base-pair may account for the decrease in peptide phosphorylation from the 24 base-pair DNA compared to the 30 base-pair duplex effector (compare Figures 8 and 10). Finally, we conducted autophosphorylation experiments both in the presence and the absence of the peptide substrate to ensure that our autophosphorylation results were consistent with the peptide-based kinase assays. Similar results were seen under both conditions (data not shown). These results indicate that length dependence may play a role in influencing autophosphorylation.

Once having determined that a single-strand overhang on the terminus of a duplex DNA effector does not increase DNA-PK activity as compared to a full duplex DNA effector, we designed a series of DNA effectors with homopolymeric overhang strands. Our previous publication indicated that DNA sequence, particularly terminal sequence, differentially affects DNA-PK activation [51]. Thus, to determine if DNA-PK exhibits sequence bias on a single-strand overhang effector,

we assessed kinase activity (phosphorylation of a synthetic peptide) with homopolymeric overhang strand effectors.  One set of effectors had 3' 6-base extensions of Ts or As (Figure 12), and this terminus was rendered the only accessible terminus by the presence of streptavidin on the opposite end.  The other set of effectors was identical except the extensions were on the 5' strand of the accessible terminus (Figure 13).  Triplicate assays were performed at two different DNA concenterations (0.5 pmol and 1.0 pmol) and in triplicate, and results revealed that DNA-PK activity from the 3' A overhang effector was slightly decreased compared to activity from the 3' T overhang effector.  This effect was observed at both concentrations (Figure 12), and mimics previous work we have done looking at sequence bias and DNA-PK activation where we showed differential activation of DNA-PK resulting from pyrimidines versus purines [51].  Interestingly, we also observed a decrease in activation from the 5'A overhang DNA effectors compared to the 5'T overhang effectors (Figure 13).  Finally, comparison of 3' and 5' overhang effectors showed greater activation from the 5' DNA effectors as compared to 3' overhang (compare overall pmol transferred in Figure 12 and 13).  This result is independent of sequence, and is completely consistent with our previous results showing that 5' extensions result in greater activity than 3' (Figure 8).

When designing the set of effectors with homopolymeric sequences, we designed them such that when individually included in a reaction, the extensions are non-compatible and thus each terminus presumably binds a single DNA-PK. However, when two effectors are combined together in a reaction, they are capable of annealing, and could potentially form a synaptic complex (Figure 3).
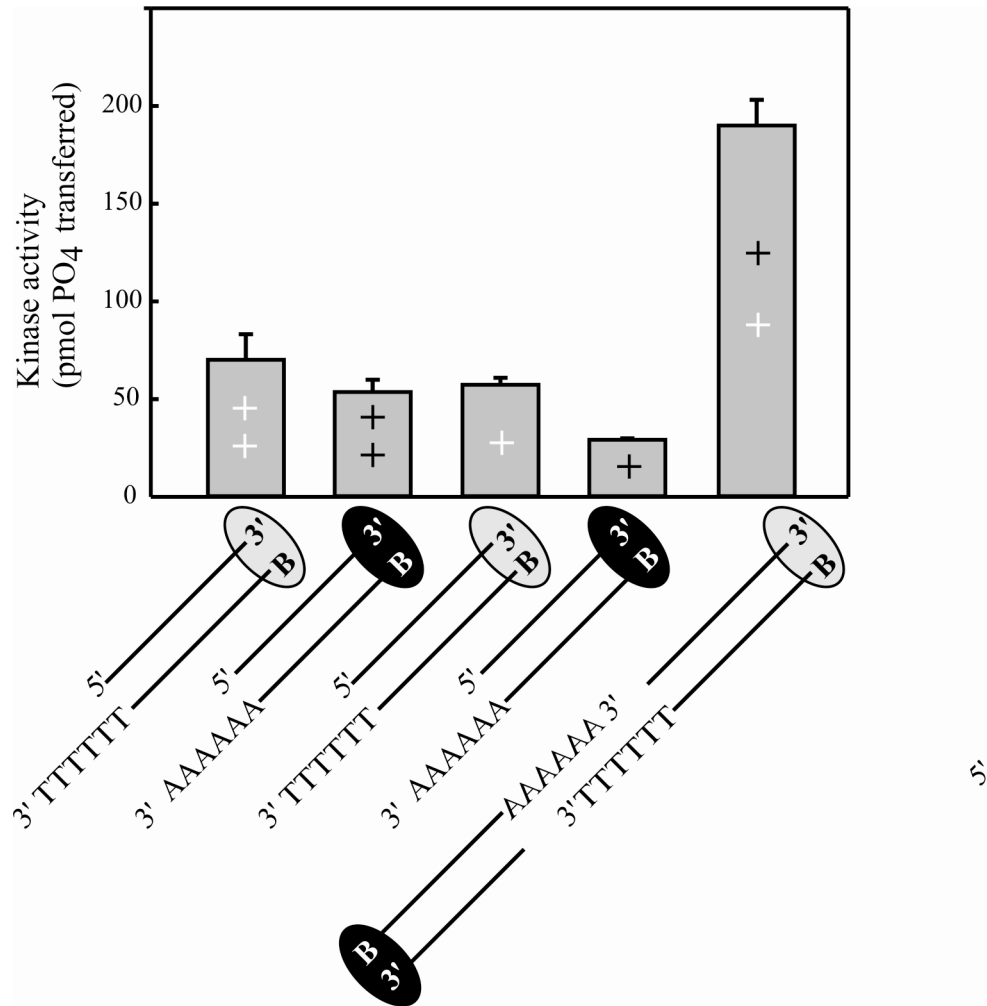
**Figure 12. Dimeric activation of DNA-PK from effectors containing 3'
compatible homopolymeric overhang ends.** Effectors with a 6-base poly-T 3'
overhang or a 6-base poly-A 3' overhang were pre-bound with heterotrimeric DNA-
PK and assayed for DNA-PK kinase activation. Assays were conducted with either 1
or 0.5 pmol of each effector per reaction, as indicated, or 0.5 pmol of each effector
was incubated together in a single reaction. 0.5 pmol of the poly-T effector is
indicated by a white plus symbol, and half a pmol of the poly-A effector is indicated
by the black plus symbol. Results are presented as the picomoles of ^{32}P transferred to
the synthetic p53 peptide in a 30-min reaction. Reactions were performed in triplicate
and the mean and standard deviation are presented.
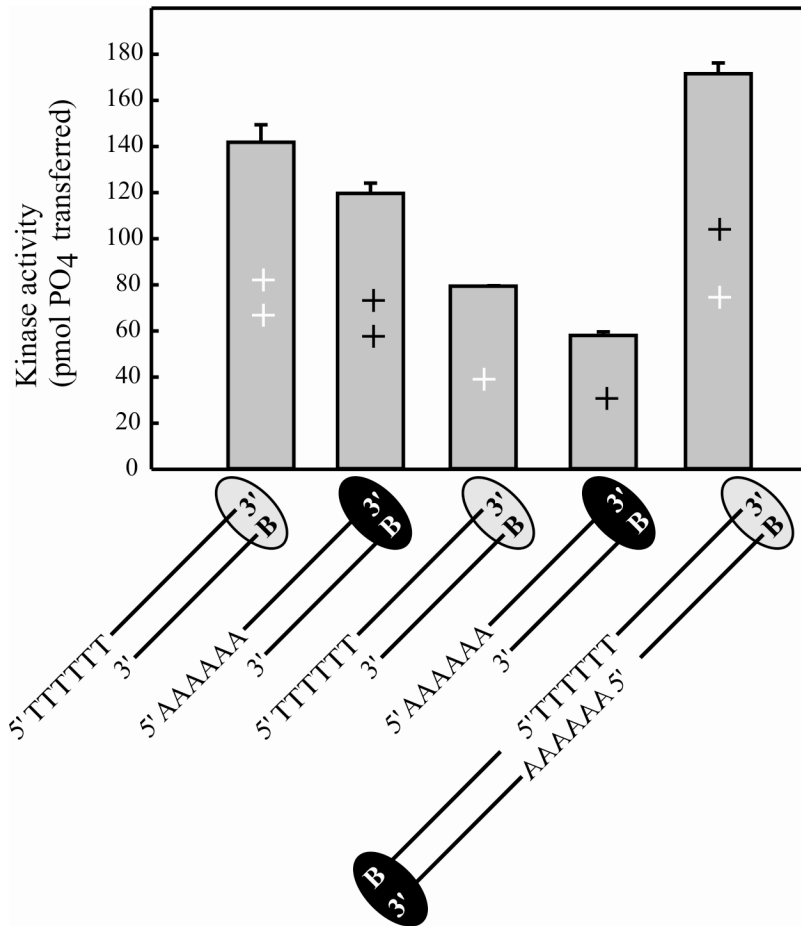
**Figure 13. Dimeric activation of DNA-PK from effectors containing 5' compatible homopolymeric overhang ends.** Effectors with either a 6-base poly-T 5' overhang or a 6-base poly-A 5' overhang were assayed for DNA-PK kinase activation as described in Figure 12. 0.5 pmol of the poly-T effector is indicated by a white plus symbol, and half a pmol of the poly-A effector is indicated by the black plus symbol.

These regions of complementarity mimic regions of microhomology such as those that occur in a cell. This experiment was performed by pre-incubating each DNA effector with DNA-PK (5 minute incubation), then incubating these pre-formed complexes together for five minutes before initiating the kinase reaction with the addition of $^{32}$P-ATP. It is important to note that each individual effector reaction was performed at two different concentrations, one being equal to the total DNA concentration in the combined reaction (1.0 pmol, Figure 12, bars 1 and 2) and one being equal to half the DNA concentration of the combined reactions (0.5pmol, Figure 12, bars 3 and 4). The experiment was designed this way in order to increase the level of activation resulting from the relatively poor DNA effectors as well as to control for total DNA in the combined reaction (where 0.5 pmol of each DNA complementary DNA effector was added, Figure 12, bar 5). In the reactions containing two 3' overhang effectors with complementary overhangs, a significant increase in activation was observed (Figure 12, bar 5) compared to the individual reactions that only contained one DNA overhang effector (at 0.5pmol or 1.0 pmol). If kinase activation was additive when combining the DNA effectors containing regions of complementarity, in this reaction we would have expected to see the sum of the activity resulting from the each DNA effector at 0.5 pmol concentration (Figure 12, bars 3 and 4), approximately 85 pmol of phosphate transferred. Furthermore, if we consider an average of the individual reactions at equal concentrations of total DNA (1 pmol, Figure 12, bars 1 and 2), we would expect approximately 65 pmol of phosphate transferred. Instead, DNA-PK activity resulting from combining two DNA effectors with regions of microhomology in the overhang strands resulted in 190 pmol

of phosphate transferred (Figure 12, bar 5). This synergistic level of kinase activity is dependent on the presence of compatible DNA termini and suggests that annealing of DNA ends influences DNA-PK activation.

The above results suggest that compatible DNA termini may play a role in DNA-PK activation. However, the described experiments do not reveal how strand orientation and polarity play a role in activation. In an effort to determine if strand orientation of a microhomologous sequence plays a role in synergistic levels of activation, we performed experiments in the same manner as Figure 12 with effectors containing identical sequences and structures as those seen in Figure 12, but with 5' extensions. 5' overhang effectors with compatible termini did produce a slight level of synergistic activation when incubated together in a reaction (Figure 13, bar 5) as compared to control reactions (Figure 13, bars 1-4), but this level of synergy was not nearly as great as that seen from incubating DNA effectors with 3' overhang compatible termini together. Additive results (0.5 pmol of each 5' overhang effector, Figure 13 bars 2-3) predicted 137 pmol of phosphate transferred, while averaging each reaction (1 pmol of each effector, Figure 13 bars 1-2) predicts a value of 130 pmol of phosphate transferred. The level of activity actually observed from incubating two effectors with 5' overhang regions of complementarity together is slightly synergistic, with 171 pmol of phosphate transferred (Figure 13, bar 5), but this increase in activity over the predicted additive and average values is not nearly as great as the synergistic increase seen with the 3' overhang effectors. These results indicate that the 3' end (over the 5' end) of a DSB is important for the DNA-PK dependent aligning and microhomology directed ligation at the site of a DSB.

66

The results described above indicate that complementary sequences in a 3' overhang region of a DNA effector have an effect on DNA-PK activation. However, as the described regions of microhomology are composed of homopolymeric sequences, we were concerned that these areas have the potential for annealing in different positions, with the potential for 2-, 3-, 4-, 5- or 6 bp annealing. This would create different protein-DNA structural complexes, with the possibility for varying lengths of nucleotide gaps to exist between the two complexes. To correct and control for this possibility, effectors were designed with a complementary mixed sequence on the 3' overhang. These effectors can only anneal in a single position, and so would only contain a nick at each junction following annealing. The kinase assay was conducted as described above, and results show that like effectors with homopolymeric regions of complementarity, effectors with 3' overhangs containing a specific annealing sequence also induce high levels of synergistic activity, 256 pmol of phosphate transferred (Figure 14). This level is significantly higher than the projected additive and average values, 136 and 108 pmol of phosphate transferred. These results support the conclusion that the 3' end is necessary for microhomology-associated annealing and solidifies the hypothesis that microhomology is important for DNA-PK activation, as the complementary sequence in these effectors is significantly more specific than the DNA effectors used in Figure 12. This indicates that the synergistic level of activity, now referred to as dimeric activation, results from two effectors having the ability to successfully anneal, and that this requires greater than one complementary base.
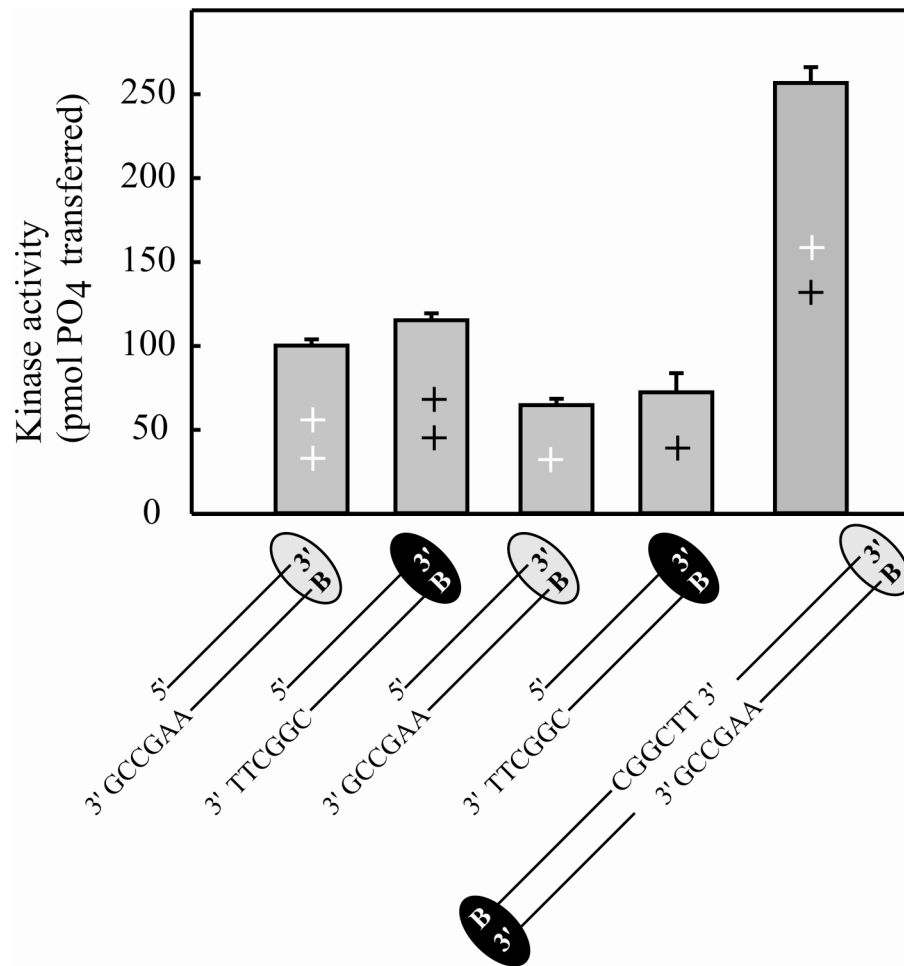
**Figure 14. Activation of DNA-PK with DNA effectors containing compatible mixed sequence overhang ends.** Effectors with 6-bp 3' overhang complementary sequences were pre-bound with DNA-PK and assayed for DNA-PK activation as described in Figure 12. Assays were conducted with 1 pmol or 0.5 pmol of a single DNA effector, or 0.5 pmol of each effector was included together in a reaction, as indicated. The white plus symbol indicates half a pmol of one DNA effector, and the black plus symbol indicates the second effector with a complementary overhang.

We hypothesized that the DNA-PK dimeric activation resulting from DNA effectors with compatible 3' overhang termini was due to an increase in formation of a synaptic complex between the two DNA effectors and the two DNA molecules. To test this, we designed a pull-down assay utilizing radiolabeled DNA. This assay was conducted under similar conditions as the kinase assays, as described in Materials and Methods. Briefly, one unlabeled DNA effector was bound to streptavidin-conjugated magnetic beads, and a $^{32}$P labeled effector with a complementary overhang sequence was bound to streptavidin molecules. DNA-PK was then pre-bound to each DNA effector (streptavidin-bead bound and streptavidin-molecule bound DNA effectors) individually, incubated together, washed extensively, and radioactive counts were read in a scintillation counter (Figure 15). Increase in radioactive counts corresponds to an increase in synaptic complex formation, and results are presented as a percent of total radiolabeled DNA-PK-DNA complex bound to unlabeled DNA-DNA-PK complex. Results from this assay revealed that a synaptic complex is formed in the presence of DNA overhang effectors and DNA-PK, as shown by the increase in percent bound in the reactions containing samples with pre-bound DNA-DNA-PK as compared to the reactions that were absent of DNA-PK (Figure 16, compare bars 1 and 2 and 3 and 4). Interestingly, DNA overhang effectors with DNA-PK bound to them formed a synaptic complex regardless of the presence of a region of microhomology within the overhang (Figure 16, bars 1 and 3). This result differs from kinase activity observed from overhang effectors containing regions of microhomology, as activity in kinase assays was increased with DNA overhang effectors with regions of microhomology. These results deomonstrate that homology

69
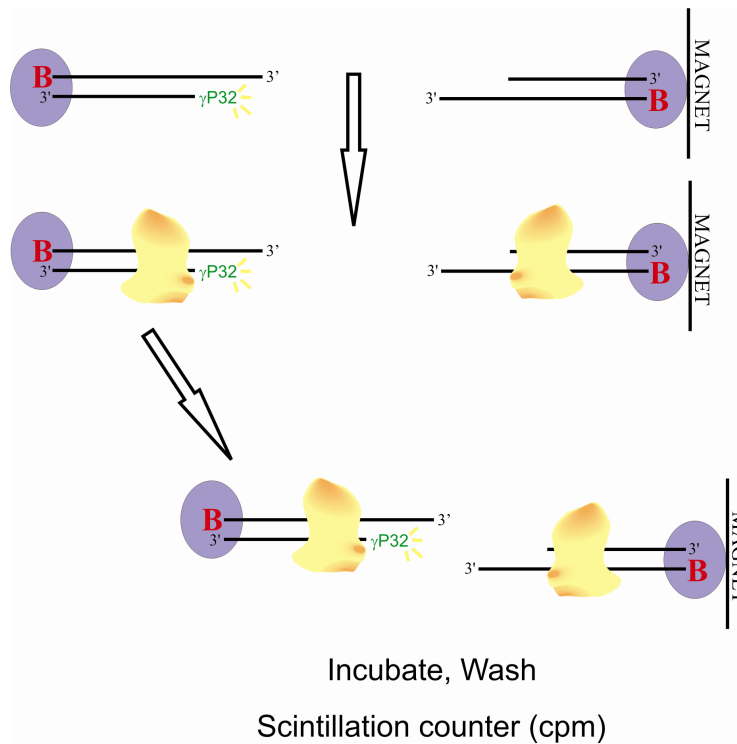
**Figure 15. Schematic of DNA-PK synaptic complex formation assay with overhang effectors.** A $^{32}$P labeled DNA effector was pre-bound with streptavidin (indicated in purple) and a unlabeled effector with complementary overhang sequence was bound to streptavidin conjugated magnetic beads. DNA-PK (indicated in yellow) was then pre-bound to each of these DNA effectors individually. These two reactions were incubated together, washed, and radioactive counts were read in a scintillation counter.
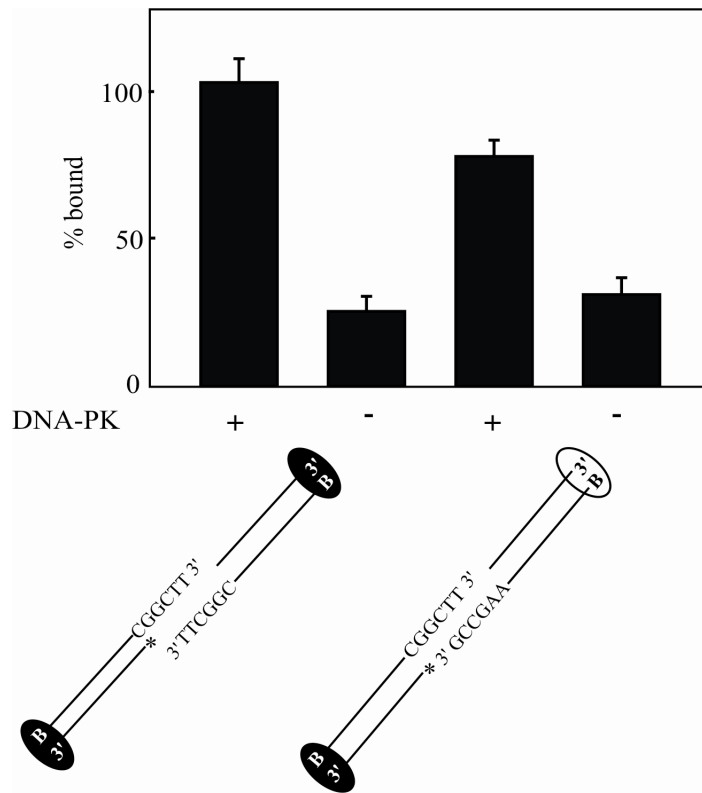
**Figure 16. DNA-PK synaptic complex formation with DNA effectors containing compatible overhang ends.** Five hundred femtomoles of each unlabeled DNA effector was bound to streptavidin magnetic beads. $^{32}$P-labeled DNA (indicated by asterisk) and the SA bound unlabeled DNA was incubated with DNA-PK or buffer as indicated, and labeled DNA was incubated in a separate tube with DNA-PK or buffer for 5 min. The labeled DNA effector prebound with DNA-PK or buffer was added to the tubes containing SA-unlabeled DNA and DNA-PK or buffer, incubated for 5 min, washed, and counts were read in a scintillation counter. Results are presented as percent of total DNA-DNA-PK complex bound to SA – DNA – DNA – PK complex.

driven dimeric activation seen in our kinase assays is a catalytic effect, and does not

result from increased binding and formation of a synaptic complex.

### 3.3. Discussion

Many studies over the years help us understand the mechanism of activation

of this unique DNA-dependent protein kinase. Convincing biochemical and

structural data have shown that DNA makes contact with DNA-PK, and recent higher

resolution structural studies present a model where DNA threads through a channel in

the protein kinase. Furthermore, it has been postulated that DNA structure, chemistry

and sequence play an important role in activation of the kinase. However, precisely

how DNA serves to activate DNA-PK is still an open question. The results we have

gathered show that in a Ku-dependent DNA-PK kinase assay, Y-shaped effectors

with single-strand ends result in activity that is similar to that seen from full duplex

DNA effectors. However, the presence of single-strand overhangs results in

significantly less activity. This finding differs from kinase assay results using Ku-

independent DNA-PKcs, where a significant increase in activity was observed with

DNA effectors containing single-strand ends [53]. Although this study revealed

interesting mechanistic insights, this design is perhaps not the most physiologically

accurate way to study mechanisms of DNA-PK. It has been shown *in vivo* that Ku

recruits DNA-PKcs to the site of a DSB, and furthermore that DNA-PK kinase

activity is significantly increased in the presence of Ku [61]. This illustrates the

importance of including the holoenzyme (Ku and DNA-PKcs) when studying

mechanism of activation. Furthermore, the difference in activation from DNA-PKcs

versus DNA-PK (the holoenzyme) resulting from a single-strand end may be

72

explained in part by an energetic argument. The presence of Ku at the termini eliminates the need for having pre-separated DNA strands, and this suggests that Ku promotes strand opening in conjunction with DNA-PKcs. This is supported by recent work arguing that Ku is able to "peel away" DNA termini from a histone surface at the site of a DSB, suggesting that the Ku structure does more than just thread onto DNA [37]. Recent work has also suggested that Ku may also play a role in end-processing during NHEJ, again supporting the theory that Ku could have some sort of influence in opening up DNA at the site of the break [110]. In any event, Ku facilitation of unwinding in conjunction with DNA-PKcs to generate the required single-strand ends could explain the differential activation as a function of single strands between assays with DNA-PKcs alone and with the heterotrimer.

The inhibition of DNA-PK activity resulting from a 3' overhang compared to a 5' overhang DNA effector, combined with the synergistic activity exhibited from complementary overhangs suggests that each single-strand terminus plays a unique role in DNA-PK activation. These results suggest that the 5' end of DNA is more important contact with the kinase, thus resulting in a greater degree of activation than the 3' end (Figure 8). Interestingly, each strand on their does not result in maximal activation of DNA-PK (as compared to double strand DNA of the same length). This indicates while each strand plays an important and unique role in activation of the kinase, both strands are still necessary maximal DNA-PK activation.

Based on the data presented above and structural and enzymatic analysis that has emerged over the last five years in the NHEJ field, we have developed a more complex model for activation of DNA-PK (Figure 17). Following Ku binding and

73

recruitment of DNA-PKcs to the site of the break, the kinase binds to the DNA

terminus.  The DNA strand is postulated to protrude through the kinase, with the

terminus appearing on the opposite opening of the kinase.  Following insertion

through the kinase, evidence points to fraying or unwinding of the DNA end [54].

Our data show that a DNA fragment with a 5' overhang induces greater DNA-PK

activation than a DNA fragment with a 3' overhang.  Yet, when two complementary

3' overhang DNA effectors are incubated together, a synergistic level of DNA-PK

activation is observed.  When two pieces of DNA with 5' complementary overhangs

are incubated together, the synergistic level of activation is significantly lower.

Combined, this data suggests that the 5' strand is important for activation, while the

3' strand may be important in scanning for regions of microhomology.

Previous studies suggest the possibility that following fraying of the DNA

ends after DNA-PK binding, the strands may insert themselves into active sites on the

perimeter of the kinase [55].  Our data suggests that each DNA termini is bound by

DNA-PK in a dimeric, or synaptic, complex independent of homology. The DNA is

scanned for regions of microhomology, which potentially pulls the DNA further

through the kinase.  Once homologous regions are identified increased kinase activity

results.   The model predicts that this activation is accompanied by insertion of the 5'

end into the active pocket on the periphery of the kinase (Figure 17 D, E).  The

formation of this synaptic complex and subsequent dimeric activation is expressed as

a synergistic level of activity when the two complementary effectors are incubated

together in an assay for DNA-PK activation.  This process could be viewed as

"useful" to NHEJ, as having the ability to scan for and identify regions of

74
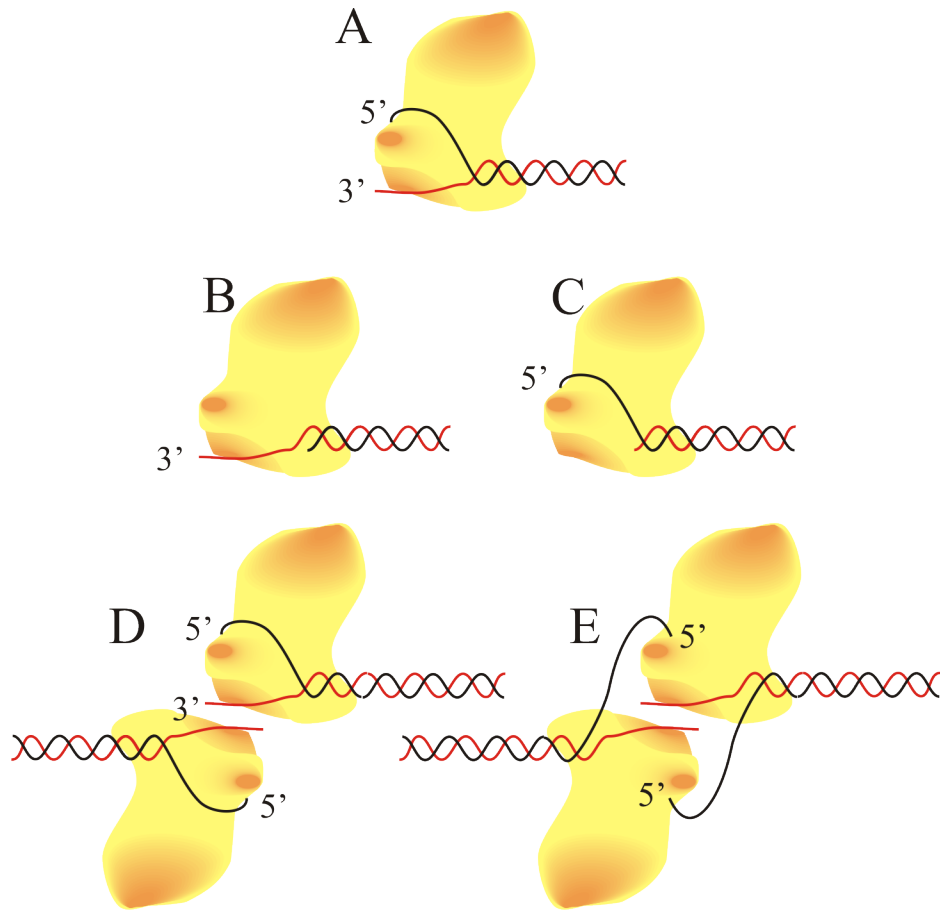
**Figure 17. Model for activation of DNA-PK.** DNA, depicted in black and orange, threads through DNA-PK, depicted in yellow. (A) When DNA of adequate length threads through the kinase, the ends separate and the 5' end can insert itself into an active site on the periphery of the kinase. (B) A 5' overhang containing effector can activate in the absence of dimerization while a 3' overhang (C) displays less activation. When the 3' overhang possesses a complementary sequence to the second DNA molecule with a 3' overhang, the two DNA ends can anneal, thus orienting the two DNA-PK molecules into a synaptic complex. The annealing may allow for more DNA to thread through the kinase, potentially making more of the 5' strand accessible for kinase activation. This activation could then occur in either a *cis* (D) or *trans* (E) fashion.

microhomology would allow for repair of a DSB without massive removal of nucleotides on flanking sequences, thus preserving genetic material. Furthermore, it is possible that annealing of 3' complementary termini releases the 5' strand for use in activating the kinase. Therefore, it is reasonable that 3' regions of microhomology increase overall kinase activity, as this would most likely increase overall NHEJ.

It is believed that when DNA-PKcs is bound to the ends of two DNA molecules at the site of a DSB, the protein kinase is responsible for bringing the two DNA ends into proximity of each other, in what is now called a synaptic complex. The formation of this synaptic complex is thought to be through the dimerization of DNA-PK. In fact, recent structural data indicates that the C-terminal region of Ku80 is both long enough and flexible enough to make contact with a DNA-PK molecule on the opposing strand. This could potentially be one of the factors responsible for formation of a synaptic complex being formed between two DNA-PK holoenzyme complexes bound to the two DNA termini at a DSB. Furthermore, it is thought that dimerization of DNA-PKcs and subsequent formation of the synaptic complex results in maximal activation of the kinase [14]. Our results are consistent with a model where dimerization of DNA-PK is independent of microhomology (Figure 13), but kinase activity is greatly influenced by end annealing. In short, synergistic activation of DNA-PK as driven by microhomology is a kinetic event.

There are two models one can envision for the role of DNA in activation of the kinase once these molecules are brought within proximity. One model involves the frayed 5' DNA end being inserted into the active site of the same DNA-PKcs molecule to which the DNA is bound [51, 54], in a *cis* orientated model (Figure 17D).

The second model positions the 5' strand interacting with the DNA-PKcs molecule that is bound to the opposite DNA strand, in a *trans* orientated model (Figure 17E) [53]. This model is supported by data suggesting that DNA-PKcs is autophosphorylated in *trans* [82]. Recent work in *Mycobacterium tuberculosis* suggests that the 3' ends of DNA at each terminus of a double strand break are important in maintaining a synaptic complex consisting of the NHEJ machinery. The authors propose that the 3' ends protruding from each LigD (analogous to DNA-PK machinery in eukaryotes) molecule can pair together, thus bringing each LigD-bound DNA termini into proximity of each other in a synaptic complex [111]. Further research in eukaryotes needs to be done to determine more precisely the role of the 3' and 5' ends in DNA-PK activation and synaptic complex formation.

It is important to point out that NHEJ-dependent joining of blunt-end substrates can occur *in vitro* and in cell culture models. These termini could be joined independent of microhomology, and would serve in the true sense of "non-homologous" end-joining, as the two blunt ends could simply be ligated together with no microhomology-dependent activity. This kinase activation mechanism may not necessarily include fraying of the termini or nuclease processing to reveal regions of microhomology. Consistent with this theory is the fact that blunt-end DNA effectors still provide the highest level of kinase activity *in vitro*, over single-strand DNA ends. However, as we have shown in the physiologically relevant context of a DNA-PK dependent synaptic complex formed at the site of DSB, DNA with regions of microhomology increases kinase activation. This kinetic data of ours is supported by work revealing that 3' or 5' overhang complementary DNA ends were joined much

more efficiently than blunt ends in cell-free NHEJ assays [9, 112]. This data suggests

that the preferred *in vivo* NHEJ substrate could potentially undergo strand separation

or contain single-strand overhangs, as well as possess regions of microhomology.

Clearly, more experimental evidence needs to be obtained to understand precisely

how DNA termini affect kinase activation, and this work needs to be expanded to

look at how microhomology and DNA-PK activation affect NHEJ *in vivo.*

## 4.  Purification of exonuclease-free Artemis and implications for DNA-PK dependent processing of DNA termini in NHEJ-catalyzed DSB repair

### 4.1.  Introduction

Ionizing radiation induced DNA DSB repaired by NHEJ can contain other DNA structural damage including thymine glycols, ring fragmentation, 3' phosphoglycolates, 5' hydroxyl groups and abasic sites.  These DNA discontinuities that arise around DNA termini at the site of a DSB usually need to be processed before ligation of the DSB by the XRCC4/Ligase IV/XLF complex can occur [1]. Many enzymes have been implicated DNA termini processing during NHEJ, including polymerases, kinases, and nucleases.  Artemis, a 76 kDa nuclease, plays a role in cleavage of DNA termini during NHEJ [74].

Artemis, a member of the metallo-β-latamase family and the β-CASP subfamily of enzymes, has been shown to have DNA-PK dependent endonuclease activity on DNA hairpin structures, and DNA-PK dependent endonuclease processing of 3' and 5' single-strand overhangs, with preferential cleavage at the dsDNA/ssDNA junction [74].  While specific mechanistic models of Artemis endonuclease activation vary, it is clear that Artemis endonuclease activity is DNA-PK and ATP dependent. Artemis has also been suggested to possess an intrinsic 5'-3' DNA-PK independent exonuclease activity based on *in vitro* analysis of partially purified preparations of Artemis.  However, recent studies raise questions about wether Artmies has intrinsic exonuclease activity.  *In vitro* studies have identified the catalytic domain and then most recently, a specific amino acid required for endonuclease activity of Artemis. Interestingly, mutational analysis of several conserved residues within the catalytic

domain successfully disrupts the endonuclease activity, but each of these mutants still maintains robust exonuclease activity [103, 113]. This could be a result of Artemis having two independent catalytic sites within the polypeptide, one for each activity (endonuclease and exonuclease). However, this would make Artemis a unique enzyme within its family, as metallo-β-lactamase fold enzymes have been classified as only having one active that has been shown to be the functional catalytic site for all activities [114]. Furthermore, the exonuclease activity has not yet been shown to have a role *in vivo*, whereas the endonuclease activity has been demonstrated both *in vitro* and *in vivo* [115]. While a variety of purification protocols have been used to obtain a purified form of Artemis, all preparations to date still include both exonuclease and endonuclease activity.

There is currently considerable conflict in the field regarding classification of the activities of Artemis. Clearly, understanding the true nature of a protein's activity will lead to a greater understanding of the role of this enzyme in NHEJ. To resolve these apparent discrepencies, we pursued the fractionation of Artemis in a baculovirus expression system to determine of the exonuclease and endonuclease activities were biochemically separable. We developed a three step purification protocol which results in the separation of the exonuclease activity from the intrinsic endonuclease activity of Artemis. Biochemical analyses revealed that the exonuclease activity associated with Artemis is not intrinsic to the Artemis polypeptide.

## 4.2. Results

N-terminal [His]$_6$ tagged human Artemis was cloned and overexpressed in insect cells as described in Materials and Methods. Briefly, the full length Artemis

coding region from GenBank was cloned from a cDNA library using standard PCR techniques. The cDNA was then sub-cloned into the pRSET-C vector (Invitrogen) to generate a N-terminal [His]$_6$ tagged Artemis fusion construct. To generate a recombinant baculovirus for expression of [His]$_6$-Artemis in insect cells (Clontech), this construct was subcloned into the pBacPA8 vector to generate BacPAK8-Art-His (Figure 18). This construct was transfected into SF9 insect cells using Bsu36I-digested BacPAK6 viral DNA (Clontech). The recombinant virus generated from the transfected cells was collected, plaque purified, and expanded according to manufacturer's directions. This expanded recombinant virus was used to infect SF9 cells to generate expression of [His]$_6$-Artemis protein. Following overexpression, Artemis was fractionated by three steps including anionic exchange, nickel affinity and hydroxyapatite column chromatography (Figure 19A).

A cell-free extract was prepared from insect cells expressing human recombinant [His]$_6$-Artemis fusion protein. To detect Artemis overexpression in the cell-free extract, we analyzed the extracted protein by SDS-PAGE, western blot and phosphorylation by DNA-PK. Coomassie Blue staining of an SDS denaturing gel revealed expression of the [His]$_6$-Artemis protein (Figure 19B). This expression was further confirmed by western blot analysis, and this revealed a dominant band at the expected molecular mass (~110 kDa) for the recombinant His-tagged fusion protein. This analysis was performed with using both a monoclonal antibody against the N-terminal [His]$_6$ fusion tag (Figure 19C) and a polyclonal antibody against the full length Artemis polypeptide (data not shown). Artemis has been shown to have eleven serine/threonine residues that are phosphorylated by DNA-PK *in vitro* [73].

Schematic of Art cloning.
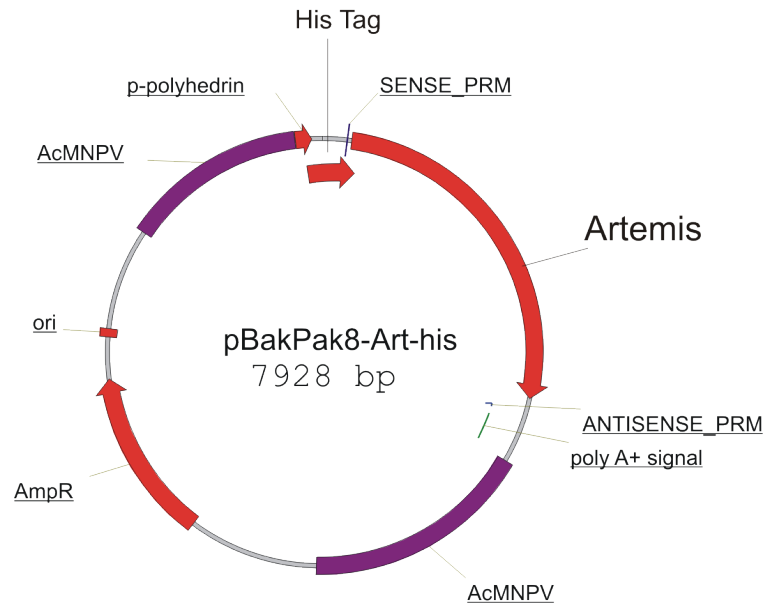


**Figure 18. Map of BacPAK-Art-His.** The Artemis gene with a N-terminal [His]$_6$ tag was subcloned into the BakPAK-8 vector for transfection into SF9 insect cells.
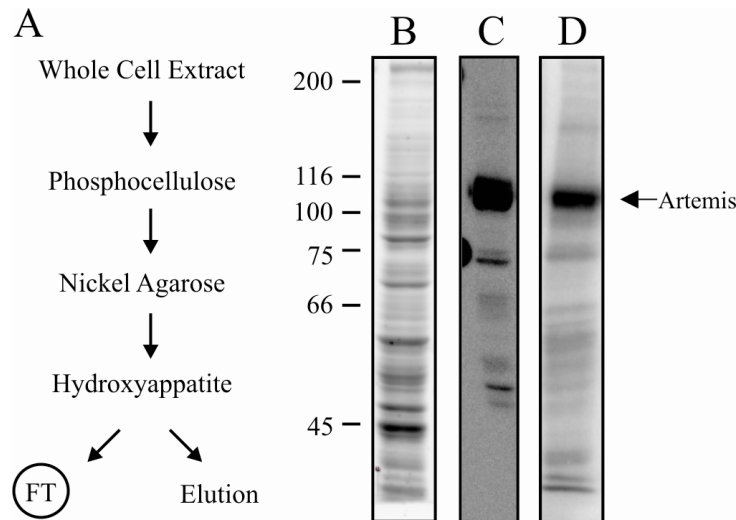
**Figure 19. Purification scheme for [His]$_6$-Artemis.** (A) A whole cell extract prepared from SF9 insect cells expressing [His[$_6$ –Artemis was fractionated over a phosphocellulose column. The flow-through was applied to a 2 mL Nickel-Agarose column, and [His]$_6$-Artemis was eluted with 200 mM imidazole. Pooled fractions were further fractionated over a 5mL hydroxyappatite column. The FT containing [His]$_6$-Artemis and elution containing exonuclease activity were collected from the HAP column. (B) Analysis of whole cell extract from SF9 insect cells containing over-expressed Artemis-[His]$_6$. Coomassie-stained SDS-PAGE gel of the whole cell extract (2.5 µg) made from insect cells infected with recombinant [His]$_6$-Artemis baculovirus. (C) Western blot analysis of whole cell extract (2.5 µg) using the anti-Xpress antibody, as described in Materials and Methods. (D) Phosphorylation of Artemis by DNA-PK was measured by incubating whole cell extract containing [His]$_6$-Artemis (5 µg) with 60 nM DNA-PK in presence of 100 nM 30-mer full duplex DNA, 125 µM ATP and 1.0 µCi [γ-$^{32}$P]-ATP as described in Materials and Methods. Reactions were terminated by addition of SDS, separated by 8 % SDS-PAGE, and the gel was dried and exposed to a PhosphorImager. Arrow depicts phosphorylated Artemis or DNA-PKcs product on each gel.

Therefore, to confirm that the baculovirus expressed [His]$_6$-Artemis that we made can be phosphorylated by DNA-PK, we conducted an *in vitro* DNA-PK phosphorylation reaction as described in Materials and Methods. Briefly, the cell-free extract was incubated with purified DNA-PK, double-strand 30-mer DNA to stimulate DNA-PK kinase activity, and [$\gamma$-$^{32}$P] ATP. Reaction products were separated by SDS-PAGE and incorporation of the radioactive phosphate into the Artemis protein was detected by PhosphorImager analysis. As seen with Commassie staining and western blot analysis, the kinase reaction resulted in a prominent band at the anticipated size for [His]$_6$-Artemis (Figure 19D). This band is indicative of DNA-PK-dependent phosphorylation of [His]$_6$-Artemis in the cell-free extract.

After preparation of the whole cell extract from insect cells infected with recombinant [His]$_6$-Artemis baculovirus, the potassium chloride concentration in the extract was increased to 0.5 M and subsequently mixed with phosphocellulose chromatography media, a cation exchange resin used to separate proteins based on charge via ion exchange. Raising the salt concentration up so high in the extract allowed for the majority of the protein in the extract (including [His]$_6$-Artemis) to flow through the matrix. This flow-through was collected and immediately loaded onto a 2 mL nickel-NTA agarose column, nickel-charged affinity resin that can be used to purify recombinant proteins containing a polyhistidine (6xHis) sequence like [His]$_6$-Artemis has. Following loading of extract, the column was washed extensively with high ionic strength buffer followed by low ionic strength buffer, both of which contained 5 mM imidazole. The washes were performed to eliminate non-specific, low affinity binding of proteins from the extract to the Ni-NTA column.

As his-tagged proteins bound to a Ni-NTA protein can be eluted by competition with imidazole, the bound protein was eluted with buffer containing 200 mM imidazole and collected in 1 mL fractions. Analyses of eluted proteins showed that the majority of $[His]_6$-Artemis bound to the Ni-NTA agarose matrix and was eluted with 200 mM imidazole. The load, flow-through and eluate from the nickel column were analyzed by SDS-PAGE and stained with Coomassie Blue (Figure 20A). Further verification was performed by western blot analysis (Figure 20B ) and phosphorylation by DNA-PK (Figure 20C). Each assay revealed that the majority of the Artemis applied to the column was retained in the imidazole elution (Figure 20A-C, compare lanes 1 and 3). Importantly, as this procedure was repeated several times, we discovered that retention of Artemis on the Ni-matrix was extremely sensitive to chromatographic conditions to the presence of reducing agents, with greater than anticipated amount of Artemis remaining in the flow-through under less than optimal conditions (data not shown). Thus, reducing agents should be avoided in purification buffers in an effort to maximize protein yield. While the results from fractionation over a Ni-NTA column indicate a degree of purity of $[His]_6$-Artemis, the Coomassie Blue stained gel and phosphorylation assay reveal significant impurities in the eluate. While not necessarily a surprising result, these results indicate the need for further fractionation to achieve a higher degree of purity.

In our attempts to further purify $[His]_6$-Artemis, the majority of the matrices at our disposal were assessed, including various anion (DEAE and Q-sepharose matrices) and cation exchanage chromatography (S-sepharose matrix), adsorption chromatography (Heparin-sepharose matrix) as well as hydrophobic interaction
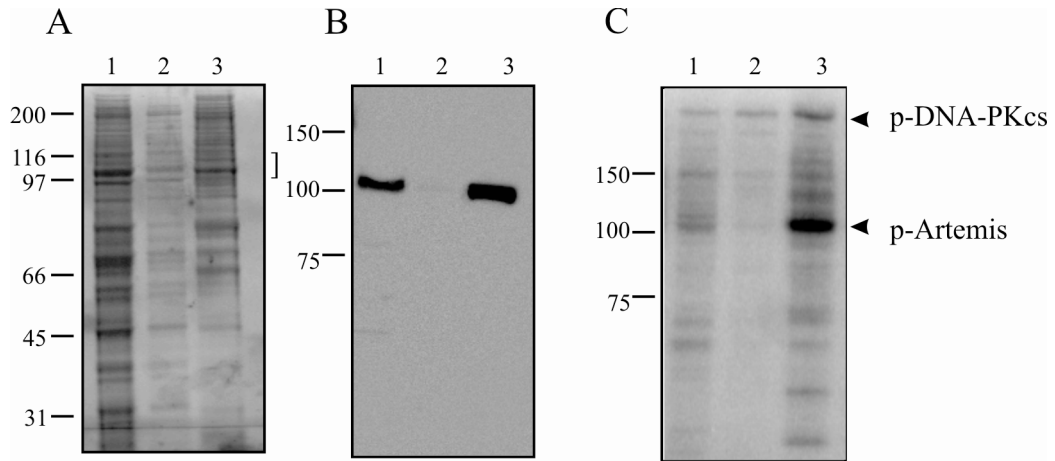
**Figure 20. Analysis of fractionation on a Nickel-Agarose column.** (A) Coomassie-Blue stained 8 % SDS-PAGE of pools from Nickel-Agarose column. The bracket indicates anticipated position of [His]$_6$-Artemis migration. (B) Western blot analysis using the anti-Xpress antibody against a portion of the 6xHis tag (Invitrogen). (C) Phosphorylation of Nickel-Agarose pools by DNA-PK. For A, B and C, Lane 1, Nickel-Agarose load, Lane 2, Nickel-Agarose flow-through, Lane 3, Nickel-Agarose pool. All assays were conducted as described in legend for Fig. 19 and arrows indicate migration the position of Artemis.

chromatography (Phenyl-sepharose matrix). The results from these matrices were universally poor (data not shown). However, fractionation by adsorption chromatography on a hydroxyapatite (HAP) matrix resulted in substantial purification of [His]$_6$-Artemis. HAP matrix consists of positively charged calcium ions and negatively charged phosphate groups. The protein-matrix interaction is complicated, but briefly, involves attraction of the positively charged amino groups and negatively charged carboxyl groups in protein to the negatively charged phosphate ions and positively charged calcium ions in the matrix. Typically, bound protein is eluted off HAP matrix by increasing phosphate concentration in a buffer with a pH of 6.5-7.0. It is important to point out that the success rate of separation on this column was achieved at a relatively high pH of 7.8. The majority of total protein applied (greater than 90 %) was retained on the HAP column, but interestingly the majority of [His]$_6$-Artemis was not retained on the HAP column and instead was found to be in the flow-through fractions. Western blot analysis of the flow-through fractions (Figure 21A) and elution fractions (21B) confirmed that the vast majority of [His]$_6$-Artemis was recovered in the flow-through fractions. Furthermore, Coomassie Blue staining of SDS-PAGE with the HAP load and flow-through fractions confirmed that the HAP FT pool had overall decreased non-specific protein while retaining Artemis (Figure 21C). Unfortunately, [His]$_6$-Artemis overexpression in baculovirus does not result in rampant overexpression of the protein, so definitive identification of Artemis by Coomassie Blue staining of SDS-PAGE is difficult. However, the Artemis containing flow-through fractions were pooled and Artemis levels in each were determined by the more quantitative *in vitro* phosphorylation analysis.
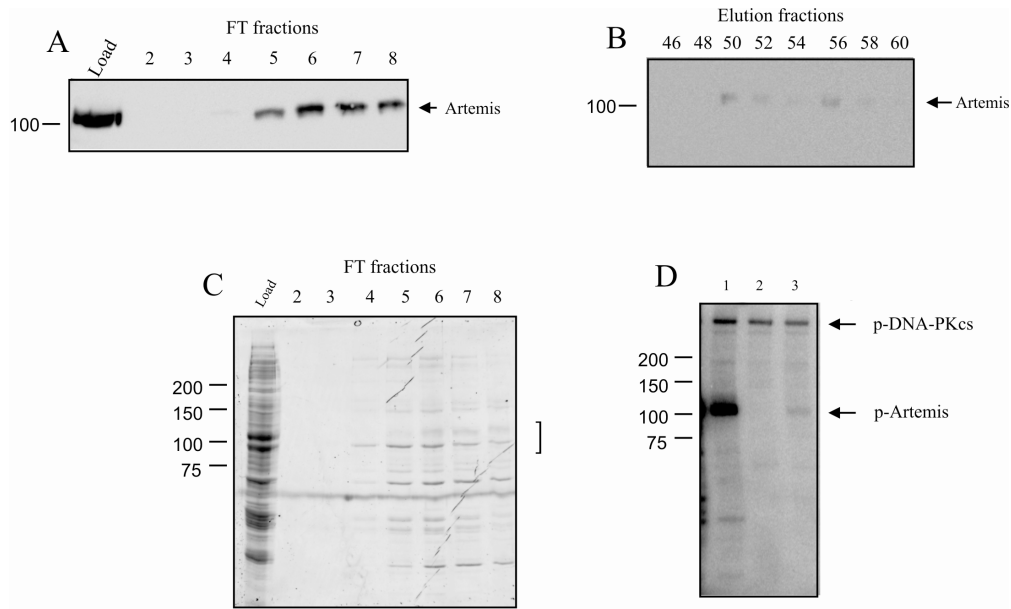
**Figure 21. Analysis of hydroxyapatite (HAP) column fractionation of Artemis.**
(A) Western blot analysis of load and flow through fractions and (B) fractions
obtained from the gradient elution. Aliquots of each fraction were separated by SDS-
PAGE, transferred, probed with anti-Xpress antibody and detected as described in
"Methods". (C) Coomassie-Blue stained SDS-PAGE analysis of the load and flow-
through fractions. Samples were processed as described in "Methods". The bracket
indicates anticipated position of [His]$_6$-Artemis migration. (D) Phosphorylation of
[His]$_6$-Artemis by DNA-PK. Reactions were performed as described in the legend
for Figure 19. Lane 1, HAP flow-through pool (140 ng), Lane 2, DNA-PK control
without Artemis. Lane 3, HAP elution pool (190 ng). Arrows indicate phosporylated
[His]$_6$-Artemis and DNA-PKcs.

This confirmed that the overwhelming majority of the Artemis protein was present in the flow-through pool and could be successfully phosphorylated by DNA-PK (Figure 21D, lane 1), as compared to control reactions without the HAP FT (lane 2). Phosphorylation of the protein in the HAP elution pool by DNA-PK revealed little to no phosphorylation of Artemis, suggesting that no Artemis protein was eluted from this column (lane 3).

Having confirmed the presence of the Artemis polypeptide following fractionation over a HAP column, we wanted to determine how HAP fractionation affected the retention of 5'-3'exonuclease activity, postulated to be an intrinsic enzymatic activity of Artemis. To determine exonuclease activity, we assayed the column fractions from the HAP column for 5'-3' exonuclease activity using a 34-base single-strand oligonucleotide with a 5' [$^{32}$P]-label. The release of a 5' radiolabeled nucleoside monophosphate is a direct measure of any 5'-3' exonuclease activity (Figure22A). Nuclease products are visualized by separating the reactions on a denaturing gel as described in Materials and Methods. Surprisingly, the majority of the exonuclease activity was resolved in six fractions that bound to the column and were then subsequently eluted during the phosphate gradient. Minimal exonuclease activity was found in the flow through fractions (Figure 23A). Quantification of the gel-based exonuclease assay further demonstrate that a small portion of the overall exonuclease activity loaded onto the HAP column was identified in the flow-through, while the majority was located in the eluate (Figure 23B). It is important to note that measurement of the bound exonuclease activity is potentially an underestimation, as all of the substrate was completely degraded in the peak elutions (fractions 48-50,

Figure 23A and 23B).  The exonuclease containing fractions were pooled and

quantitative nuclease and Artemis expression analysis was performed.  The percent of

total antibody reactivity or exonuclease activity resolved in the two pools of protein

(flow-through and elution) was determined and the results demonstrate that greater

than 90 % of Artemis protein loaded onto the HAP column was recovered in the HAP

flow-through material, while less than 10 % was recovered in the gradient elution

pool.  In accordance with Figure 23A and 23B, only 10 % of the overall exonuclease

activity loaded onto the HAP column was identified in the flow-through, while 90 %

of it was located in the eluate (Figure 23C).  As seen in Figure 21, the majority of the

Artemis polypeptide was found in the flow-through fractions and minimal Artemis

was in the elutions, while enzymatic results show that the majority of exonuclease

activity is in the elutions and not the flow-through.  These results suggest that $[His_6]$-

Artemis does not bind to a HAP column under specific fractionation conditions while

the majority of exonuclease activity remains bound under these same conditions and

can be eluted with high phosphate.

Discussions with colleagues within the field led to questions concerning the

origination of the exonuclease activity found in our Artemis prep.  We designed a

purification experiment to determine whether the exonuclease activity is a

contaminating nuclease that has a high affinity for a nickel-agarose column.  To

accomplish this, we overexpressed another His-tagged DNA repair protein, XPA,

using recombinant baculovirus.  This DNA-binding protein, frequently used in our

lab, has no intrinsic nuclease activities and minimal protein interaction domains.

Following expression of recombinant $[His]_6$-XPA in insect cells using baculovirus
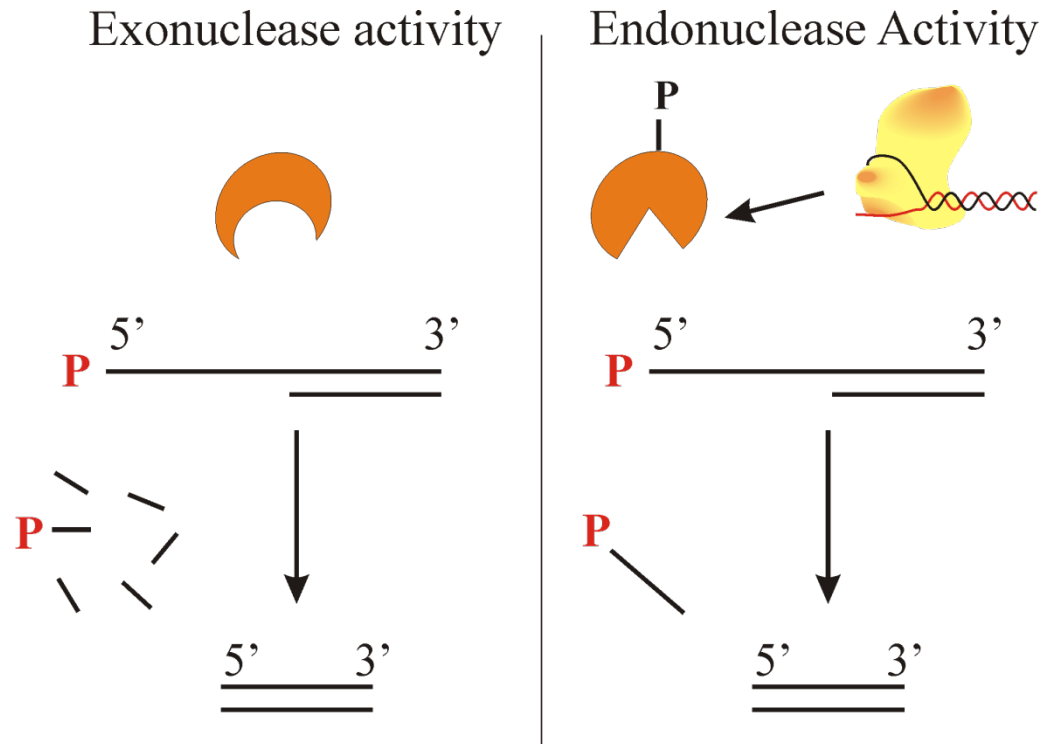
**Figure 22.  Exonuclease activity and DNA-PK dependent endonuclease activity.**
(A) Exonuclease activity.  Exonucleases cleave phosphodiester bonds at the end of
polynucleotide chains.  (B) Endonucleases cleave phosphodiester bonds internally,
producing polynucleotide or oligonucleotides.  The nuclease Artemis cleaves
phosphodiester bonds internally to produce oligonucleotide fragments in the presence
of DNA-PK and ATP.
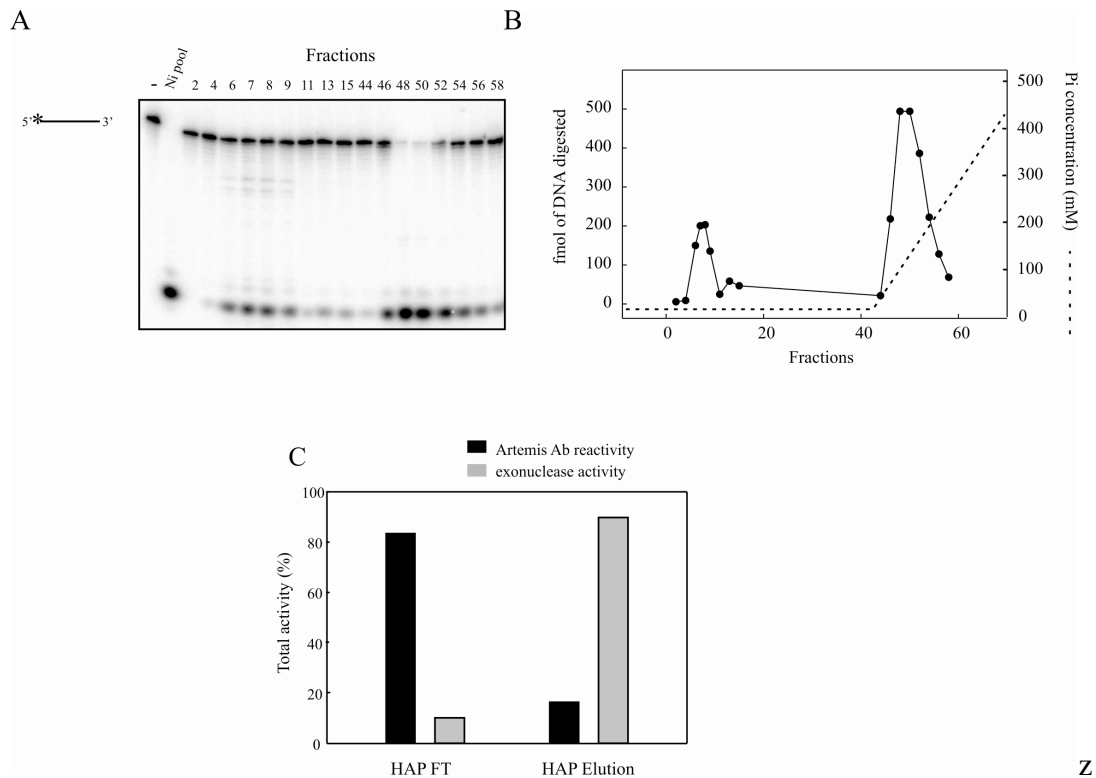
**Figure 23. Quantitative assessment of exonuclease activity from HAP fractionation of [His]$_6$-Artemis.** (A) A 2 µL aliquot of each 1mL HAP fraction from a [His]$_6$-Artemis purification was assayed for exonuclease activity using a 5'[$^{32}$P] labeled single-strand DNA 30 bases in length. Reaction products were separated and visualized as described in Materials and Methods. (B) Quantification of exonuclease activity from (A). (C) Quantified antibody reactivity and exonuclease activity from the HAP flow-through and HAP elution pools. Total intensity of antibody reactivity was obtained from MultiGauge analysis (Fuji) of representative western blots and total exonuclease activity was quantified using ImageQuant (Amersham) analysis of product released.

expression system, a whole cell extract was prepared under the same conditions and procedures as for $[His]_6$-Artemis and the identical purification protocol that was used for overexpressed $[His]_6$-Artemis was applied to $[His]_6$-XPA fractionation. Following fractionation over the nickel-agarose column and HAP column, fractions were assayed for exonuclease activity on a radiolableled DNA substrate. Robust exonuclease activity was seen in the whole cell extract as well as in nickel-agaorse elution fractions. Fractions from the nickel-agarose elution containing exonuclease activity and subsequently XPA protein were pooled and further fractionated over a HAP column as described for $[His]_6$-Artemis. As seen with the $[His]_6$-Artemis preps, exonuclease assays from the HAP column loaded with XPA again revealed a minimal amount of exonuclease activity flowing through the column (Figure 24A and 24B). In addition, the peak of exonuclease activity eluted from the HAP column with the phosphate gradient coincides exactly with the peak of exonuclease activity eluted from the HAP column in the $[His]_6$-Artemis prep. Importantly, the low level of exonuclease activity seen flowing through the HAP column coincides with the low level of exonuclease activity seen flowing through the HAP column from the $[His]_6$-Artemis prep (compare Figures 23 and 24). In order to further demonstrate that Artemis was not in the pool of protein with exonuclease activity, protein pools from the nickel-agarose elution, HAP flow-through and HAP elution were examined for DNA-PK dependent endonuclease activity. All pools were completely devoid of DNA-PK dependent endonuclease activity (Figure 25).

Following our discovery of exonuclease separation via fractionation over a HAP column, we performed scrupulous quantitative analysis on the nickel-agarose
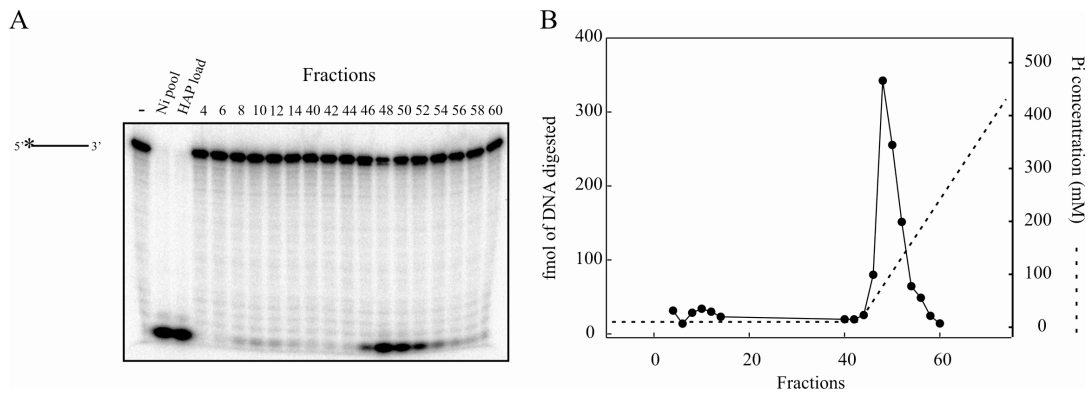
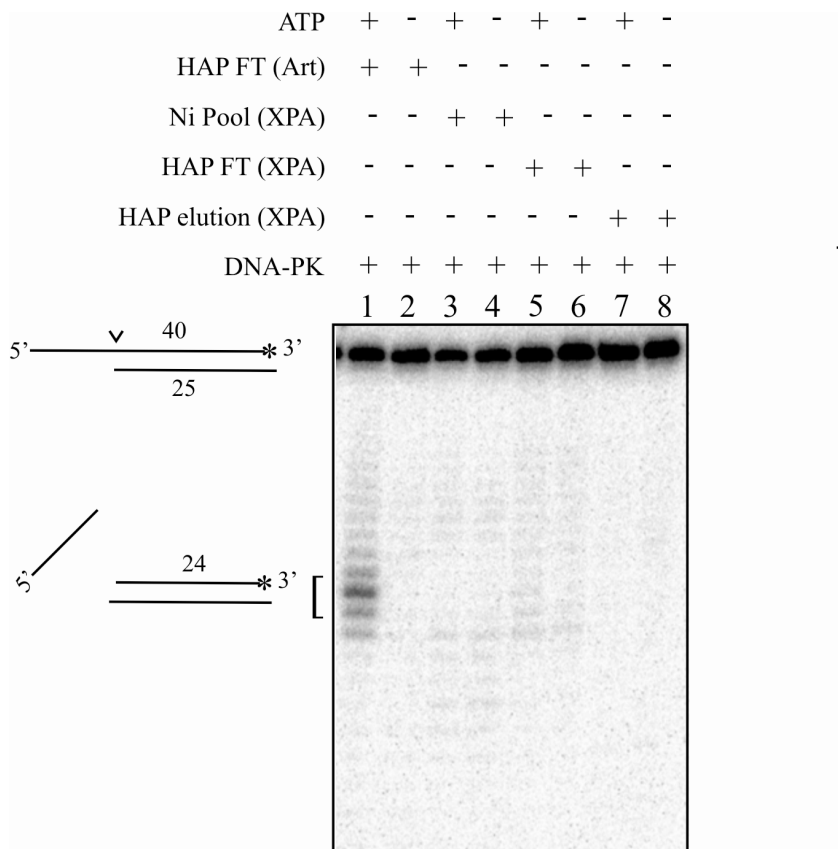**Figure 24. Quantitative assessment of exonuclease activity from HAP fraction of a [His]$_6$-XPA.** (A) A 2 µL aliquot of each 1mL HAP fraction from a [His]$_6$-XPA purification was assayed as described in Figure 23. (B) Quantification of exonuclease activity from (A).

**Figure 25. Analysis of endonuclease activity on a 3' radiolabeled DNA substrate with a 5' single-strand overhang from [His]$_6$-XPA preparation.** Reaction conditions were conducted as described in "Methods and Materials". The DNA substrate is depicted above the gel and the position of the [$^{32}$P] label is denoted by the asterisk and the position of Artemis endonuclease activity is denoted by the carat. DNA strand lengths of each DNA substrate are also noted in the figure. A positive control demonstrating ATP dependent endonuclease activity in the HAP FT fraction from a [His]$_6$ Artemis preparation is presented in lanes 1 and 2, while no endonuclease activity is observed in any fractions from the XPA preparation 3-8.

elution and HAP FT pools of protein to ensure that separation of enzymatic activities occurred. A portion of each pool of protein, nickel-agarose elution and HAP FT, was dialyzed into identical buffer made up of 50 mM Tris pH 7.5, 200 mM KCl, 20 % glycerol and 1 mM DTT and succumbed to a battery of assays. Dialysis into identical buffer was performed in an effort to minimize any difference in reaction conditions from the different buffers each pool of protein had originally been in that could affect enzymatic activities (inhibitory or stimulatory) of the pools of protein. Comparison of the Ni pool and HAP FT by western blot analysis revealed the presence of a significant level of Artemis in each pool, as expected (Figure 26A) and this was confirmed by analysis of DNA-PK phosphorylation of each pool (Figure 26B and 26C). These results definitively prove that the Artemis polypeptide is located in both pools of protein from the nickel and HAP columns.

As previously explained, the flow-through fractions from the HAP column retained minimal exonuclease activity on single-strand DNA, an activity in the literature previously attributed to the Artemis polypeptide (lieber cell 2002). As seen in Figure 26, each pool of protein contained [His]$_6$-Artemis and we wanted to directly compare the exonuclease activity in each pool of protein, Ni and HAP FT. Increasing amounts of the nickel pool of protein and the HAP FT pool of protein were incubated with a 5' radiolabeled oligonucleotide and release of the 5' deoxynucleoside monophosphate (dNMP) was monitored. Increasing concentrations of Ni pool containing Artemis resulted in increased 5'-3' exonuclease activity. In contrast, the Artemis containing HAP flow-through pool revealed an NMP product that was barely above the detection limit of our assay. These results demonstrate that the HAP FT

96
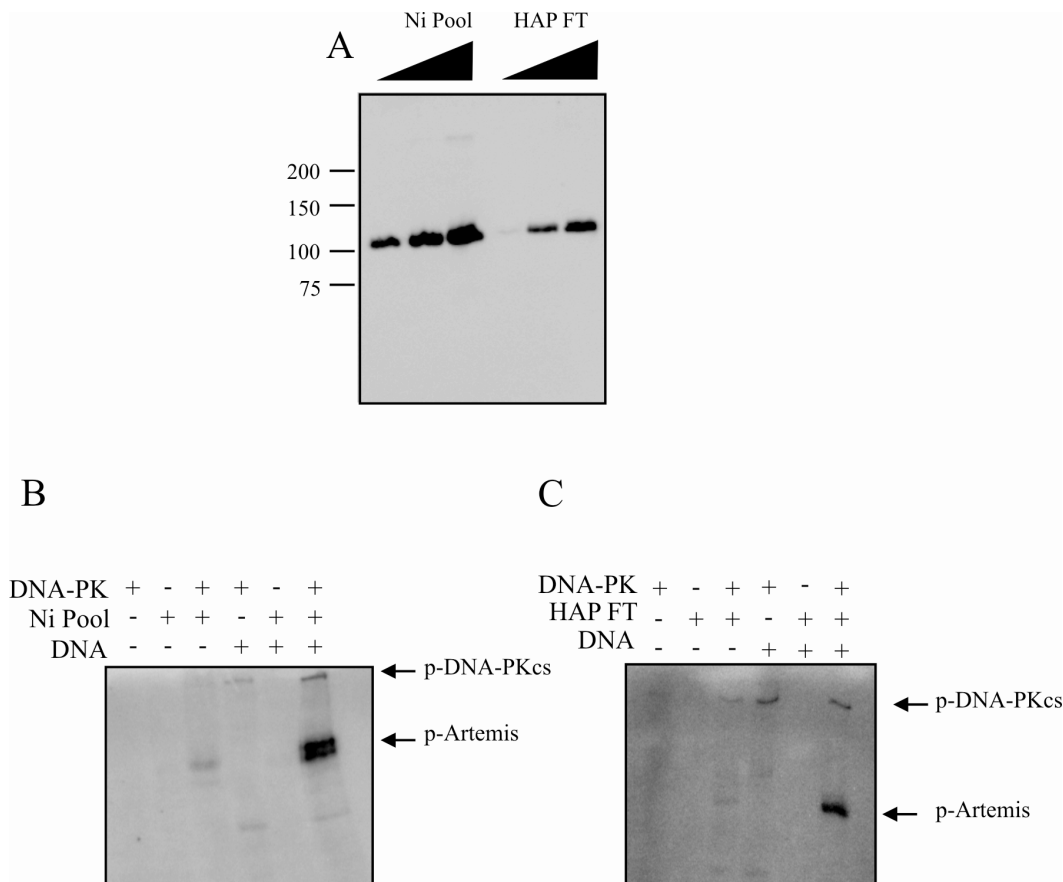
**Figure 26. Identification of [His]$_6$-Artemis polypeptide in Nickel-Agarose and HAP flow-through pools of protein.** (A) Western blot analysis. Nickel-Agarose pool (200 ng, 1 µg and 2 µg) and HAP flow-through (10 ng, 20 ng and 50 ng) were analyzed by Western blot using an anti-Artemis antibody. DNA-PK phosphorylation of Nickel (B) and HAP FT (C) pool of protein. *In vitro* phosphorylation reactions were conducted as described in Materials and Methods and contained DNA-PK, [His]$_6$-Artemis and DNA as indicated. Reaction products were separated via SDS PAGE and products visualized by phosphorImager analysis.

97

pool of protein does not contain 5'-3' exonuclease activity (Figure 27A). It is necessary to point out that there are preparation specific variations of exonuclease activity, and differences observed in the analysis of column fraction versus pools. Despite these differences, it is evident from results that the majority of the HAP polypeptide was flowing through the HAP column and this pool of protein was devoid of the majority of exonuclease activity.

The more relevant activity of Artemis, found both *in vitro* and *in vivo*, is the DNA-PK dependent hairpin-opening activity and the 5' and 3' overhang endonuclease activity. In an effort to ensure that the HAP FT pool of $[His]_6$-Artemis devoid of exonuclease activity still retained its endonuclease activity, the Ni and HAP FT pools of protein were assayed for hairpin-opening activity. To conduct these assays, a 5' radiolabeled hairpin substrate containing a 6 base 5' overhang was incubated with Ni or HAP FT pools of protein, buffer, heterotrimeric DNA-PK. 30-mer double-strand DNA was also added where indicated, as it has been reported that Artemis exhibits increased endonuclease activity when double-strand DNA is incubated in the reaction so as to increase kinase activity of DNA-PK, thus increasing phosphorylation of Artemis. Previous groups have shown that DNA-PK dependent Artemis endonuclease cleavage of this hairpin substrate yields a product of approximately 28 bases in length [74]. Both the Ni pool and HAP FT pools of protein catalyzed hairpin-opening activity in the presence of ATP and DNA-PK on this substrate (Figure 27B, lanes 6 and 7 and lanes 10 and 11, respectively). Interestingly, there is slightly more endonuclease activity in the HAP FT pool of protein, as evidenced by the slightly more prominent cleavage product (Figure 27B,

lanes 10 and 11).  It is important to point out that this could be from the lack of

exonuclease activity in the HAP FT, which would necessarily result in less

endonucleolytic removal of the 5' label on the cleavage product thus creating a darker

band at this product size.  Interestingly, the presence of the 30-mer cold double-strand

substrate does not seem to result in increased cleavage product with this substrate

(Figure 27B, lane 8), and this result will be discussed further in conclusion.  Also

evident, though of reduced intensity compared to the hairpin opening activity, are

products that range in size from 5-7 nucleotides and are postulated to result from the

5' overhang cleavage activity of Artemis.  Importantly, the 5' dNMP product

produced by exonuclease activity cleaving the 5' label on the hairpin substrate is

evident in reactions performed with the nickel pool, but is substantially reduced in

reactions performed using the HAP flow-through fractions.  This result is clearer

following reduced exposure of the gel to minimize bleed-over from the Ni pool

fractions (Figure 27B, bottom panel).  These results show that separation of

exonuclease activity from DNA-PK dependent Artemis endonuclease activity occurs

following fractionation over a HAP column.

We were concerned that the radiolabeled products from a substrate containing

a 5' radioactive label observed in Figure 27A were potentially being misinterpreted.

Despite experimental precautions taken, it was difficult to determine if the

radiolabeled product at the bottom of the gel (Figure 27A) was actually a dNMP or a

larger product.  To ensure that the dNMP products observed (from the Ni pool) were

in fact the result of exonuclease activity and not a dinucleotide product produced by

an endonuclease activity, we assessed nuclease activity of each pool of protein on a
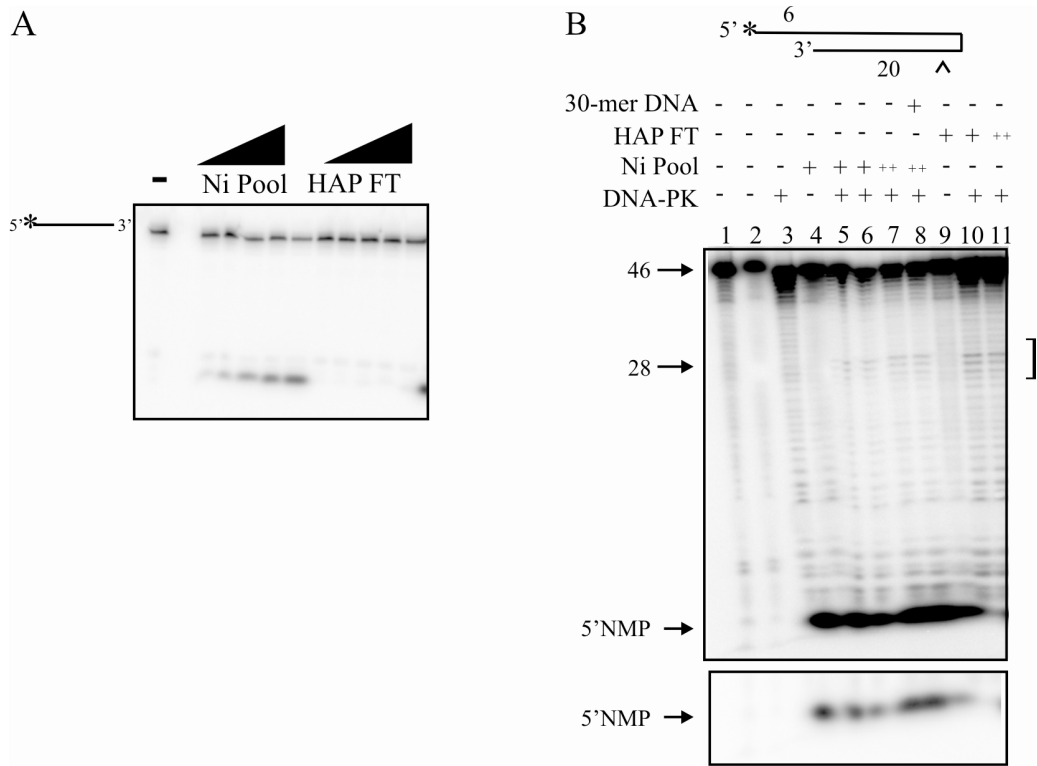
**Figure 27.  Biochemical characterization of Nickel-Agarose and HAP flow-through pools of [His]$_6$-Artemis.** (A) Analysis of [His]$_6$-Artemis Ni pool and HAP FT exonuclease activity on 30 base 5' radiolabed single-strand DNA.  Increasing amounts of Ni pool (100 ng to 1 µg) or HAP FT (5 ng to 50 ng) pool was assayed for exonuclease activity using 50 fmol of 5' [$^{32}$P] single-strand DNA substrate as described in Materials and Methods.  (B) Analysis of hairpin opening activity.  Ni pool (400 ng and 1 µg) or HAP FT (20 ng and 50 ng) was incubated with 250 fmol of 5' radiolabeled hairpin DNA substrate, 200 nM double-strand cold DNA (30-mer), and 50 nM of DNA-PK as indicated.  Following endonuclease cleavage, reaction products were separated and visualized as described in Materials and Methods.

100

single-strand DNA substrate with a 3' radiolabeled terminus. Increasing amounts of the nickel pool of protein resulted in a ladder of products that was consistent with sequential single nucleoside monophosphate removal from the 5' terminus of the oligonucleotide (Figure 28A). The HAP FT pool of protein contained barely detectable 5'-3' single-strand exonuclease activity, consistent with activity seen in this pool in Figure 27A. Importantly, overexposure of the gels in Figures 27A and 28A did reveal products indicative of low levels of exonuclease activity, but this activity comprised less than 1 % of those seen in Ni pool. These results confirm that while [His]$_6$-Artemis fractionated over a nickel column retains significant 5'-3' exonuclease activity, subsequent fractionation of this protein over a HAP column results in near quantitative separation of the exonuclease from the Artemis protein.

As it appears that [His]$_6$-Artemis fractionated over a HAP column is devoid of 5'-3' exonuclease activity but still has hairpin opening activity, we wanted to examine DNA-PK dependent Artemis overhang cleavage activity to ensure that all *in vivo* intrinsic enzymatic activities are retained in this purified preparation of protein. To accomplish this, we prepared a 5'-radiolabeled DNA substrate with a 3' single-strand overhang. It has been previously reported that in the presence of DNA-PK and ATP, Artemis cleaves this substrate close to the single-strand/double-strand junction, resulting in a cleavage product around 26 bases long [74]. Incubation of this overhang substrate with DNA-PK, ATP and the two pools of [His$_6$-Artemis] protein resulted in a 26 base cleavage product, and as expected this was dependent on DNA-PK and ATP (Figure 28B, lanes 4, 5 and 6 and lanes 8, 9 and 10). Again, the 5' NMP product is apparent in reactions performed with the nickel pool of protein but is

A

B

C
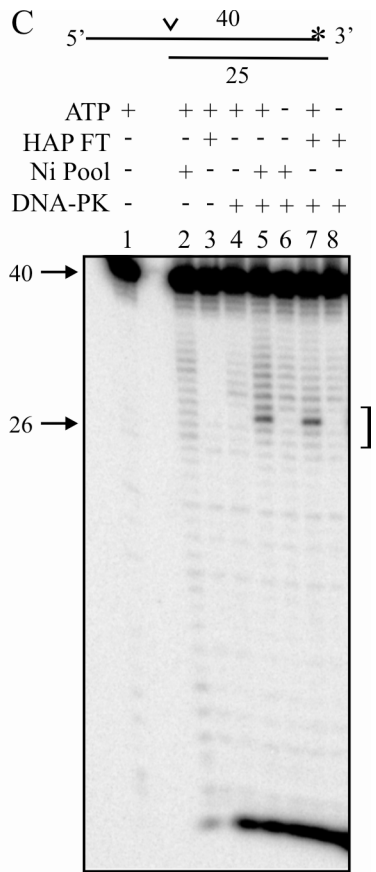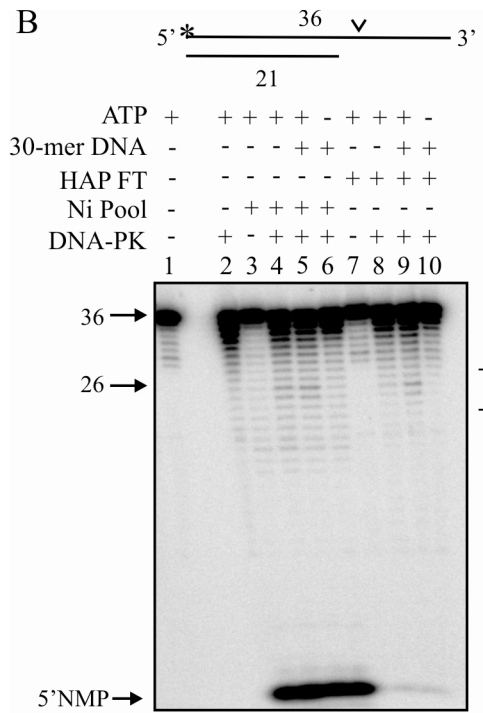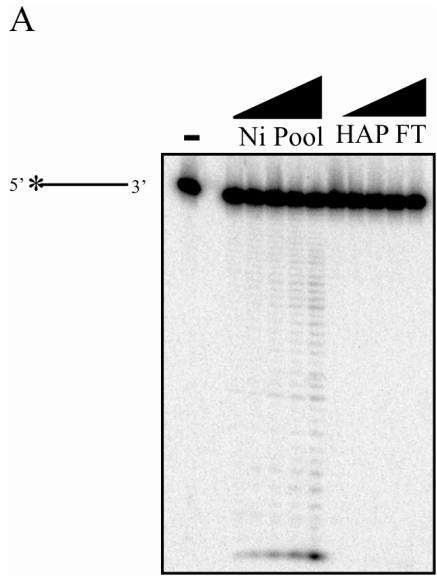
**Figure 28. Characterization of Artemis nuclease activity.** (A) Analysis of Ni pool and HAP FT exonuclease activity on single-strand DNA with a 3' $^{32}$P label. Assays were conducted as described in the legend to figure 4B), except the single-strand oligonucleotide was radiolabeled by incorporation of [α-$^{32}$P] on the 3' termini. (B) Analysis of endonuclease activity on a 5' radiolabeled DNA substrate with a 3' single-strand overhang. Reactions were conducted as described in 4C, except Ni pool, HAP FT, 250 µM of ATP and 200 nM of cold duplex DNA (30-mer) were added as indicated. (C) Analysis of endonuclease activity on a 3' radiolabeled DNA substrate with a 5' single-strand overhang. Reaction conditions were conducted as described in "Methods and Materials". Each DNA substrate is depicted above the gel and the position of the [$^{32}$P] label is denoted by the asterisk and the position of Artemis endonuclease activity is denoted by the carat. DNA strand lengths of each DNA substrate are also noted in the figure. The 5' nucleoside monophosphate product (5' dNMP) is indicated by the arrows in panel B.

reduced to background levels in reactions containing the HAP flow-through pool

(Figure 28B, compare lanes 3-6 to lanes 7-10). For further verification of

endonuclease activity, a DNA substrate with a 5' single-strand overhang and a 3' [α-

$^{32}$P] dCMP label was used to assay endonuclease activity on a 5' overhang. Previous

results have shown that in the presence of DNA-PK and ATP, Artemis

endonucleolytically cleaves this substrate close to the single-strand/double-strand

junction resulting in a cleavage product of approximately 24-26 nucleotides long

(lees-miller paper). In the presence of DNA-PK and ATP, both the nickel pool of

protein and the HAP FT pool endonucleolytically cleaved the 5' overhang (Figure

28C, compare lanes 5 and 6 and lanes 7 and 8, respectively). In our hands, the

resulting cleavage product is 26 nucleotides. A product that is consistent with

exonuclease activity appears at the bottom of the gel, but only appears in lanes that

contain DNA-PK in them, including but not limited to the lane that contains DNA-PK

alone (Figure 28C, lane 4), this product is attributed to a contaminating 3'

exonuclease from our preparation of DNA-PK from Hela cells. The combined data

from Figures 27 and 28 demonstrate that both the Ni and HAP FT pools of protein

maintain DNA-PK and ATP dependent hairpin opening and endonuclease activity on

single-strand overhangs, identical to the activity previously reported on Artemis.

However, while the Artemis polypeptide is in both these pools of protein (Figure

26A), the HAP FT pool of protein no longer exhibits single-strand exonuclease

activity despite the fact that it retains DNA-PK dependent endonuclease activity.

These results show that our purification procedure results in biochemical separation

of exonuclease activity from Artemis, and further suggest that the exonuclease activity previously attributed to Artemis is not an intrinsic part of the polypeptide.

In an effort to thoroughly ensure that we separated exonuclease activity away from Artemis, exonuclease and endonuclease activities were tracked throughout the HAP column, 100 % of the endonuclease activity is recovered in the HAP FT pool, resulting in a 30-fold level of purification (Table 2).  However, only 2.5 % of the exonuclease activity is retained in the same HAP FT pool, with no increase in specific activity despite the loss of 96 % of the total protein.  These results are consistent with successful biochemical separation of the exonuclease activity from the Artemis polypeptide while maintaining DNA-PK dependent endonuclease activity, thereby indicating that exonuclease activity is not an intrinsic component of the Artemis polypeptide.

Having obtained a preparation of Artemis that we believe to be more enzymatically pure than any other lab has previously obtained, we were anxious to pursue further experiments to assess the role of DNA-PK dependent Artemis catalyzed nuclease activity on a variety of DNA substrates containing different structures, sequences and regions of microhomology.  The substrates used in endonuclease assays discussed above were all previously published substrates and so activity of Artemis on these substrates has been characterized.  Unfortunately, these substrates are not necessarily reminiscent of a DNA termini at the site of an IR induced DNA DSB.  A DNA substrate physiologically mimicking IR induced DSB is anticipated to have a much shorter DNA overhang.  As a substrate with shorter overhangs has not been studies by any other lab, we assessed more physiologically

| Endonuclease activity | | | | | |
|---|---|---|---|---|---|
| Fraction | Protein (mg) | Specific activity (units/mg) | Total activity (units)* | Purification -fold | Yield % |
| Ni Pool | 1.2 | 1.57 | 1883.45 | 1.00 | 100.00 |
| HAP FT | .04 | 47.01 | 1880.30 | 29.95 | 99.83 |

| Exonuclease activity | | | | | |
|---|---|---|---|---|---|
| Fraction | Protein (mg) | Specific activity (units/mg) | Total activity (units)* | Purification -fold | Yield % |
| Ni Pool | 1.2 | 27.00 | 32400.00 | 1.00 | 100.00 |
| HAP FT | .04 | 20.00 | 800.00 | 0.74 | 2.47 |

**Table 2.** Purification table of [His]$_6$-Artemis protein preparation.

relevant DNA substrates with 6-base single-strand overhangs. In an effort to measure endonuclease activity on a DNA substrate that more closely resembles a DNA terminus following IR, we assessed cleavage of a 24-base double-strand substrate with a 6-base 5' single-strand overhang and a 3' [$\alpha$-$^{32}$P] dCMP label (KSP 11.3/5'30). In an effort to avoid any sequence bias that might exist, the single-strand overhang region is made up of a mixed nucleotide sequence. Results show that in the presence of DNA-PK and ATP, Artemis cleaves this substrate at the double-strand/single-strand junction to create a product of 24 bases (Figure 29, lane 4). This is evidence that Artemis is capable of cleaving shorter DNA overhangs like the types of overhangs one would expect to see at the site of an IR induced DNA DSB. We went on to asses two additional DNA substrates that were identical to the substrates in Figure 29 except with homopolymeric overhangs, one with a 6-base 5'A overhang (KSP 11.3/5'24+6A) and one with 6-base 5'T (KSP 11.3/5'24+6T) (Figure 30). Again, Artemis was able to efficiently cleave the 6-base overhang on these two substrates, but the cleavage product was not as homogeneous as the product observed in Figure 29, where the predominant cleavage product was 24 bases long. In Figure 30, cleavage products are more heterogeneous, with cleavage products that vary between 23 and 25. While it appears that Artemis can still cleave these two substrates at the double-strand/single-strand junction (24 bases), cleavage is also occurring at n+1 and n-1 positions. As the only difference between these two substrates and the one assessed in Figure 29 is sequence, it is presumed that this difference in cleavage pattern is a result of a sequence bias. Furthermore, there appears to be greater cleavage of the DNA substrate with a 5' T overhang (Figure 30, lanes 2 and 13).

107
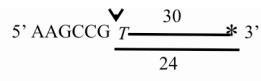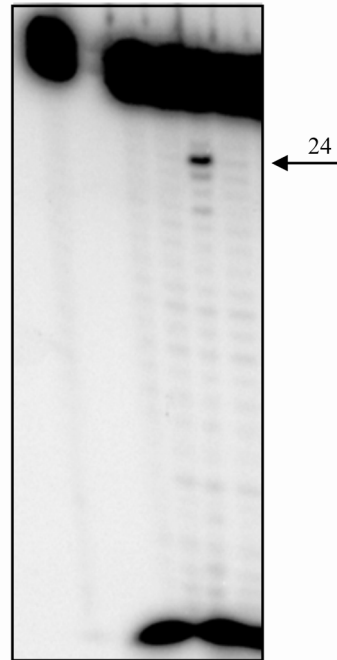
**Figure 29. Characterization of Artemis endonuclease activity on a short DNA overhang substrate.** Artemis endonuclease cleavage of 3' radiolabeled 6-base 5' single-strand overhang with a 24 basepair region was analyzed. Reaction conditions were conducted as described in "Methods and Materials". The DNA substrate is depicted above the gel and the position of the [$^{32}$P] label is denoted by the asterisk and the position of Artemis endonuclease activity is denoted by the arrow.
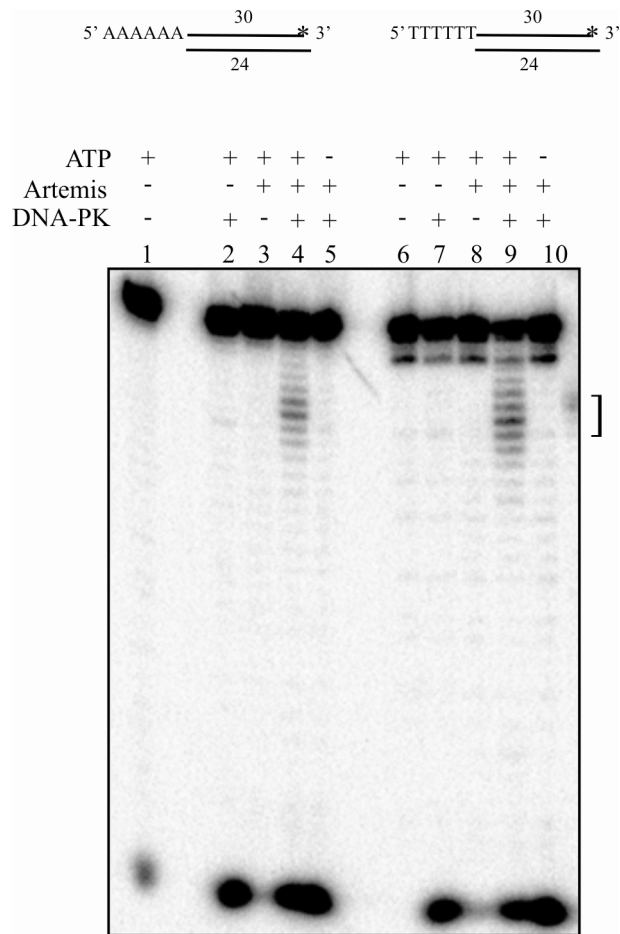
**Figure 30.  Characterization of Artemis sequence bias on short DNA overhang substrates.**  Artemis endonuclease cleavage of 3' radiolabeled 6-base single-strand overhang of 5' A or 5'T was analyzed.  Reaction conditions were conducted as described in "Methods and Materials".  The DNA substrates are depicted above the gel and the position of the [$^{32}$P] label is denoted by the asterisk and the position of Artemis endonuclease activity is denoted by the bracket.

In order to further explore Artemis sequence bias, DNA substrates with homopolymeric sequences of A or T in a 15-base 5' single-strand overhang region were analyzed (KSP 11.1/11.0C and KSP 11.2/11.0C). While both substrates were cleaved by Artemis, results clearly show a cleavage sequence bias, with 5'T substrates preferentially cleaved compared to 5'A (Figure 31). This is supported by recent data showing that Artemis possesses DNA-PK dependent endonuclease activity on single-strand DNA, with a sequence preference favoring cleavage of thymidines [108]. In summary, analysis of Artemis mediated cleavage reveals that this nuclease is capable of cleaving much shorter overhang regions than those previously published, and both the cleavage activity and pattern of cleavage is affected by length and sequence. Further studies with DNA substrates of different length and sequence will reveal the intricacies of Artemis cleavage and potentially indicate a mechanism of Artemis-DNA interaction.
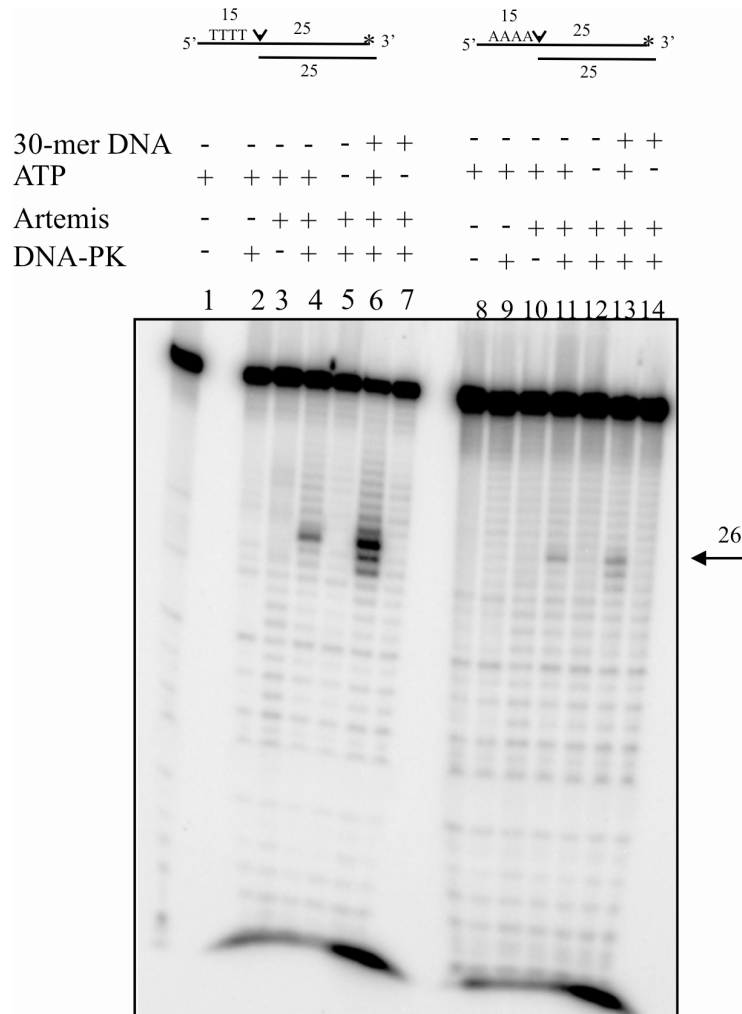
**Figure 31. Characterization of Artemis sequence bias on long DNA overhang substrates.** Artemis endonuclease cleavage of 3' radiolabeled 15-base single-strand overhang of 5' A or 5'T was analyzed. Reaction conditions were conducted as described in "Methods and Materials". The DNA substrates is depicted above the gel and the position of the [$^{32}$P] label is denoted by the asterisk and the position of Artemis endonuclease activity is denoted by the bracket.

## 4.3.  Discussion

Our design and implementation of a novel purification procedure of $[His]_6$-Artemis resulted in the biochemical separation of exonuclease activity from DNA-PK dependent endonuclease activity.  Interestingly, other laboratories have made mutations in various positions throughout the Artemis polypeptide in an effort to identify the nuclease active site.  Some of these mutations have resulted in disruption of the endonuclease activity but have had no effect on exonuclease activity [73, 103, 106, 113, 116, 117].  For example, N-terminal Artemis mutations located in the enzymatically important metallo-β-lactamase and β-CASP domains resulted in identification of a sub-set of mutants that functionally abrogated endonuclease activity by disrupting metal coordination [113].  Importantly, biochemical analysis of these mutants resulted in no loss of exonuclease activity.  Additional work with a phosphorylation mutant that is associated with partial immunodeficiency in a mouse model exhibited reduced endonucleasee activity but nearly complete retention of exonuclease activity [118].  It is possible that the exonuclease activity could be located in another active site other than those identified by the extensive set of mutant generated.  However, this seems unlikely as it is thought that metallo-β-lactamse fold enzymes have one active site that is responsible for all enzymatic processing [114]. This hypothesis is further supported by data published on SNM1, a 5'-3'mammalian exonuclease classified in the metallo-β-lactamase superfamily.  SNM1 is characterized by having only exonuclease activity on single-strand DNA, with no accompanying endonuclease activity.  A mutation of a conserved aspartate (D736) in the β-lactamase domain resulted in functional disruption of the 5'-3' exonuclease

activity [117, 119]. Another group had made a mutation of this same conserved aspartate residue in Artemis (D37) that completely eliminated endonuclease activity of Artemis, but the exonuclease activity associated with Artemis remained in the mutant [113]. This is genetic evidence to further support our biochemical evidence indicating that the exonuclease activity is not located in the same active site as the endonuclease activity. Importantly, the extensive Atremis mutational analysis done to date has yet to locate an exonuclease active site within Artemis. These genetic studies coupled with our biochemical analysis indicate that not only is the exonuclease activity separate from the endonucleolytic active site, but it is not part of the Artemis polypeptide at all.

The purification scheme presented in this chapter was developed and then executed over multiple protein purification preparations. While every successful preparation resulted in separation of the two nuclease activities as described, it is important to point out that separation of the activities did vary between protein preparations. As development of the purification procedure progressed, variations in procedure would at times result in small changes in the separation of the exonuclease activity from the Artemis endonuclease activity. For example, we found that greater separation of activity was achieved on a 5 mL HAP column compared to a 2 mL HAP column, despite the fact that the 2 mL column contained more than enough binding capacity for the protein amount that we applied to the column. Importantly, the residual exonuclease activity that flowed through the 2 mL HAP column (and thus contaminated our Artemis pool of protein that also flowed through the column) could be successfully separated by re-running the FT pool over a second HAP column.

This was an interesting finding, as it suggests that the 2 mL HAP column could become saturated with exonuclease activity and lead to poor separation of the exonuclease and endonuclease activity. We also noticed variations in separation when the pH of buffers used for the HAP column was altered with lower pH resulting in poorer separation of the exonuclease activity, so our buffers contain a relatively pH of 7.85. Typically binding to a HAP column is performed at a lower pH as the lower the pH, the more protein binds to the matrix. [His]$_6$-Artemis does not bind to the HAP column and this is likely the result of the higher pH buffer. Many other proteins do not bind to the HAP column under these conditions as well, as evidenced by the amount of non-specific proteins in the HAP FT (Figure 21C). Interestingly, the exonuclease activity remains bound to the column under these conditions. It is also important to point out that we observed a nominal amount of Artemis in many of the fractions collected from the HAP column, including the wash and elution (Figure 21B and data not shown). These levels of protein were low enough that they could only be observed by western blot analysis, and even then the signal was very low. This phenomenon was also observed during fractionation over the nickel-agarose column, indicating a certain degree of spreading of the fusion protein during all fractionation steps. Interestingly, spreading of the protein was also seen over other columns (ie. ion exchange), leading us to conclude that this protein has propensity for multiple matrices. This could also explain the fairly high amount of non-specific proteins that we see eluting with Artemis off of different columns. In short, Artemis may be a very "sticky" protein, perhaps due to one or several disordered regions, that gives it an

affinity for multiple matrices as well as attracts a variety of protein-protein interactions.

Our study demonstrates that the exonuclease activity of Artemis previously reported is not an intrinsic component of the Artemis polypeptide, and there are many possibilities to explain the presence of the exonuclease activity found in less-pure fractions of Artemis. It is possible that the exonuclease activity is simply a contaminating enzyme that is endogenously expressed in the SF9 insect cells we use to overexpress Artemis and co-purifies with over-expressed Artemis independent of any biologically relevant interaction. This possibility is supported by our observations of Artemis being a "sticky" protein with an affinity for non-specific interactions. It is further supported by our data showing single-strand 5'-3' exonuclease activity co-purifying with another DNA binding protein, $[His]_6$-XPA, overexpressed in insect cells. This result suggests the possibility of the contaminating exonuclease having an affinity for nickel-agarose resin, as both the XPA and Artemis preparations were fractionated over this column first. This is not an unlikely scenario, as insect cells have been shown to contain many endogenous nucleases and the 5'-3' exonuclease SNM1 was also identified in *D. Melanogaster* [120]. It is also possible that the exonuclease is another enzyme that is associated with Artemis and plays a physiological role with Artemis in the cell. This possibility will have to be further investigated.
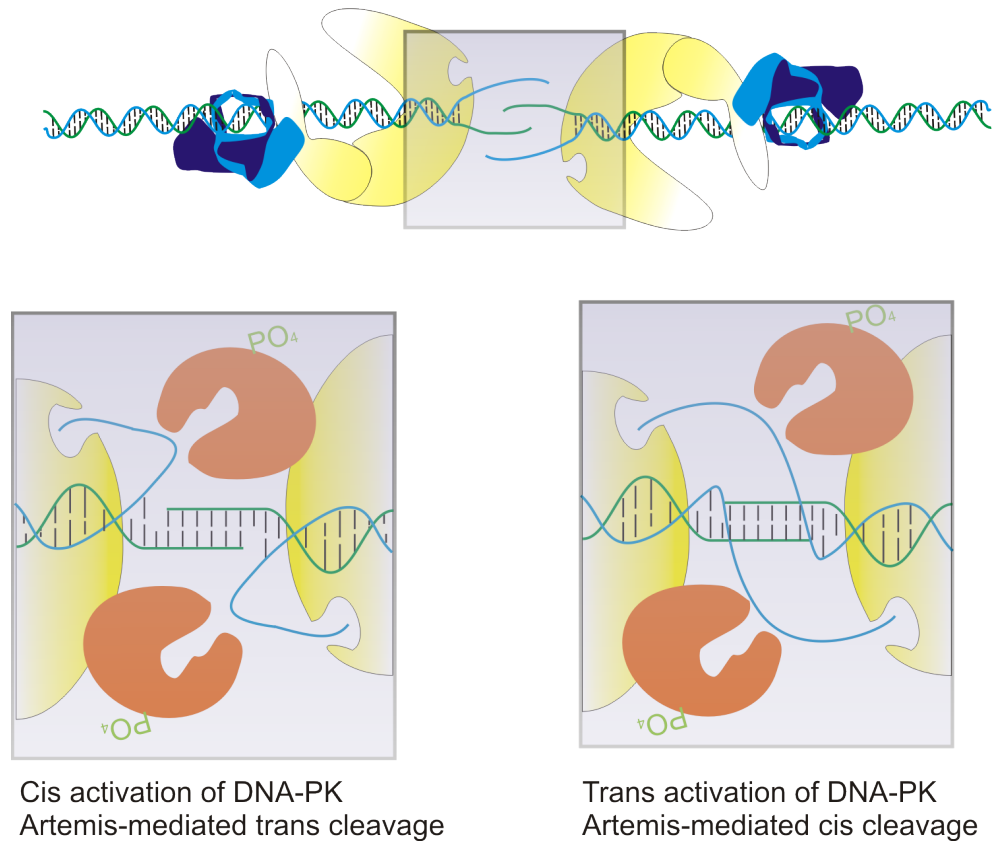
Our purification scheme resulted in a preparation of Artemis that is devoid of exonuclease activity that was previously thought to be intrinsic to Artemis but maintains the biologically relevant DNA-PK and ATP dependent endonuclease

activity. With this preparation of Artemis, we began to conduct experiments to further understand the role of this endonuclease activity in NHEJ. Our studies with more biologically relevant substrates containing shorter overhang regions have shown that Artemis is capable of cleaving shorter overhang regions. Furthermore, a sequence bias is observed, with Artemis preferentially cleaving DNA substrates with 5' T overhangs as compared to 5' A overhangs. The explanation for sequence bias could be as simple as thymine fitting into the Artemis active site better than other bases. Support for this hypothesis is seen in Figure 29, where a cleavage predominantly occurs at the double-strand junction. This substrate has an overhang made up of a mixed 6-base substrate consisting of G, C and A in the overhang region, with a T as the first nucleotide in the double-strand region (*T*GCCGAA). This data suggests that Artemis preferentially cleaves thymines, and as the resulting cleavage product is 24 bases long (with the 6-base single-strand overhang endonucleolytically cleaved off), this cleavage would have to occur on the 5' end of the nucleotide. Interestingly, sequence bias appears to be more important when a DNA overhang is longer as the difference in Artemis cleavage between 5'T and 5'A 15-base overhangs is much more pronounced than the difference in 5'T and 5'A 6-base overhang cleavage, but the relevance of these results is still unclear. Additional biochemical studies with DNA substrates needs to be done to understand how sequence bias and strand length affect DNA-PK and ATP dependent Artemis-catalyzed cleavage.

## 5. Summary and Perspectives

NHEJ, the major pathway responsible for the repair of DNA DSB, was originally defined as a simple pathway that crudely joined DNA DSB with the help of a handful of proteins, Ku, DNA-PKcs, and Ligase IV/XRCC4.  Extensive research in the field over the years has changed our view of NHEJ, and it is now apparent that this is a complex and intricate pathway that includes a variety of other proteins including processing enzymes Artemis, DNA polymerases μ and λ and the Ligase IV associated protein XLF.  Biochemical and structural analysis has resulted in fairly detailed characterization of many of these proteins.  However, many unanswered questions regarding molecular mechanism of these proteins remain.

Our work has further characterized the largest enzyme in this pathway, DNA-PK, and results suggest a model for activation of DNA-PK.  In our proposed model, DNA threads through a channel in DNA-PKcs following binding of this large kinase to a DSB (Figure 32A).  Strand separation of the DNA terminus likely occurs, with the 5' strand being inserted into an active site on the periphery of the kinase and the 3' strand potentially annealing with a 3' strand on the opposite DNA terminus.  This 3' strand-dependent interaction may be responsible for further pulling the DNA through the kinase structure, and thus increasing overall kinase activity.  This DNA strand interaction may also play a role in stabilizing a synaptic complex of the two DNA termini-protein complexes.  Elegant work has shown that DNA-PK autophosphorylation occurs in a *trans* fashion [82], however this does not necessarily mean that the protein-DNA interaction that drives activation occurs in a trans fashion. Activation of the kinase by the 5' strand could occur in either a *cis* or *trans* fashion

Cis activation of DNA-PK
Artemis-mediated trans cleavage

Trans activation of DNA-PK
Artemis-mediated cis cleavage

**Figure 32. DNA-PK activation and Artemis-mediated cleavage.** (A) DNA threads through the ring-like structure of the Ku heterodimer (blue doughnut structure) and through a channel in DNA-PKcs (yellow structure). Following threading of the DNA, strand separation occurs and the 3' strand (depicted in green) drives homology-mediated interactions with the opposite 3' strand, aiding in formation of a synaptic complex between the two DNA termini. The purple shadow indicates the magnification of the region in figure 4B and 4C. (B) *Cis* activation of DNA-PK (yellow structure) occurs by the 5' strand (depicted in blue) interacting with an active site that can accommodate single-strand DNA on the periphery of the same DNA-PK molecule that is bound to the DNA terminus. Artemis (orange structure) interacts with DNA-PK and cleaves DNA in a *trans* fashion by cleaving a single-strand overhang on the opposite DNA terminus. (C) *Trans* activation occurs by 5' single-strand DNA interacting with the active on the DNA-PK molecule bound to the opposite DNA terminus. Artemis interacts with DNA-PK and cleaves DNA in a *cis* fashion by cleaving a single-strand overhang on the same terminus with which DNA-PK and Artemis are interacting.

(Figure 32B and C). Further studies are needed to determine DNA-mediated activation of the kinase.

Biochemical and structural work has shown that *trans a*utophosphorylation of the ABCDE cluster allows for rearrangement of the protein-DNA complex such that the DNA ends are made accessible for processing enzymes [63]. Autophosphorylation induced conformational changes appear to occur mainly in the head domain of DNA-PKcs. This is the region where the kinase domain is thought to be located, and it is possible that conformational changes could result in generation of a platform for enzymes to engage in processing of the DNA termini. This model suggests that DNA-PK is responsible for holding DNA termini in place while processing of the ends occurs. This is an interesting idea, as it suggests that DNA-PK remains bound to DNA while processing occurs. Previous models have suggested that dissociation of DNA-PK is occurs following autophosphorylation. However, in the model described above, autophosphorylation of one cluster of residues has already occurred in order to leave DNA ends accessible for processing but dissociation of DNA-PK has not yet occurred. Therefore, this suggests that a second round of DNA-PK autophosphorylation that results in dissociation of the kinase may occur following DNA end processing. It is very possible that a different set of residues (other than the ABCDE cluster) must be phosphorylated to initiate DNA-PK dissociation from the termini. Further studies are needed to determine the mechanisms and dynamics of DNA end processing and DNA-PK dissociation.

Biochemical studies of Artemis to date clearly indicate that more research is necessary to fully understand the molecular mechanism of DNA-PK and Artemis-

mediated DNA cleavage in NHEJ. Combined results from the field suggest a model

for DNA-PK and Artemis interactions with DNA ends. DNA strand polarity clearly

plays a role, as 3' and 5' cleavage of single-strand overhangs varies slightly, with a 3'

overhang getting cleaved to within 4 nt of the double-strand junction while 5'

overhangs are cleaved predominantly at the double-strand junction with minor

cleavage events at n+1, n-1 [74, 106]. Our lab and others have also shown that a 3'

overhang results in a more heterogeneous cleavage set, with the n+4 position being

cleaved more predominantly but additional cleavage of surrounding nucleotides, up to

two in either direction, occurs as well. This differs from the homogenous cleavage

pattern of a 5' overhang resulting in predominant cleavage at the double strand

junction. It is possible that this variation is a product of DNA positioning as driven

by DNA-DNA-PK interactions. Our data demonstrates that 5' overhangs may be

crucial for activation and thus may possess more well defined interactions with the

DNA-PKcs subunit, which could create a uniform alteration in the DNA structure to

allow more precise cleavage by Artemis at the single-strand/double-strand junction

(Figure 33A). 3' overhangs do not necessarily have such a defined interaction with

DNA-PKcs, as Artemis is forced to interact with DNA overhangs in a stochastic

manner, creating a more random cleavage pattern that results in cleavage products of

assorted sizes (Figure 33B). Further work analyzing DNA substrate length, structure

and sequence will result in an increased understanding of the molecular mechanism of

Artemis and its overall role in NHEJ.

Despite the biochemical data gathered, many questions remain regarding

DNA-PK dependent Artemis endonuclease activity. It is clear that Artemis requires
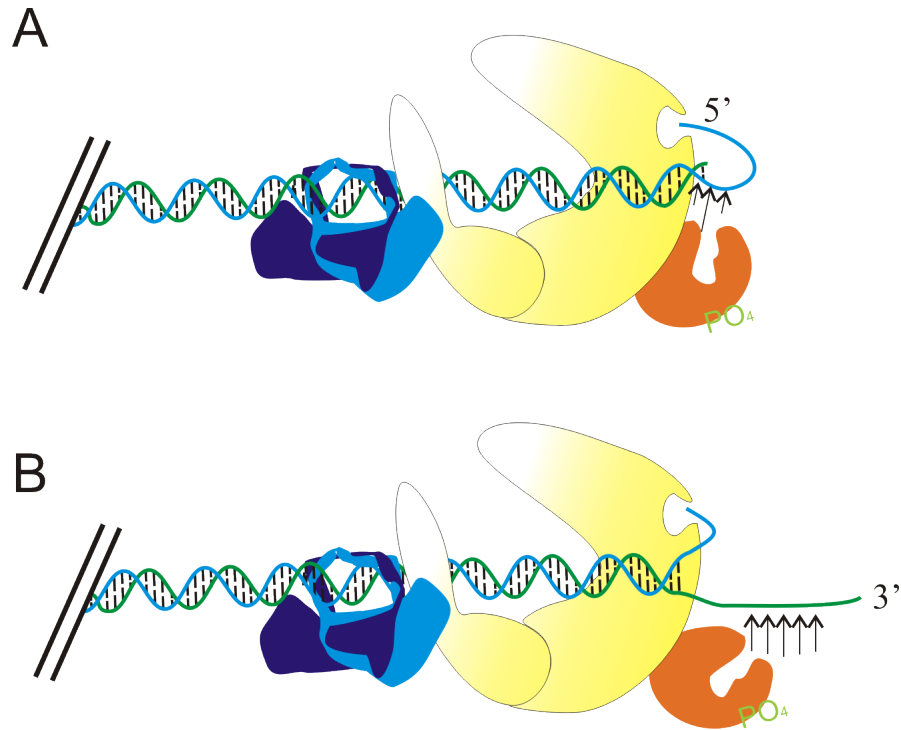
**Figure 33. Artemis endonuclease activity on single-strand overhangs.** DNA-PK dependent Artemis-mediated cleavage of overhangs varies based on strand polarity. Ku heterodimer is depicted in blue, DNA-PKcs is depicted in yellow, and Artemis is depicted in orange. (A) Artemis cleaves 3' overhangs in a heterogenous manner, with cleavage products occurring at the n+6, n+5, n+4, n+3 and n+2 positions. All of these potential cleavage products result in a 3' overhang remaining at the DNA terminus. (B) Artemis cleaves 5' overhangs in a homogeneous, with cleavage mainly occurring at the single-strand/double-strand junction and a few cleavage events occurring at the n+1 or n-1 positions.

121

DNA-PK and ATP for endonuclease activity, but it is unclear if this activation by DNA-PK is through a *cis* or *trans* mechanism. Several labs have performed *in vitro* nuclease assays with a radiolabeled overhang substrate, but include unlabeled double-strand DNA to increase DNA-PK activity, arguing that this increases the endonuclease activity of Artemis. However, it is hard to imagine an *in vivo* scenario at the site of a DSB where DNA-PK is acting *in trans* to activate Artemis (Figure 34). In fact, work by Povirk's group has shown that Artemis nuclease activity is not increased in the presence of a dsDNA stimulus [99], and Lees-Miller group observes robust endonuclease stimulation in the absence of stimulating dsDNA [106]. Rather, an alternative is that DNA-PK is bound to the site of a DSB, Artemis is recruited to this same DNA end and Artemis is activated in *cis* by this DNA-PK molecule. Once DNA-PK dependent Artemis-catalyzed endonuclease cleavage is activated, cleavage events could occur through a *cis* or *trans* mechanism. The DNA/DNA-PK/Artemis complex described could be envisioned to stimulate *trans* endonucleolytic cleavage. That is, just as *trans* autophosphorylation of DNA-PK occurs, Artemis too could be bound to one terminus in a complex with DNA-PK and act catalytically across the synaptic complex to cleave DNA on the opposite terminus (Figure 32B). As a DNA DSB induced by IR can be very complex, with a variety of DNA discontinuities on either terminus at the site of the DSB, it is possible that Artemis cleaves a DNA terminus in *trans* that needs to be processed, even if the side it is bound to does not require processing. It is also possible that Artemis cleaves a DNA strand in *cis* (Figure 32C), similar to DNA-PK being activated in *cis*.
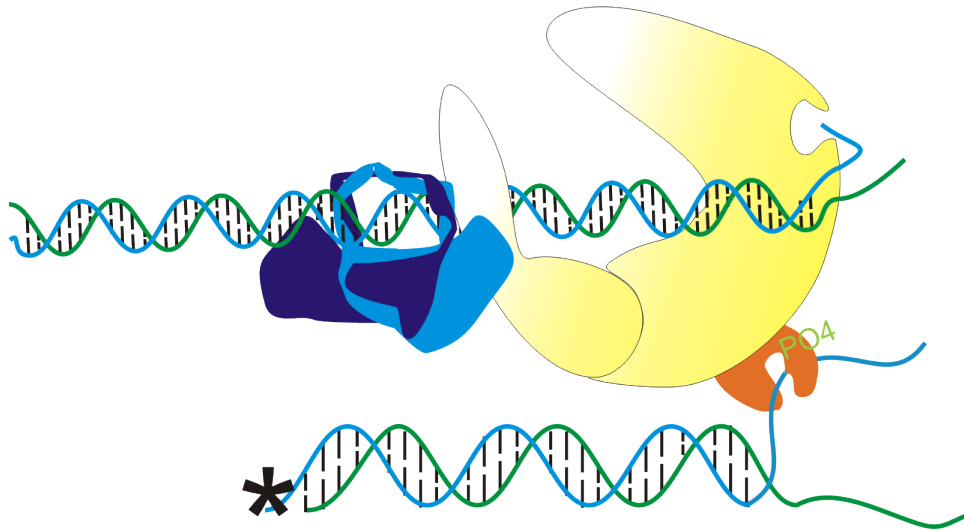
**Figure 34. Activation of Artemis endonuclease activity.** Artemis endonuclease activity is dependent on DNA-PK and ATP, and this activation event could occur in *trans* by a DNA-PK molecule bound to a different DNA terminus than the terminus Artemis is cleaving. Activation of Artemis endonuclease activity could also occur in *cis* by a DNA-PK molecule that is bound to the same DNA terminus that Artemis is cleaving (see Figure 33).

It is becoming increasingly clear that processing during NHEJ is an important

yet complicated step that requires regulation at the molecular level.   In the context of

a DNA DSB induced by IR, a small amount of processing can be extremely useful.  It

is becoming more apparent that regions of microhomology, embedded within the

DNA sequence in the vicinity of a double strand break, may play a role in successful

re-joining of broken DNA (see Chapter 3).  Artemis-catalyzed nuclease activity to

excise nucleotides, revealing regions of microhomology may be a critical step in

NHEJ.   Processing of DNA termini to remove forms of DNA damage (like 3'

phosphoglycolates or abasic sites) that would otherwise impede DNA ligation of the

DSB or cause further harm to the cell is another example of useful DNA processing

during NHEJ.  This "micro" type of processing is less detrimental than massive

processing that would result in depletion of a large amount of genetic material.

Furthermore, it is more energetically favorable for the cell to have mechanisms in

place to remove DNA damage while repairing the DNA DSB.  The opposite scenario

would result in DNA damage, such as an abasic site, persisting in the DNA and

having to be removed via another repair process after resolving the DSB.  It is

important to point out that this minimal amount of processing described, while

favorable for the cell probably requires a variety of enzymes to accomplish specific

processing events like synthesis or degradation of DNA ends to get to a region of

microhomology or to remove/repair other types of DNA damage around the terminus

with minimal loss of nucleotides. Elaborate processing events are important in the

context of repair of IR induced DNA DSB, as IR can result in a variety of DNA

damage at the site of a break that would need to be removed for efficient and effective

NHEJ.  As these breaks can be so complex, it is likely that there are several enzymes involved in the processing steps of NHEJ that have yet to be identified.

REFERENCE LIST

[1] B.L.Mahaney, K.Meek, S.P.Lees-Miller. Repair of ionizing radiation-induced DNA double-strand breaks by non-homologous end-joining, Biochem. J. 417 (2009) 639-650.

[2] A.R.Lehmann, R.P.Fuchs. Gaps and forks in DNA replication: Rediscovering old models, DNA Repair (Amst) 5 (2006) 1495-1498.

[3] M.Gellert. V(D)J recombination: RAG proteins, repair factors, and regulation, Annual Review of Biochemistry 71 (2002) 101-132.

[4] J.Erenpreisa, M.Kalejs, F.Ianzini, E.A.Kosmacek, M.A.Mackey, D.Emzinsh, M.S.Cragg, A.Ivanov, T.M.Illidge. Segregation of genomes in polyploid tumour cells following mitotic catastrophe, Cell Biol. Int. 29 (2005) 1005-1011.

[5] M.Shrivastav, L.P.De Haro, J.A.Nickoloff. Regulation of DNA double-strand break repair pathway choice, Cell Res. 18 (2008) 134-147.

[6] J.F.Ward. Radiation mutagenesis: the initial DNA lesions responsible, Radiat. Res. 142 (1995) 362-368.

[7] E.Pastwa, R.D.Neumann, K.Mezhevaya, T.A.Winters. Repair of radiation-induced DNA double-strand breaks is dependent upon radiation quality and the structural complexity of double-strand breaks, Radiat. Res. 159 (2003) 251-261.

[8] M.R.Lieber. The Mechanism of Double-Strand DNA Break Repair by the Nonhomologous DNA End-Joining Pathway, Annu. Rev. Biochem. (2010).

[9] J.Budman, G.Chu. Processing of DNA for nonhomologous end-joining by cell-free extract, EMBO J. 24 (2005) 849-860.

[10] D.B.Roth, J.H.Wilson. Nonhomologous recombination in mammalian cells: role for short sequence homologies in the joining reaction, Mol. Cell Biol. 6 (1986) 4295-4304.

[11] K.Meek, S.Gupta, D.A.Ramsden, S.P.Lees-Miller. The DNA-dependent protein kinase: the director at the end, Immunological Reviews 200 (2004) 132-141.

[12] S.P.Lees-Miller, K.Meek. Repair of DNA double strand breaks by non-homologous end joining, Biochimie 85 (2003) 1161-1173.

[13] M.R.Lieber, Y.M.Ma, U.Pannicke, K.Schwarz. Mechanism and regulation of human non-homologous DNA end- joining, Nature Reviews Molecular Cell Biology 4 (2003) 712-720.

[14] L.G.DeFazio, R.M.Stansel, J.D.Griffith, G.Chu. Synapsis of DNA ends by DNA-dependent protein kinase, EMBO J. 21 (2002) 3192-3200.

[15] S.J.Collis, T.L.DeWeese, P.A.Jeggo, A.R.Parker. The life and death of DNA-PK, Oncogene 24 (2005) 949-961.

[16] M.R.Lieber, H.Lu, J.Gu, K.Schwarz. Flexibility in the order of action and in the enzymology of the nuclease, polymerases, and ligase of vertebrate non-homologous DNA end joining: relevance to cancer, aging, and the immune system, Cell Res. 18 (2008) 125-133.

[17] M.R.Lieber. The mechanism of human nonhomologous DNA end joining, J. Biol. Chem. 283 (2008) 1-5.

[18] S.Rooney, F.W.Alt, D.Lombard, S.Whitlow, M.Eckersdorff, J.Fleming, S.Fugmann, D.O.Ferguson, D.G.Schatz, J.Sekiguchi. Defective DNA repair and increased genomic instability in artemis-deficient murine cells, J. Exp. Med. 197 (2003) 553-565.

[19] K.N.Mahajan, S.A.Nick McElhinny, B.S.Mitchell, D.A.Ramsden. Association of DNA polymerase mu (pol mu) with Ku and ligase IV: role for pol mu in end-joining double-strand break repair, Mol. Cell Biol. 22 (2002) 5194-5202.

[20] M.R.Lieber, U.Grawunder, X.Wu, M.Yaneva. Tying loose ends: roles of Ku and DNA-dependent protein kinase in the repair of double-strand breaks. [Review] [68 refs], Current Opinion in Genetics & Development 7 (1997) 99-104.

[21] J.Gu, H.Lu, A.G.Tsai, K.Schwarz, M.R.Lieber. Single-stranded DNA ligation and XLF-stimulated incompatible DNA end ligation by the XRCC4-DNA ligase IV complex: influence of terminal DNA sequence, Nucleic Acids Res. 35 (2007) 5755-5762.

[22] P.Ahnesorg, P.Smith, S.P.Jackson. XLF Interacts with the XRCC4-DNA Ligase IV Complex to Promote DNA Nonhomologous End-Joining, Cell. 124 (2006) 301-313.

[23] T.Mimori, J.A.Hardin, J.A.Steitz. Characterization of the DNA-binding protein antigen Ku recognized by autoantibodies from patients with rheumatic disorders, J. Biol. Chem. 261 (1986) 2274-2278.

[24] C.W.Anderson, T.H.Carter. The DNA-activated protein kinase -- DNA-PK, Curr. Top. Microbiol. Immunol. 217 (1996) 91-111.

[25] M.Koike, T.Shiomi, A.Koike. Dimerization and nuclear localization of ku proteins, J. Biol. Chem. 276 (2001) 11167-11173.

[26] Y.Gu, S.Jin, Y.Gao, D.T.Weaver, F.W.Alt. Ku70-deficient embryonic stem cells have increased ionizing radiosensitivity, defective DNA end-binding activity, and inability to support V(D)J recombination, Proc. Natl. Acad. Sci. USA 94 (1997) 8076-8081.

[27] B.K.Singleton, A.Priestley, H.Steingrimsdottir, D.Gell, T.Blunt, Jackson, SP, A.R.Lehmann, P.A.Jeggo. Molecular and biochemical characterization of xrs mutants defective in Ku80, Mol. Cell Biol. 17 (1997) 1264-1273.

[28] J.A.Downs, S.P.Jackson. A means to a DNA end: the many roles of Ku, Nature Reviews Molecular Cell Biology 5 (2004) 367-378.

[29] P.R.Blier, A.J.Griffith, J.Craft, J.A.Hardin. Binding of Ku protein to DNA. Measurement of affinity for ends and demonstration of binding to nicks, J. Biol. Chem. 268 (1993) 7594-7601.

[30] M.Yaneva, T.Kowalewski, M.R.Lieber. Interaction of DNA-dependent protein kinase with DNA and with Ku: biochemical and atomic-force microscopy studies, EMBO J. 16 (1997) 5098-5112.

[31] W.S.Dynan, S.Yoo. Interaction of Ku protein and DNA-dependent protein kinase catalytic subunit with nucleic acids., Nucleic Acids Res. 26 (1998) 1551-1559.

[32] S.Yoo, W.S.Dynan. Geometry of a complex formed by double strand break repair proteins at a single DNA end: recruitment of DNA-PKcs induces inward translocation of Ku protein, Nucleic Acids Res. 27 (1999) 4679-4686.

[33] S.Yoo, A.Kimzey, W.S.Dynan. Photocross-linking of an oriented DNA repair complex - Ku bound at a single DNA end, J. Biol. Chem. 274 (1999) 20034-20039.

[34] Y.Ma, M.R.Lieber. DNA length-dependent cooperative interactions in the binding of Ku to DNA, Biochemistry 40 (2001) 9638-9646.

[35] J.J.Turchi, K.M.Henkels, Y.Zhou. Cisplatin-DNA adducts inhibit translocation of the Ku subunits of DNA-PK, Nucleic Acids Res. 28 (2000) 4634-4641.

[36] B.Kysela, A.J.Doherty, M.Chovanec, T.Stiff, S.M.Ameer-Beg, B.Vojnovic, P.M.Girard, P.A.Jeggo. Ku stimulation of DNA ligase IV-dependent ligation requires inward movement along the DNA molecule, J. Biol. Chem. 278 (2003) 22466-22474.

[37] S.A.Roberts, D.A.Ramsden. Loading of the nonhomologous end joining factor, Ku, on protein-occluded DNA ends, J. Biol. Chem. 282 (2007) 10605-10613.

[38]   D.Gell, S.P.Jackson. Mapping of protein-protein interactions within the DNA-dependent protein kinase complex, Nucleic Acids Res. 27 (1999) 3494-3502.

[39]   J.R.Walker, R.A.Corpina, J.Goldberg. Structure of the Ku heterodimer bound to DNA and its implications for double-strand break repair, Nature 412 (2001) 607-614.

[40]   Z.Zhang, W.Hu, L.Cano, T.D.Lee, D.J.Chen, Y.Chen. Solution structure of the C-terminal domain of Ku80 suggests important sites for protein-protein interactions, Structure. 12 (2004) 495-502.

[41]   R.Harris, D.Esposito, A.Sankar, J.D.Maman, J.A.Hinks, L.H.Pearl, P.C.Driscoll. The 3D solution structure of the C-terminal region of Ku86 (Ku86CTR), J. Mol. Biol. 335 (2004) 573-582.

[42]   R.T.Abraham. PI 3-kinase related kinases: 'big' players in stress-induced signaling pathways, DNA Repair (Amst) 3 (2004) 883-887.

[43]   C.W.Anderson, J.J.Dunn, P.I.Freimuth, A.M.Galloway, M.J.lalunis-Turner. Frameshift mutation in PRKDC, the gene for DNA-PKcs, in the DNA repair-defective, human, glioma-derived cell line M059J, Radiat. Res. 156 (2001) 2-9.

[44]   R.B.West, M.Yaneva, M.R.Lieber. Productive and nonproductive complexes of Ku and DNA-dependent protein kinase at DNA termini, Mol. Cell Biol. 18 (1998) 5908-5920.

[45]   A.Kurimasa, S.Kumano, N.V.Boubnov, M.D.Story, C.S.Tung, S.R.Peterson, D.J.Chen. Requirement for the kinase activity of human DNA-dependent protein kinase catalytic subunit in DNA strand break rejoining, Mol. Cell Biol. 19 (1999) 3877-3884.

[46]   P.Baumann, S.C.West. DNA end-joining catalyzed by human cell-free extracts, Proc. Natl. Acad. Sci. USA 95 (1998) 14066-14070.

[47]   S.P.Jackson. The DNA-damage response: new molecular insights and new approaches to cancer therapy, Biochem. Soc. Trans. 37 (2009) 483-494.

[48]   T.M.Gottlieb, S.P.Jackson. The DNA-dependent protein kinase: requirement for DNA ends and association with Ku antigen, Cell 72 (1993) 131-142.

[49]   S.Gupta, K.Meek. The leucine rich region of DNA-PKcs contributes to its innate DNA affinity, Nucleic Acids Res. 33 (2005) 6972-6981.

[50]   A.Suwa, M.Hirakata, Y.Takeda, S.A.Jesch, T.Mimori, J.A.Hardin. DNA-dependent protein kinase (Ku protein-p350 complex) assembles on double-stranded DNA, Proc. Natl. Acad. Sci. USA 91 (1994) 6904-6908.

[51] K.S.Pawelczak, B.J.Andrews, J.J.Turchi. Differential activation of DNA-PK based on DNA strand orientation and sequence bias, Nucleic Acids Res. 33 (2005) 152-161.

[52] O.Hammarsten, G.Chu. DNA-dependent protein kinase: DNA binding and activation in the absence of Ku, Proc. Natl. Acad. Sci. USA 95 (1998) 525-530.

[53] O.Hammarsten, L.G.DeFazio, G.Chu. Activation of DNA-dependent protein kinase by single-stranded DNA ends, J. Biol. Chem. 275 (2000) 1541-1550.

[54] M.Jovanovic, W.S.Dynan. Terminal DNA structure and ATP influence binding parameters of the DNA-dependent protein kinase at an early step prior to DNA synapsis, Nucleic Acids Res. 34 (2006) 1112-1120.

[55] K.K.Leuther, O.Hammarsten, R.D.Kornberg, G.Chu. Structure of DNA-dependent protein kinase: implications for its regulation by DNA, EMBO J. 18 (1999) 1114-1123.

[56] J.Boskovic, A.Rivera-Calzada, J.D.Maman, P.Chacon, K.R.Willison, L.H.Pearl, O.Llorca. Visualization of DNA-induced conformational changes in the DNA repair kinase DNA-PKcs, EMBO J. 22 (2003) 5875-5882.

[57] A.Rivera-Calzada, J.P.Maman, L.Spagno, L.H.Pearl, O.Llorca. Three-dimensional structure and regulation of the DNA-dependent protein kinase catalytic subunit (DNA-PKcs), Structure 13 (2005) 243-255.

[58] D.R.Williams, K.J.Lee, J.Shi, D.J.Chen, P.L.Stewart. Cryo-EM structure of the DNA-dependent protein kinase catalytic subunit at subnanometer resolution reveals alpha helices and insight into DNA binding, Structure. 16 (2008) 468-477.

[59] B.L.Sibanda, D.Y.Chirgadze, T.L.Blundell. Crystal structure of DNA-PKcs reveals a large open-ring cradle comprised of HEAT repeats, Nature 463 (2010) 118-121.

[60] B.K.Singleton, M.I.Torres-Arzayus, S.T.Rottinghaus, G.E.Taccioli, P.A.Jeggo. The C terminus of Ku80 activates the DNA-dependent protein kinase catalytic subunit, Mol. Cell. Biol. 19 (1999) 3267-3277.

[61] N.Uematsu, E.Weterings, K.Yano, K.Morotomi-Yano, B.Jakob, G.Taucher-Scholz, P.O.Mari, G.van, B.P.Chen, D.J.Chen. Autophosphorylation of DNA-PKCS regulates its dynamics at DNA double-strand breaks, J. Cell Biol. 177 (2007) 219-229.

[62] E.Weterings, N.S.Verkaik, G.Keijzers, B.I.Florea, S.Y.Wang, L.G.Ortega, N.Uematsu, D.J.Chen, G.van. The Ku80 carboxy terminus stimulates joining and artemis-mediated processing of DNA ends, Mol. Cell Biol. 29 (2009) 1134-1142.

[63] M.Hammel, Y.Yu, B.L.Mahaney, B.Cai, R.Ye, B.M.Phipps, R.P.Rambo, G.L.Hura, M.Pelikan, S.So, R.M.Abolfath, D.J.Chen, S.P.Lees-Miller, J.A.Tainer. Ku and DNA-dependent protein kinase dynamic conformations and assembly regulate DNA binding and the initial non-homologous end joining complex, J. Biol. Chem. 285 (2010) 1414-1423.

[64] D.Pang, S.Yoo, W.S.Dynan, M.Jung, A.Dritschilo. Ku proteins join DNA fragments as shown by atomic force microscopy, Cancer Res. 57 (1997) 1412-1415.

[65] T.M.Bliss, D.P.Lane. Ku selectively transfers between DNA molecules with homologous ends, J. Biol. Chem. 272 (1997) 5765-5773.

[66] C.F.Chiu, T.Y.Lin, W.G.Chou. Direct transfer of Ku between DNA molecules with nonhomologous ends, Mutat. Res. 486 (2001) 185-194.

[67] D.Merkle, W.D.Block, Y.Yu, S.P.Lees-Miller, D.T.Cramb. Analysis of DNA-dependent protein kinase-mediated DNA end joining by two-photon fluorescence cross-correlation spectroscopy, Biochemistry 45 (2006) 4164-4172.

[68] Y.Yu, B.L.Mahaney, K.Yano, R.Ye, S.Fang, P.Douglas, D.J.Chen, S.P.Lees-Miller. DNA-PK and ATM phosphorylation sites in XLF/Cernunnos are not required for repair of DNA double strand breaks, DNA Repair (Amst) 7 (2008) 1680-1692.

[69] P.Calsou, C.Delteil, P.Frit, J.Droulet, B.Salles. Coordinated assembly of Ku and p460 subunits of the DNA- dependent protein kinase on DNA ends is necessary for XRCC4- ligase IV recruitment, J. Mol. Biol. 326 (2003) 93-103.

[70] Y.G.Wang, C.Nnakwe, W.S.Lane, M.Modesti, K.M.Frank. Phosphorylation and regulation of DNA ligase IV stability by DNA-dependent protein kinase, J. Biol. Chem. 279 (2004) 37282-37290.

[71] D.W.Chan, R.Ye, C.J.Veillette, S.P.Lees-Miller. DNA-dependent protein kinase phosphorylation sites in Ku 70/80 heterodimer, Biochemistry 38 (1999) 1819-1828.

[72] P.Douglas, S.Gupta, N.Morrice, K.Meek, S.P.Lees-Miller. DNA-PK-dependent phosphorylation of Ku70/80 is not required for non-homologous end joining, Dna Repair 4 (2005) 1006-1018.

[73] Y.M.Ma, U.Pannicke, H.H.Lu, D.Niewolik, K.Schwarz, M.R.Lieber. The DNA-dependent protein kinase catalytic subunit phosphorylation sites in human artemis, J. Biol. Chem. 280 (2005) 33839-33846.

[74] Y.M.Ma, U.Pannicke, K.Schwarz, M.R.Lieber. Hairpin opening and overhang processing by an Artemis/DNA- dependent protein kinase complex in nonhomologous end joining and V(D)J recombination, Cell 108 (2002) 781-794.

[75] D.W.Chan, S.P.Lees-Miller. The DNA-dependent protein kinase is inactivated by autophosphorylation of the catalytic subunit, J. Biol. Chem. 271 (1996) 8936-8941.

[76] D.Merkle, P.Douglas, G.B.G.Moorhead, Z.Leonenko, Y.P.Yu, D.Cramb, D.P.Bazett-Jones, S.P.Lees-Miller. The DNA-dependent protein kinase interacts with DNA to form a protein-DNA complex that is disrupted by phosphorylation, Biochemistry 41 (2002) 12706-12714.

[77] P.Douglas, G.P.Sapkota, N.Morrice, Y.P.Yu, A.A.Goodarzi, D.Merkle, K.Meek, D.R.Alessi, S.P.Lees-Miller. Identification of in vitro and in vivo phosphorylation sites in the catalytic subunit of the DNA-dependent protein kinase, Biochemical Journal 368 (2002) 243-251.

[78] W.D.Block, Y.Yu, D.Merkle, J.L.Gifford, Q.Ding, K.Meek, S.P.Lees-Miller. Autophosphorylation-dependent remodeling of the DNA-dependent protein kinase catalytic subunit regulates ligation of DNA ends, Nucleic Acids Res. 32 (2004) 4351-4357.

[79] X.Cui, Y.Yu, S.Gupta, Y.M.Cho, S.P.Lees-Miller, K.Meek. Autophosphorylation of DNA-dependent protein kinase regulates DNA end processing and may also alter double-strand break repair pathway choice, Mol. Cell Biol. 25 (2005) 10842-10852.

[80] Y.V.Reddy, Q.Ding, S.P.Lees-Miller, K.Meek, D.A.Ramsden. Non-homologous end joining requires that the DNA-PK complex undergo an autophosphorylation-dependent rearrangement at DNA ends, J. Biol. Chem. 279 (2004) 39408-39413.

[81] E.Weterings, N.S.Verkaik, H.T.Bruggenwirth, J.H.J.Hoeijmakers, D.C.van Gent. The role of DNA dependent protein kinase in synapsis of DNA ends, Nucleic Acids Res. 31 (2003) 7238-7246.

[82] K.Meek, P.Douglas, X.Cui, Q.Ding, S.P.Lees-Miller. trans Autophosphorylation at DNA-dependent protein kinase's two major autophosphorylation site clusters facilitates end processing but not end joining, Mol. Cell Biol. 27 (2007) 3881-3890.

[83] K.Meek, V.Dang, S.P.Lees-Miller. DNA-PK: the means to justify the ends?, Adv. Immunol. 99 (2008) 33-58.

[84] H.Willers, J.Husson, L.W.Lee, P.Hubbe, F.Gazemeier, S.N.Powell, J.hm-Daphi. Distinct mechanisms of nonhomologous end joining in the repair of site-directed chromosomal breaks with noncomplementary and complementary ends, Radiat. Res. 166 (2006) 567-574.

[85] X.Wu, T.E.Wilson, M.R.Lieber. A role for FEN-1 in nonhomologous DNA end joining: the order of strand annealing and nucleolytic processing events, Proc. Natl. Acad. Sci. U. S. A 96 (1999) 1303-1308.

[86] F.Karimi-Busheri, A.Rasouli-Nia, J.lalunis-Turner, M.Weinfeld. Human polynucleotide kinase participates in repair of DNA double-strand breaks by nonhomologous end joining but not homologous recombination, Cancer Res. 67 (2007) 6619-6625.

[87] J.J.Perry, S.M.Yannone, L.G.Holden, C.Hitomi, A.Asaithamby, S.Han, P.K.Cooper, D.J.Chen, J.A.Tainer. WRN exonuclease structure and molecular mechanism imply an editing role in DNA end processing, Nat. Struct. Mol. Biol. 13 (2006) 414-422.

[88] R.Kusumoto, L.Dawut, C.Marchetti, L.J.Wan, A.Vindigni, D.Ramsden, V.A.Bohr. Werner protein cooperates with the XRCC4-DNA ligase IV complex in end-processing, Biochemistry 47 (2008) 7548-7556.

[89] J.H.Lee, T.T.Paull. Direct activation of the ATM protein kinase by the Mre11/Rad50/Nbs1 complex, Science 304 (2004) 93-96.

[90] J.W.Lee, L.Blanco, T.Zhou, M.Garcia-Diaz, K.Bebenek, T.A.Kunkel, Z.Wang, L.F.Povirk. Implication of DNA polymerase lambda in alignment-based gap filling for nonhomologous DNA end joining in human nuclear extracts, J. Biol. Chem. 279 (2004) 805-811.

[91] B.Bertocci, S.A.De, J.C.Weill, C.A.Reynaud. Nonoverlapping functions of DNA polymerases mu, lambda, and terminal deoxynucleotidyltransferase during immunoglobulin V(D)J recombination in vivo, Immunity. 25 (2006) 31-41.

[92] S.A.Nick McElhinny, D.A.Ramsden. Sibling rivalry: competition between Pol X family members in V(D)J recombination and general double strand break repair, Immunol. Rev. 200 (2004) 156-164.

[93] Y.M.Ma, H.H.Lu, B.Tippin, M.F.Goodman, N.Shimazaki, O.Koiwai, C.L.Hsieh, K.Schwarz, M.R.Lieber. A biochemically defined system for mammalian nonhomologous DNA end joining, Molecular Cell 16 (2004) 701-713.

[94] J.M.Daley, R.L.Laan, A.Suresh, T.E.Wilson. DNA joint dependence of pol X family polymerase action in nonhomologous end joining, J. Biol. Chem. 280 (2005) 29030-29037.

[95] A.F.Moon, M.Garcia-Diaz, K.Bebenek, B.J.Davis, X.Zhong, D.A.Ramsden, T.A.Kunkel, L.C.Pedersen. Structural insight into the substrate specificity of DNA Polymerase mu, Nat. Struct. Mol. Biol. 14 (2007) 45-53.

[96] S.A.Nick McElhinny, J.M.Havener, M.Garcia-Diaz, R.Juarez, K.Bebenek, B.L.Kee, L.Blanco, T.A.Kunkel, D.A.Ramsden. A gradient of template dependence defines distinct biological roles for family X polymerases in nonhomologous end joining, Mol. Cell 19 (2005) 357-366.

[97] R.Juarez, J.F.Ruiz, S.A.Nick McElhinny, D.Ramsden, L.Blanco. A specific loop in human DNA polymerase mu allows switching between creative and DNA-instructed synthesis, Nucleic Acids Res. 34 (2006) 4572-4582.

[98] P.Andrade, M.J.Martin, R.Juarez, S.F.Lopez de, L.Blanco. Limited terminal transferase in human DNA polymerase mu defines the required balance between accuracy and efficiency in NHEJ, Proc. Natl. Acad. Sci. U. S. A 106 (2009) 16203-16208.

[99] L.F.Povirk, T.Zhou, R.Zhou, M.J.Cowan, S.M.Yannone. Processing of 3'-phosphoglycolate-terminated DNA double strand breaks by Artemis nuclease, J. Biol. Chem. 282 (2007) 3547-3558.

[100] I.Callebaut, D.Moshous, J.P.Mornon, J.P.de Villartay. Metallo-beta-lactamase fold within nucleic acids processing enzymes: the beta-CASP family, Nucleic Acids Res. 30 (2002) 3592-3601.

[101] D.Moshous, I.Callebaut, R.de Chasseval, C.Poinsignon, I.Villey, A.Fischer, J.P.de Villartay. The V(D)J recombination/DNA repair factor artemis belongs to the metallo-beta-lactamase family and constitutes a critical developmental checkpoint of the lymphoid system, Immune Mechanisms and Disease 987 (2003) 150-157.

[102] E.Cattell, B.Sengerova, P.J.McHugh. The SNM1/Pso2 family of ICL repair nucleases: From yeast to man, Environ. Mol. Mutagen. (2010).

[103] J.P.de Villartay, N.Shimazaki, J.B.Charbonnier, A.Fischer, J.P.Mornon, M.R.Lieber, I.Callebaut. A histidine in the beta-CASP domain of Artemis is critical for its full in vitro and in vivo functions, DNA Repair (Amst) 8 (2009) 202-208.

[104] S.Soubeyrand, L.Pope, C.R.de, D.Gosselin, F.Dong, J.P.de Villartay, R.J.Hache. Artemis phosphorylated by DNA-dependent protein kinase associates preferentially with discrete regions of chromatin, J. Mol. Biol. 358 (2006) 1200-1211.

[105] J.Drouet, P.Frit, C.Delteil, J.P.de Villartay, B.Salles, P.Calsou. Interplay between Ku, artemis, and the DNA-dependent protein kinase catalytic subunit at DNA ends, J. Biol. Chem. 281 (2006) 27784-27793.

[106] A.A.Goodarzi, Y.Yu, E.Riballo, P.Douglas, S.A.Walker, R.Ye, C.Harer, C.Marchetti, N.Morrice, P.A.Jeggo, S.P.Lees-Miller. DNA-PK autophosphorylation facilitates Artemis endonuclease activity, EMBO J. 25 (2006) 3880-3889.

[107] S.M.Yannone, I.S.Khan, R.Z.Zhou, T.Zhou, K.Valerie, L.F.Povirk. Coordinate 5' and 3' endonucleolytic trimming of terminally blocked blunt DNA double-strand break ends by Artemis nuclease and DNA-dependent protein kinase, Nucleic Acids Res. 36 (2008) 3354-3365.

[108] J.Gu, S.Li, X.Zhang, L.C.Wang, D.Niewolik, K.Schwarz, R.J.Legerski, E.Zandi, M.R.Lieber. DNA-PKcs regulates a single-stranded DNA endonuclease activity of Artemis, DNA Repair (Amst) (2010).

[109] L.Spagnolo, A.Rivera-Calzada, L.H.Pearl, O.Llorca. Three-dimensional structure of the human DNA-PKcs/Ku70/Ku80 complex assembled on DNA and its implications for DNA DSB repair, Mol. Cell 22 (2006) 511-519.

[110] S.A.Roberts, N.Strande, M.D.Burkhalter, C.Strom, J.M.Havener, P.Hasty, D.A.Ramsden. Ku is a 5'-dRP/AP lyase that excises nucleotide damage near broken ends, Nature 464 (2010) 1214-1217.

[111] N.C.Brissett, R.S.Pitcher, R.Juarez, A.J.Picher, A.J.Green, T.R.Dafforn, G.C.Fox, L.Blanco, A.J.Doherty. Structure of a NHEJ polymerase-mediated DNA synaptic complex, Science 318 (2007) 456-459.

[112] J.Budman, S.A.Kim, G.Chu. Processing of DNA for nonhomologous end-joining is controlled by kinase activity and XRCC4/ligase IV, J. Biol. Chem. 282 (2007) 11950-11959.

[113] U.Pannicke, Y.M.Ma, K.P.Hopfner, D.Niewolik, M.R.Lieber, K.Schwarz. Functional and biochemical dissection of the structure-specific nuclease ARTEMIS, EMBO J. 23 (2004) 1987-1997.

[114] Z.Dominski. Nucleases of the metallo-beta-lactamase family and their role in DNA and RNA metabolism, Crit Rev. Biochem. Mol. Biol. 42 (2007) 67-93.

[115] K.Dahm. Functions and regulation of human artemis in double strand break repair, J. Cell Biochem. 100 (2007) 1346-1351.

[116] D.Niewolik, U.Pannicke, H.Lu, Y.Ma, L.C.Wang, P.Kulesza, E.Zandi, M.R.Lieber, K.Schwarz. DNA-PKcs dependence of Artemis endonucleolytic activity, differences between hairpins and 5' or 3' overhangs, J. Biol. Chem. 281 (2006) 33900-33909.

[117] A.Hazrati, M.Ramis-Castelltort, S.Sarkar, L.J.Barber, C.J.Schofield, J.A.Hartley, P.J.McHugh. Human SNM1A suppresses the DNA repair defects of yeast pso2 mutants, DNA Repair (Amst) 7 (2008) 230-238.

[118] Y.Huang, W.Giblin, M.Kubec, G.Westfield, C.J.St, L.Chadde, S.Kraftson, J.Sekiguchi. Impact of a hypomorphic Artemis disease allele on lymphocyte development, DNA end processing, and genome stability, J. Exp. Med. 206 (2009) 893-908.

[119] J.Hejna, S.Philip, J.Ott, C.Faulkner, R.Moses. The hSNM1 protein is a DNA 5'-exonuclease, Nucleic Acids Res. 35 (2007) 6115-6123.

[120] A.Laurencon, C.M.Orme, H.K.Peters, C.L.Boulton, E.K.Vladar, S.A.Langley, E.P.Bakis, D.T.Harris, N.J.Harris, S.M.Wayson, R.S.Hawley, K.C.Burtis. A large-scale screen for mutagen-sensitive loci in Drosophila, Genetics 167 (2004) 217-231.

CURRICULUM VITAE

**Katherine S. Pawelczak**

Education

2005-2010    Ph.D., Biochemistry and Molecular Biology, Indiana University, Indianapolis, IN

1997-2001    B.A. Biology, Earlham College, Richmond, IN

Research Experience

2005-2010    **Graduate Research Assistant,** Indiana University School of Medicine, Department of Biochemistry and Molecular Biology, Indianapolis, IN
- Thesis title: Determining the Molecular Mechanisms of DNA Non-Homologous End Joining Proteins.  Advisor: Dr. John Turchi

2002-2005    **Research Assistant,** Wright State University, Department of Biochemistry and Molecular Biology, Dayton, OH
- Performed research on my own project involving DNA repair proteins and their interactions with DNA.  Supervisors: Dr. John Turchi and Dr. Pat Dennis

2001-2002    **Research Assistant,** Indiana Crop Improvement Association/Purdue University, Lafayette, IN
- Performed extensive laboratory research on the genetics and biochemistry of a new line of soybean, CystX, and its interactions with the Soybean Cyst Nematode.  Supervisors: Dr. Rick Vierling, Dr. Virginia Ferris and Dr. Jalal Faghihi.

Bibliography, Journal Articles, Peer-reviewed

1) Bennett SM, **Pawelczak KS**, Woods D, and Turchi JJ.  Analysis of the C-term domain of Ku80 reveals interactions with both Ku and DNA-PKcs.  *In preparation.*

2) **Pawelczak KS**, Bennett SM, and Turchi JJ.  Coordination of DNA-PK activation and nuclease processing of DNA termini in NHEJ.  *Antioxidants and Redox Signalling.*  Accepted, August 2010.

3) **Pawelczak K.S.**, and Turchi J.J. (2009).  Purification and characterization of exo-nuclease free Artemis: Implications for DNA-PK dependent processing of DNA termini in NHEJ catalyzed DSB repair.  *DNA Repair.*  June 4; **9**(6): 670-7.

4) **Pawelczak K.S.**, and Turchi J.J. (2008).  A mechanism for DNA-Pk activation requiring unique contributions from each strand of a DNA terminus and implications for microhomology-mediated nonhomologous DNA end joining.  *Nucleic Acids Research.* July, **36**(12): 4022-31.

5)  Rahal E.A**.**, Henricksen L.A., Li Y., Turchi J.J., **Pawelczak K.S.**, Dixon, K. (2008).  ATM mediates repression of DNA end-degradation in an ATP-dependent manner.  *DNA Repair*.  Mar 1; **7**(3): 464-75.

6)  **Pawelczak K.S.**, Andrews B.J., and Turchi J.J. (2005).  Differential activation of DNA-PK based on DNA strand orientation and sequence bias.  *Nucleic Acids Research*.  Jan 7; **33**(1): 152-161.

Honors/Awards

1) Young Investigator Award Recipient, 11th International Workshop on Radiation Damage to DNA, Atlanta, GA, May, 2010.
2) Selected to give an oral presentation at a post-doctoral recruiting symposium for CGSTP candidates, National Cancer Institute, NIH, Frederick, MD, November, 2009.

3) 4th Annual NIH Graduate Student Research Festival, Bethesda, MD, November, 2009.

4) Travel Award, 3rd ASM Conference on DNA Repair and Mutagenesis, Whister, B.C., Canada, May, 2009.

5) Travel Award, Indiana University School of Medicine, used towards ASPCC in Verona, Italy, November, 2007.

6) Best Oral Presentation, 9th Annual Midwest DNA Repair Conference, Columbus, OH, May, 2007.

Oral Presentations, Selected from Abstracts, * *depicts oral presenter*

1)  **Katherine S. Pawelczak\*** and John J. Turchi.  Purification and characterization of exo-nuclease free Artemis: Implications for DNA-PK dependent processing of DNA termini in NHEJ catalyzed DSB repair.  11th International Workshop on Radiation Damage to DNA, Atlanta, GA, May, 2010.

2)  **Katherine S. Pawelczak\*** and John J. Turchi.  Purification and characterization of exo-nuclease free Artemis: Implications for DNA-PK dependent processing of DNA termini in NHEJ catalyzed DSB repair.  11th Annual Midwest DNA Repair Conference, Ann Arbor, MI, May 2009.

3)  **Katherine S. Pawelczak\*** and John J. Turchi.  Influence of DNA structure and orientation on activation of DNA-PK.  9th Annual Midwest DNA Repair Conference, Columbus, OH, May 2007.

Bibliography, Abstracts, Non-peer reviewed, International, National and Regional conferences, * *depicts poster presenter*

1)  **Katherine S. Pawelczak\*** and John Turchi**.**  Purification and characterization of exo-nuclease free Artemis: Implications for DNA-PK dependent processing of DNA termini in NHEJ catalyzed DSB repair.  3rd ASM Conference on DNA Repair and Mutagenesis, Whistler, British Columbia, Canada, May 30-June 6, 2009.

2) Sarah Bennett*, **Katherine S. Pawelczak** and John Turchi. Elucidating the role of the Ku80 C-terminal domain in DNA-PKcs activation. 3rd ASM Conference on DNA Repair and Mutagenesis, Whistler, British Columbia, CA, May 30-June 6, 2009.

3) **Katherine S. Pawelczak*** and John Turchi**.** Purification and characterization of exo-nuclease free Artemis: Implications for DNA-PK dependent processing of DNA termini in NHEJ catalyzed DSB repair. 11th Annual Midwest DNA Repair Conference, Ann Arbor, MI, May 2009.

4) **Katherine S. Pawelczak*** and John Turchi. Influence of DNA structure and orientation on activation of DNA-PK. 10th Annual Midwest DNA Repair Conference, Pittsburgh, PA, May10-11, 2008.

5) Elias Rahal*, Leigh A. Henrickson, Yuling Li, John J. Turchi, **Katherine S. Pawelczak**, and Kathleen Dixon. ATM represses DNA end-degradation in an ATP-dependent manner. 10th Annual Midwest DNA Repair Conference, Pittsburgh, PA, May10-11, 2008.

6) **Katherine S. Pawelczak*** and John Turchi. Influence of DNA structure and orientation on activation of DNA-PK. 10th International Symposium on Platinum Coordination Compounds in Cancer Chemotherapy, Verona, Italy, Nov. 30-Dec 3, 2007.

7) **Katherine S. Pawelczak*** and John J. Turchi. Influence of DNA structure and orientation on activation of DNA-PK. 9th Annual Midwest DNA Repair Conference, Columbus, OH, 2007

8) **Katherine S. Pawelczak***, Brooke J. Andrews, Jason Lehman, and John J. Turchi. Influence of sequence bias/strand orientation and redox effect on proteins involved in DNA double-strand break repair. 8th Annual Midwest DNA Repair Conference, Indianapolis, IN, May 20-21, 2006.

9) **Katherine S. Pawelczak** and John Turchi. Cloning, over-expression and purification of un-modified, full-length Artemis: Characterization of nuclease activity and its role in non-homologous end Joining. 7th Annual Midwest DNA Repair Conference, Detroit, MI. May 20-21, 2005.

10) **Katherine S. Pawelczak***, Brooke J. Andrews and John J. Turchi. Differential activation of DNA-PK based on DNA strand orientation and sequence bias. 2[nd]ASM Conference on DNA Repair and Mutagenesis, Southhampton, Bermuda, Nov.14-20, 2004.

11) **Katherine Pawelczak***, Brooke Andrews and John Turchi. The effect of cisplatin adduct position, orientation and strand bias on the activation of DNA-PK. 6th Annual Midwest DNA Repair Conference, Lexington, KY, June, 2003.

12) Brooke J. Andrews*, **Katherine S. Pawelczak** and John J. Turchi. Development of solution based assays to analyze the interaction of Ku with cisplatin-damaged DNA and determine the effect of orientation on binding. 6th Annual Midwest DNA Repair Conference, Lexington, KY, June, 2003.

13) **Katherine Pawelczak\***, John Turchi and Patrick Dennis.  DNA Replication Fork Collapse signals to the mTOR/S6K pathway.  Cold Spring Harbor Meeting on Eukaryotic DNA replication.  Cold Spring Harbor, NY., Sept. 3-7, 2003.

14) **Katherine Pawelczak\***, John Turchi and Patrick Dennis.  Crosstalk between DNA Replication Fork Collapse and the mTOR/S6K pathway.  5th Annual Midwest DNA Repair Conference, Rochester, MN.  May 23-25, 2003.

Conferences Attended, International, National and Regional

1)  11th International Workshop on Radiation Damage to DNA, Atlanta, GA.  May 16-20, 2010.
2)  4th Annual NIH Graduate Student Research Festival, Bethesda, MD.  November, 2009.
3)  3rd ASM Conference on DNA Repair and Mutagenesis, Whistler, British Columbia, Canada.  May 30-June 5, 2009.
4)  11th Annual Midwest DNA Repair Conference, Ann Arbor, MI.  May 16-17, 2009.
5)  10th Annual Midwest DNA Repair Conference, Pittsburgh, PA.  May 17-18, 2008.
6)  10th International Symposium on Platinum Coordination Compounds, Verona, Italy.  November 30-Dec. 3, 2007.
7)  9th Annual Midwest DNA Repair Conference, Columbus, OH.  May 19-20, 2007.
8)  8th Annual Midwest DNA Repair Conference, Indianapolis, IN.  May 20-21, 2006.
9)  2nd ASM Conference on DNA Repair and Mutagenesis, Southhampton, Bermuda. Nov.14-20, 2004.
10) 6th Annual Midwest DNA Repair Conference, Lexington, KY. June, 2003.
11) Cold Spring Harbor Meeting on Eukaryotic DNA replication, Cold Spring Harbor, NY.  Sept. 3-7, 2003.
12) 5th Annual Midwest DNA Repair Conference, Rochester, MN.  May 23-25, 2003.

Invited Talks, * depicts presenter
**Katherine Pawelczak\*** and John J. Turchi.  DNA Repair and cancer therapy; a study of Nucleotide Excision Repair and Non Homologous End Joining.  Biology Monthly Symposium, Earlham College, Richmond, Indiana.  October 28, 2009.

Teaching Experience and Service

March 25-26, 2010, Earlham College, Richmond, IN
**Oral Examiner for Biology/Biochemistry Comprehensive Exams**

Spring 2001, Earlham College, Richmond, IN
**Supplemental Tutor, Introductory Cellular Biology Lecture**

Spring 2000, Spring 2001, Earlham College, Richmond, IN
**Teaching Assistant, Introductory Cellular Biology Lab**

Fall 2000, Earlham College, Richmond, IN
**Teaching Assistant, Anatomy and Physiology Lecture and Lab**

Spring 1999, Earlham College, Richmond, IN
**Lab assistant, Drosophila Stock keeper**